Spring 5-31-2003

Modification of biodegradable polyesters with inorganic fillers

Georgia Chouzouri
New Jersey Institute of Technology

ABSTRACT

MODIFICATION OF BIODEGRADABLE POLYESTERS WITH INORGANIC FILLERS

by

Georgia Chouzouri

In attempts to address the growing need of materials with controlled degradation characteristics and good mechanical properties for tissue engineering applications, composites based on biodegradable polymers and a potentially bioactive novel inorganic synthetic filler were produced and characterized. Composites were produced by solution mixing of a commercial polylactic acid, as well as a biodegradable thermoplastic polyester based on butylene adipate/succinate, with synthetic magnesium/aluminum carbonate minerals, known as hydrotalcites. Two types of hydrotalcites, at 30 wt% filler level, were used: surface coated and uncoated. Composites were also melt-mixed in a twin-screw extruder for comparison.

Differential Scanning Calorimetry (DSC), Thermogravimetric Analysis (TGA), and Melt Rheology were used to characterize the unfilled polymers and their composites. Results of long-term degradation data *in vitro* in a PBS solution are also presented. The polylactic acid composites showed significant differences compared to the unfilled polymers and the copolyester composites. The copolyester composites showed only slight thermal and hydrolytic short and long-term degradation. By contrast, hydrotalcites appear to promote in all cases degradation of the matrix in the polylactic acid composites. During the course of long-term degradation of the polylactic acid and its composites, Elemental Analysis for released Mg and Al ions was performed, as well as measurement

of pH changes. Scanning Electron Microscopy was also used to study morphological changes of the composites. Further investigation is needed involving degradation experiments *in vivo* for the most promising polylactic acid/hydrotalcite composites.

MODIFICATION OF BIODEGRADABLE POLYESTERS WITH INORGANIC FILLERS

by
Georgia Chouzouri

A Thesis
Submitted to the Faculty of
New Jersey Institute of Technology
In Partial Fulfillment of the Requirements for the Degree of
Master of Science in Chemical Engineering

Otto H. York Department of Chemical Engineering

May 2003

APPROVAL PAGE

MODIFICATION OF BIODEGRADABLE POLYESTERS WITH INORGANIC FILLERS

Georgia Chouzouri

Dr. Marino Xanthos, Thesis Advisor — Date
Professor of Chemical Engineering, NJIT

Dr. Costas Gogos, Committee Member — Date
Research Professor of Chemical Engineering, NJIT

Dr. Michael Huang, Committee Member — Date
Assistant Professor of Chemical Engineering, NJIT

BIOGRAPHICAL SKETCH

Author: Georgia Chouzouri

Degree: Master of Science

Date: May 2003

Undergraduate and Graduate Education:

- Master of Science in Chemical Engineering,
  New Jersey Institute of Technology, Newark, NJ, 2003

- Bachelor of Science in Chemical Engineering.
  National Technical University of Athens, Athens, Greece, 1998

Major: Chemical Engineering

Presentations and Publications:

Georgia C. and Xanthos M.,
"Modification of biodegradable polyesters with inorganic fillers",
Proc. 61st Society of Plastic Engineers Annual Technical Conference, (2003)

"The ideas that have lighted my way and time after time have given me new courage to face life cheerfully, have been Kindness, Beauty and Truth"
Albert Einstein

To my beloved grandparents who passed away and to my husband for his encouragement, love and understanding

ACKNOWLEDGMENTS

First and foremost, I would like to express my deepest gratitude for my thesis advisor, Professor Marino Xanthos. I could not begin to explain my appreciation for his guidance and invaluable teaching in polymer chemistry and processing, which strengthened and provided a solid basis for my future endeavors in this field. It was a great privilege to have him as my mentor. It would be impossible for me to fully express how his moral and emotional support helped me persevere through circumstances that would otherwise be overwhelming.

I would also like to thank my Committee members, Professor Huang and Professor Gogos for agreeing to be part of my work. I appreciate their input, and I thank them for their constructive comments.

I would also like to thank the staff of the Polymer Processing Institute (PPI), Newark, NJ for providing a friendly and productive environment. Their invaluable assistance and cooperation is greatly appreciated.

In addition, I would like to thank Dr. V. Tan of PPI for his guidance and help with the DSC experiments and Dr. S. Patel of PPI for providing guidance in developing my experimental skills. Also, Mr. C. Wan for his help with the SEM and Melt Rheology experiments and Mr. Dale Conti for his timely support and assistance with experimental equipments in the PPI laboratory. Last, but not least, Dr. Z. Ophir of the Center for Biomaterials for his assistance with the TGA measurements, Professor Jing Wu and Mr. Jing Zhang of NJIT for providing the PLLA polymer and Professor Soohan Kwon, of

Chungbuk National University in Cheongju, Korea for providing the hydrotalcite samples.

Financial support for this work was provided by the Society of Plastic Engineers (SPE), Palisades Section, through the Melville M. Gerson scholarship.

It would be inexcusable not to mention my colleague and friend Dr. Rahul Dhavalikar for all the emotional support, comraderie and caring he provided.

Lastly, I take this opportunity to sincerely thank my family and friends for their love and understanding. Specifically, my mother's advice has encouraged and inspired me to stay focused and head towards the right direction. Last, but not least, I am thankful to my husband for love, patience, understanding and his confidence in me. I thank him for always being there for me.

TABLE OF CONTENTS

TABLE OF CONTENTS
(Continued)

LIST OF TABLES

Table **Page**

LIST OF FIGURES

LIST OF FIGURES
(Continued)

Figure **Page**

LIST OF FIGURES
(Continued)

Figure **Page**

LIST OF FIGURES
(Continued)

Figure **Page**

LIST OF FIGURES
(Continued)

Figure **Page**

LIST OF ACRONYMS

AFS:	Atomic force microscopy
AVR:	Average value
BMP-2:	Bone morphogenetic protein-2
CV:	Coefficient of variation
DMA:	Dynamic mechanical tests
DSC:	Differential scanning calorimetry
ICP:	Inductively coupled plasma
NMR:	Nuclear magnetic resonance
OMLS:	Organically modified layered silicate
PBS:	Phosphate buffer saline
PCL:	Polycaprolactone
PHBV:	Poly(hydroxybutyrate valerate)
PLLA:	Polylactic acid
PST:	Poly (1,4-butylene adipate-co-1,4-butylene succinate)
SBF:	Simulated body fluid
SCA:	Cellulose acetate
SCORIM™:	Shear controlled orientation in injection molding
SEM:	Scanning electron microscopy
SEVA-C:	Blend of starch with ethylene vinyl alcohol
SR-PGA:	Self reinforced polyglycolide
SR-PLLA:	Self reinforced poly L-lactide

STDEV:	Standard deviation
TGA:	Thermogravimetric analysis
WAXS:	Wide-angle X-ray scattering
XRD:	X-ray diffraction

CHAPTER 1

INTRODUCTION

During the past two decades, significant interest has been developed in the area of biomaterials based on biodegradable and bioresorbable polymers. It is already well known that polymers with a combination of desirable mechanical and physical properties, good degradation characteristics and biocompatibility have been widely used in biomedical applications such as sutures, tissue engineering scaffolds, tissue replacements and drug delivery carriers. Nevertheless, the never ending necessity for more improved and precise solutions in tissue engineering applications, has led to the development of biomaterials with better mechanical properties and controlled degradation characteristics. As a result, in the past few years, researchers have started to study systems of biodegradable polymers reinforced with inorganic or organic bioactive fillers.

1.1 Definitions

According to Vert et al. (1992), there are certain definitions given to the words "biodegradable", "bioerodible", "bioresorbable" and "bioabsorbable" that one should be familiar with, in order to better understand the tissue engineering literature; these are as follows:

"Biodegradable" polymeric materials are the ones that follow macromolecular degradation when they are dispersed *in vivo*, without any evidence of elimination from the body being noticeable. Some biological elements attack these systems resulting to

remains or other degradation by-products that are capable of moving away of their location but not necessarily from the body.

"Bioerodible" are polymers that undergo surface degradation and also resorb *in vivo*. There is also the possibility of bioerosion, which leads to total elimination of the initial material as well as of the low molecular weight substances with no residual side effects.

"Bioresorbable" are the polymeric materials that undergo bulk degradation and resorb *in vivo*. They can also follow bioresoption, which in this case involves total elimination of the initial material and of the bulk degradation by-products with no side effects left behind.

"Bioabsorbable" are the polymers that can dissolve in body fluids without any polymer chain cleavage or decrease of molecular mass. An example is a water-soluble implant that can follow slow dissolution in body fluids. When the dispersed macromolecules are excreted, a bioabsorbable polymer can also be considered as being bioresorbable.

Another definition that is essential to be aware of, is "biocompatibility". "Biocompatibility" is the ability of the material to perform with the appropriate host response in the particular biomedical application. Generally, biocompatible is a material that has no toxic or injurious defects on biological systems. A polymer is considered being biocompatible when the degradation by-products have no toxicity to the biological environment they are dispersed in.

1.2 Degradation Characteristics

Degradation of a polymer follows different pathways depending on the medium in which this takes place. According to Ray et al. (2003), degradation under compost is a complex process that involves water absorption, chain cleavage and formation of oligomeric compounds, solubilization of the oligomeric compounds, and diffusion of the soluble compounds by bacteria. Therefore, the rate of the degradation depends on the factors that increase the hydrolysis of the polymer.

Hydrolysis is also a very important step during the degradation of a polymer in the body. Kim (2002) claimed that hydrolysis of a polymer to oligomeric compounds implicates two different mechanisms depending on whether the system follows enzymatic or non-enzymatic pathways. In the case of an enzymatic system the enzymes interact with the polymer and decomposition results. When a non-enzymatic system is operational the decomposition depends on the structure of the main chain. The other step that fulfills the degradation is the absorption that takes place with the metabolic cycle of the bioorganisms. There are certain differences in biodegradability depending on the kind of the polymer. When the degradation involves a natural polymer, complete biodegradability occurs with certain disadvantages such as complexity to estimate the degradation rate, and poor strength of the polymer due to water absorption. However, when the degradation involves a synthetic polymer, selected biodegradability can ensue.

On the whole, certain features exist, which have an effect on the degradability of a polymer such as the chemical structure that includes the polarity of the main chain, the side groups, and the hydrophobic or hydrophilic character of the polymer. Added features are the architecture (block, branches, etc), the molecular weight, the morphology and the

surface area. The character of the medium that the polymer is surrounded with is also a very important degradability factor. In general, the higher the molecular weight and the strength of the polymer, the slower the degradation rate, according to Kim. All of the above factors provide the criteria of selecting a suitable polymer for a specific application with certain degradation characteristics.

1.3 Polymers Suitable for Biomedical Applications

Some of the most common biodegradable polymers that have been used for biomedical applications and, according to Tormala et al. (1999), are suitable for biocomposites are polylactic acid, polyglycolic acid, polycaprolactone, poly-d-valerolactone, poly-b-hydroxybutyrate, polyorthoesters, ethylene-vinyl alcohol, polybutylene/succinate, and polybutylene/adipate, as well as blends of the above polymers. In the case of polylactic acid, one can also use its stereocopolymers like poly-L-lactide, poly-DL-lactide and L-lactide/DL-lactide copolymers.

All the previous polymers have been studied to variable degrees and results have been reported regarding their usage as well as their properties and characteristics. Their reinforcement with organic or inorganic fillers has led to a significant modification of their properties so that a variety of new applications can now be attained.

1.4 Reinforcements Suitable for Polymers in Biomedical Applications

Depending on the intended application of the biopolymer, there are several types of reinforcing materials. These can be organic or inorganic. In the category of the organic reinforcements starch is one of the most widely studied materials having been blended with many different polymers in order to produce scaffolds for tissue engineering applications.

Inorganic fillers have also been used, especially those being bioactive. Bioactivity is the ability of promoting an interfacial bone bonding with the host tissue and, consequently, supporting tissue regeneration. During the last few years, as mentioned by Engin and Tas (2002) there is a growing demand of such bioactive materials. Their biocompatibility, bioactivity and osteoconduction characteristics have made these materials necessary for all kinds of biomedical applications where a bone bonding with the host tissue is crucial. Examples of these reinforcing materials as stated by Tormala et al. (1999) are synthetic hydroxyapatite, tricalcium phosphate, other calcium phosphates, Bioglass, Ceravital, Alumina, Zirconia, bioactive gel-glass, bioactive glasses and Alpha Wollastonite glass ceramics.

It is very essential to empathize that no one reinforcement is suitable for all applications. As stated by Hench (1996), depending on the type of the tissue attachment that needs to be fixed, only certain bioceramic materials can be used. For example, tricalcium phosphate and other calcium phosphates are grafted in a way that they can be gradually replaced by the bone. In the case of bioactive glasses, bioactive glass ceramics and hydroxyapatite, Hench states that they are attached directly to the bone by chemical bonding. Hench uses the term "bioactive fixation" for this attachment type. Another term

called "biological fixation", takes place in the case of Al_2O_3 and hydroxyapatite-coated porous metals where the bone is mechanically attached to them and bone ingrowth occurs.

According to Lutton et al. (2001), the major elements of the bone are: type I collagen, calcium phosphate minerals (mainly hydroxyapatite), carbonate-substituted apatite and water. These constituents, in addition to the facts that the bone remodels in response to age and health and also has the ability to regenerate in case of injury, led to the investigation of these minerals as potential reinforcements in biocomposites.

1.5 Acid Neutralizing Ability of Carbonated Minerals

Although biodegradable polymeric composites with the above reinforcing materials have certain advantages in biomedical applications, a considerable problem arises due to the formation of acidic low molecular weight fragments during polymer degradation. Schiller and Epple (2003) investigated the behavior of carbonated calcium phosphates materials acting as basic fillers to neutralize the acidity and provide pH control. According to the authors, the choice of the filler is important for the long-term performance of the composite in a given application. Even though in some cases the body can compensate for the release of the acid, it is healthier if the released acid can be compensated by appropriate buffer capacities that surround the tissue. As Schiller and Epple suggested, this can be provided by the use of carbonate calcium phosphates that may keep the pH within the physiological range (around 7.4).

1.6 Objective of This Study

Based on the above considerations, the objective of the present study is to investigate biocomposites based on degradable polyesters, such as a thermoplastic polyester based on butylene adipate / succinate and a commercial polylactic acid, containing a synthetic inorganic mineral as a novel bioactive reinforcement. This is a coprecipitated magnesium / aluminum carbonate compound known as hydrotalcite. Hydrotalcite has been orally administered as acid neutralizing compound for gastric fluids. Although the use of the hydrotalcite as an implant material is not well known, the Mg and Al ions that it contains in its layers have been already found, according to Hench (1996), in the form of MgO and Al_2O_3 in bioceramics used in medical devices. Its reinforcing characteristics, degradation enhancement, bioactivity and acid neutralizing ability as well as its capacity for pH control during degradation were the fields of examination. Long-term degradation experiments were performed *in vitro* in the presence of a phosphate buffered saline solution and compared with short-term data.

CHAPTER 2

LITERATURE REVIEW

Biomaterials are in the center of interest for many researchers. Throughout the years, significant research has been performed and a wide range of techniques has been developed for producing materials for biomedical applications. Tissue engineering implants where the biomaterial plays a significant role of tissue replacement or fixation have been examined.

Malafaya et al. (2002), consider the need of better biocompatible filler materials in orthopedic applications that can actually improve the patients' lives. According to them, one can apply a tissue engineering approach successfully, if takes into consideration three main factors, such as the cells, the growth factors and their scaffolds. In general, there is a necessity to increase the number of cells around the tissue and have the appropriate structure to support those cells. In addition, the usage of growth factors that can promote cell proliferation is essential, since this helps the regeneration of the tissue.

2.1 Biocomposites with Organic Fillers

In this context, Malafaya et al. (2002), studied and reported results on a blend of corn starch with ethylene vinyl alcohol (SEVA-C) using a microwave based processing route for the production of a porous delivery system. Following the full characterization of this system, Malafaya et al. developed a material with interesting mechanical behavior, which, in turn, can be used as non-loaded or loaded scaffolds for bone tissue-engineering

applications. In the second part of their work, they produced starch microspheres using an emulsion crosslinking technique, which can be applied to drug delivery carriers. This development needs further exploitation to confirm its applicability. Although further studies are needed, it is of interest that this system seems to be pH-dependent. The release of the drug *in vivo* applications seemed to be slower after a certain period due to lower pH than the physiological of the body. It is also of interest, as stated by the authors that for longer release periods an increase in the pH causes increase in the drug release.

Similarly, Reis (2002) reviewed the development of numerous natural origin polymers such as starch blended with ethylene vinyl alcohol, cellulose acetate, polylactic acid and polycaprolactone, casein and soybean proteins, chitin and chitosan. Based on these materials, scaffolds with suitable properties that can be used in tissue engineering applications are developed and characterized. According to the author, a material that will be used in load bearing sites must have mechanical properties similar to the regenerated human tissue. Simultaneously, degradation characteristics suitable for the healing of the tissues to be regenerated as well as surface characteristics capable of cell adhesion, proliferation and differentiation are required. In addition, this performance should be coupled with biocompatible behavior. Various processing methods for the production of the 3D porous architectures have been discussed. In this work two main types of scaffolds have been developed: materials with a compact dense surface layer and a foamed porous core, and fully porous architectures. The processing methods depending on the type of the scaffold constitute the following: (a) Injection molding and Extrusion, (b) Compression molding – particulate leaching, (c) Solvent casting – particulate leaching, (d) Microwave baking and (e) In – situ polymerization. Occasionally, the

polymers are reinforced with bioactive ceramics, so that the scaffolds intake bioactive characteristics. Several characterization techniques have been implemented, such as scanning electron microscopy (SEM) for the porous structure of the materials as well as for testing bioactivity, dynamic mechanical tests (DMA), nuclear magnetic resonance (NMR) for surface characterization and others.

Gomes et al. (2002), reported the use of cellulose acetate and ethylene vinyl alcohol to produce scaffolds based on starch blends. Scanning electron micrographs were taken in order to display the structure of scaffolds obtained by extrusion and *in situ* polymerization. The scaffolds that were obtained from extrusion showed an important development in the percentage of porosity and interconnectivity in the porous surfaces, whereas the ones obtained by *in situ* polymerization had the advantage of treating the defect by being injected directly and consequently taking immediately the appropriate shape. Degradation behavior was characterized by immersing the materials in an isotonic saline solution at 37^0C and measuring weight changes after several periods to determine the water uptake. The study revealed different results depending on the processing method, processing conditions and also on the final porosity of the obtained biomaterials.

Reis et al. (2001), had further explored the design of tissue engineering scaffolds based on three different blends of starch with ethylene vinyl alcohol, cellulose acetate and poly-ε-caprolactone. Their main scope was for the scaffolds to have three-dimensional geometries, adequate porosity and porous size and tissue matching mechanical properties. All of the above are very important for tissue regeneration. By using different methods, scaffolds with different structures were obtained, which can be suitable in specific tissue engineering applications.

2.2 Biocomposites with Inorganic Fillers

A preliminary study on the development of a new method for tissue engineering scaffolds from biodegradable polymers reinforced with hydroxyapatite was published by Gomes et al. (2001). Blends of starch with ethylene vinyl alcohol (SEVA-C) and cellulose acetate (SCA) were premixed with the blowing agent in a bi-axial rotating drum and then reinforced with 10 and 30-wt% of hydroxyapatite by processing in an injection molding machine. These porous scaffolds showed good mechanical and degradation properties as well as a bioactive behavior due to the hydroxyapatite. The authors concluded that there is a possibility to modify the final properties and the morphology of the scaffolds by varying the processing parameters, the materials formulation and quantity of blowing agent.

Sousa et al. (2002), explored composites of starch blends with ethylene vinyl alcohol (SEVA-C) filled with 10, 30 and 50 wt% of hydroxyapatite molded by two different molding techniques: injection molding and shear controlled orientation in injection molding (SCORIM)™. The hydroxyapatite reinforcement proved again to improve mechanical properties and provide bioactivity to the composites. In comparison with the injection molding technique, the composites that were molded by SCORIM had enhanced stiffness, which in turn allowed for an effective control of their mechanical performance.

Since it has been already shown that a blend of starch with ethylene vinyl alcohol (SEVA-C) has a degradable behavior with good mechanical properties, and it can be bioactive when reinforced with hydroxyapatite, Leonor et al. (2003), studied *in vitro* bioactivity of such a composite. The polymer was reinforced with 30% by weight of

hydroxyapatite. The composite was immersed in a simulated body fluid (SBF) and the *in vitro* bioactivity of the composite was studied as a function of time. Atomic force microscopy (AFS) was used *in situ* and confirmed results previously obtained from the scanning electron microscopy (SEM). The polymer absorbs water while it is in the SBF, degradation occurs, which results to the exposure of the hydroxyapatite particles in the solution and consequently supplies the nucleation and growth of the calcium phosphate layer. The ion concentration of the Ca and the P were measured by inductively coupled plasma emission (ICP) spectroscopy. These results indicate the potential use of the composites in bone bonding applications by *in vivo* experiments. A concern that arises is that when just the polymer matrix is immersed in the SBF, the pH drops; however, when the composite was immersed in the SBF, a pH balance over a period of time was observed. Further investigation was necessary according to the authors, to elucidate the effect of the neutralizing capacity of the filler.

Lewandrowki et al. (2002), explored *in vivo* screw implants made of poly(L-co-D,L)lactide, reinforced with 25 wt% hydroxyapatite. The composites were mixed overnight in a rotary blender and the screw implants were obtained by injection molding. One screw was implanted per rabbit in a total of 24, and follow up times were 8 and 16 weeks. Radiographic as well as histological studies were performed for all specimens, which showed that repaired tissue was formed around the area of the implant. This was mainly consistent with newly formed bone. The specimens that were implanted for a 16-week period were the ones with the highly osteoid formation. The formation of the new bone is considered to be achieved due to the addition of the hydroxyapatite. Hydroxyapatite, according to the authors was used both due to its bioactivity and

neutralizing capability. Specifically, hydroxyapatite reflects 65% neutralization of the acidic degradation by-products of the polymer. The above composites might be suitable for fixation of small bone fractures, as Lewandrowki et al. stated.

Lutton et al. (2001), developed a method of producing nano-composites by poly (hydroxybutyrate valerate) (PHBV) as a matrix and up to 50%vol nano sized hydroxyapatite as a reinforcement and also techniques of designing scaffolds capable of load bearing applications. When PHBV degrades hydrolytically, produces hydroxybutyric acid, which can be found in human blood. In addition, PHBV has longer degradation times allowing the scaffold to maintain its mechanical properties until the bone growth is satisfactory around the implant. For a scaffold to be successfully designed, it is very essential for researchers to achieve the control of its architecture, which includes features as pore size and shape. Lutton et al. solved that difficult technical challenge by developing a laser ablation process that provides accurate controlling structural characteristics.

Calandrelli et al. (2000), used ossein, a biological hydroxyapatite which consists of elemental calcium and phosphorous, as a filler for biodegradable composites. Polylactic acid (PLLA), polycaprolactone (PCL), and three different copolymers of the above were used as matrices for the obtained composites. According to the authors these polymers have poor hydrophilic properties and consequently prevent cell adhesion. By preparing such composites with 5wt % of ossein, hydrophilic behavior was enhanced and a positive cellular response was achieved. The amount of the filler added was decided, taking into consideration the improvement of the physical and morphological characteristics without sacrificing mechanical performance. The thermal, morphological,

mechanical and biochemical properties of the resulting materials were tested. Calandrelli et al. demonstrated that by using this biological hydroxyapatite filler with 60 μm or less particle size, modulus of the composites appeared to improve even at this low concentration. Biocompatibility tests using primary cultures of human osteoblastic cells as model systems were reported. Surface adhesion of the growing cells, as investigated by SEM micrographs, was enhanced due to the hydrophilic characteristics of the ossein component. Some preliminary positive results in the synthesis of proteins were also observed.

Taking an extra step in their research Laurencin et al. (2001), investigated a biodegradable poly(lactide-co-glycolide)- hydroxyapatite scaffold in which a growth factor was added, in order to promote bone formation. Particularly, bone morphogenetic protein-2 (BMP-2), which is an osteoinductive protein and has been reported to elicit the healing of bone defects, was used. *In vitro* studies showed bioactivity of the system, which was also confirmed by studies *in vivo.* The models used were severe combined immune deficient mice. The scaffolds were found to function effectively as delivery carriers for BMP-2 and according to the researchers they may be considered as an alternative to usual bone grafting techniques.

There also exists another group of researchers that investigated the preparation of nanocomposites, based on biodegradable polymers filled with different types of montmorillonites. Paul et al. (2003) considered the modification of plasticized poly(L-lactide) with organo-modified or unmodified montmorillonites as reinforcements. Poly(L-lactide), poly(ethyleneglycol) which acted as a plasticizer and the clay particles were blended in a Brabender counter-rotating mixer. The obtained materials were

analyzed and characterized by wide-angle X-ray scattering (WAXS), thermogravimetric analysis (TGA) and differential scanning calorimertry (DSC). The formation of intercalated nanostructures was suggested by WAXS. Both WAXS and DSC showed that poly(L-lactide) and poly(ethyleneglycol) competed with each other for intercalation. Furthermore, an increase in the amount of clay appears to delay thermal degradation. The nanoscale distribution of high aspect ratio fillers like montmorillonites, contributed to the remarkably improved mechanical properties of the composite as compared to the matrix.

In two similar studies, Ray et al. (2002, 2003), produced polylactide – montmorillonite nanocomposites. Organically modified layered silicate (OMLS) was produced by exchanging Na^+ ion in montmorillonite with trimethyl octadecyl – ammonium cation. The OMLS was dry mixed with polylactide and then melt extruded. Three different nanocomposites were obtained, having 4,5 and 7 wt% of OMLS respectively. WAXD and transmission electron microscopy were used for product observation. The silicate layers of the clay were intercalated and randomly distributed in the polymeric matrix. All the nanocomposites revealed enormous improvement in mechanical melt and solid properties including flexural properties. These results are in agreement with the study of Paul et al. Ray et al. took the extra step in examining biodegradability of the nanocomposites concluding that OMLS enhances biodegradability after one month; this is considered to be critical for the heterogeneous hydrolysis to start.

Mitsunaga et al. (2002), used polycaprolactone and polybutylene succinate as biodegradable polymeric matrices to create nanocomposites. Each of the polymers was grafted with maleic anhydride to increase the compatibility between the matrix and the clay. The filler that was used for the production of the nanocomposites was once more

montmorillonite organoclay as in the previous studies. The degree of delamination of the nanocomposites was examined by using X-ray diffraction measurements (XRD), which also showed an increase in crystallinity of the polymer. Delamination, led to remarkable improvement on the material strength of each composite as expected.

A composite produced from biodegradable polymers and bioactive glasses as fillers is another difficult technical challenge that researchers have to face in the biomaterials field. Fujibayashi et al. (2003), studied materials consisting of five different types of bioactive glasses having varying compositions of Na_2O, CaO and SiO_2 and being free of P_2O_5. As mentioned above, these materials are capable of creating a bond to the living bone through formation of an apatite layer. This can be proven *in vivo* as well as *in vitro* in simulated body fluid (SBF), containing certain concentration of phosphate ions. In this study, scanning electron microscopy (SEM) was used to demonstrate the depth of bone ingrowths after the bioactive materials were implanted into a defected femoral condyle of rabbits.

In the case of the biologic behavior of a composite, Nahri et al. (2003), explored a copolymer of poly(ε- caprolactone-co-DL-lactide) filled with bioactive glass (S53P4) in experimental bone defects in rabbits. Bioactive glass was in the form of granules and different amounts of small and large granules acted as fillers for each composite in order to enhance bone healing. The bone bonding ability of bioactive glasses was established by the release of Si and Ca ions that led to formation of an apatite layer. Bone ingrowth was mainly investigated in the composites with the large glass granules. Also, their presence in the composites appeared to enhance degradation since the granules increased

the water absorption. The study of these composites concluded that bioactive glass granules improve the bone response of the copolymer matrix.

A number of different bioabsorbable scaffolds have designed by Kellomäki et al. (2000) using bioabsorbable polymers and bioactive glass. The polymers used in that study were: self reinforced polyglycolide (SR-PGA), self reinforced poly L-lactide (SR-PLLA), copolymer of ε-caprolactone and L-lactic acid, other stereocopolymers of lactic acid, and Polyactive®, which is a block copolymer of polyethylene oxide and polybutylene terephthalate. The bioactive glass no. 13-93 used, was in the form of crushed particles or spheres with 6% Na_2O, 12% K_2O, 5% MgO, 20% CaO, 4% P_2O_5 and 53% SiO_2 weight composition. The obtained composites were incubated in phosphate buffer saline, pH 7.4, at 37^0 C for up to 52 weeks for *in vitro* analysis. After certain periods, the materials were removed from the buffer solution, rinsed with distilled water and dried in vacuum for seven days. Morphological changes were studied using scanning electron microscopy. Bioactivity of the composites was shown after the formation of a silica rich layer, which turned to apatite precipitation, having, as a result, enhancement of the bone growth to the surface. *In vivo* analysis was also performed in 30 growing rabbits addressing bone formation as well as interactions between the bone and the biodegradable materials. The authors concluded that, depending on the application and the strength needed by the composite, different development techniques are to be used.

Rhee (2003) examined composites of poly(ε-caprolactone) with bioactive silica nano-hybrids, produced by a sol-gel method. The variable to be studied was the different molecular weights of the polymer. The bioactivity of the PCL/silica nano-hybrids that also contained a fixed content of calcium salt resulted from the inorganic part of the

hybrid, such as Si-OH and Ti-OH groups, as expected. By immersing the materials in the SBF rapid and homogeneous nucleation and growth of the apatite crystals were observed for the systems containing the low molecular weight polymer. According to the author, the main reason for such a result was the even distribution and fine dispersion of the silica-rich domains in the low molecular polymer matrix. An additional reason is the faster degradation of the polymer phase, which led to faster release of calcium in the SBF.

In the patent literature, Tormala et al. (1999) reported on a composite material used for bone fracture fixation devices, that had a biodegradable polymer as a matrix and two reinforcements, a biodegradable polymer reinforcement and a bioceramic or bioglass filler as a second reinforcement. According to the inventors, having a polymeric reinforcing element solves the problems of inadequate strength and brittleness of the device, whereas having a bioactive reinforcing element provides bone growth and accelerates the healing time for bone defects. In the case of the bioceramics, it was proven that the particle size of the ceramic element has an important role in the biocompatibility of the device. Specifically, the larger the particle size of the ceramic, the better the biocompatibility of the composite. Certain additives and modifiers have been used to improve the processability of the composites and also some pharmaceutical active agents, such as wound healing agents and growth hormones to develop a faster healing process. Melt, powder or solvent mixing had been used for the polymeric matrix and the bioactive reinforcement. The polymeric reinforcement was used as a plain fiber or in a modified form. Composites of several biodegradable polymers and bioactive fillers as

hydroxyapatite, tricalcium phosphates were obtained and studied *in vivo* showing promising results.

As a result of the growing demand of biomaterials and the significant research work reported in this chapter, it is clear that there is a need of developing biocomposites with a good balance of degradation characteristics and physical properties. In the present study, two biodegradable polymers including a copolyester based on butylene adipate/succinate and a commercial polylactic acid, containing the synthetic reinforcing inorganic mineral hydrotalcite, potentially bioactive, were evaluated. Methods for producing such biocomposites as well as their characterization and studies *in vitro* will be reported in the following chapters.

CHAPTER 3

EXPERIMENTAL

3.1 Materials

3.1.1 Polyesters

Two different polyesters were chosen and used for the experimental study. Both of them are biodegradable and can be processed as conventional thermoplastic polyesters. They are as follows:

1. Poly (1, 4-butylene adipate-co-1,4-butylene succinate) [PST], extended with 1,6-diisocyanatohexane, a biodegradable thermoplastic polyester (CAS No. 119553672) obtained from Sigma-Aldrich. The measured carboxyl content CC_p of the pellets was 0.0535 eq./10^6g, corresponding to an acid number of 3.0. This polyester was used for producing biocomposites by solution as well as melting mixing techniques.

2. Poly-L-lactate [PLLA] (trade name Biomer L9000) (CAS No. 26680-10-4) obtained from Biomer. Polylactic acid is derived from naturally occurring lactic acid, which has two isomers as can be seen in Figure 3.1. The measured carboxyl content CC_p of the pellets was 0.0247 eq./10^6g, corresponding to an acid number of 1.4. This resin was used only for producing composites by solution mixing.

The properties and characteristics of the polyesters are listed in Table 3.1.

Lactic Acid Structure.

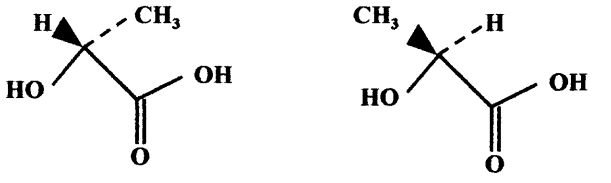

(R) D (-) Lactic Acid
(Levorotatory)

(S) L (+) Lactic Acid
(Dextrorotatory)

Figure 3.1 Isomers of lactic acid.

Table 3.1 Characteristics of Polyesters

Designation	Chemical Structure	Form	Supplier	Trade Name	Acid Number (mg KOH/g)
PST	$[-CO(CH_2)_nCO_2(CH_2)_4O-]_x$ $[-CONH(CH_2)_6NHCO-]$ $[-O(CH_2)]$	pellets	Sigma-Aldrich	-	3.0
PLLA	$H[-O-CH(CH_3)COO-]_nOH$	pellets	Biomer, Germany	Biomer L9000	1.4

3.1.2 Minerals Used as Fillers

The composites were formed by adding uncoated hydrotalcite (HT-U) (trade name CLC-120), and a surface coated with stearic acid version (HT-C), as per company's sources (Doobon Yuhwa Co, Ltd, S. Korea). Stearate coating is presumably added to facilitate dispersion and melt processability. The hydrotalcites are synthetic inorganic minerals, belonging to the group of layered double hydroxides, or so called anionic clays (Carlino, 1997). The Mg/Al ratio in the hydrotalcite used is 4.0-5.0. The molecular structure of the hydrotalcite can be seen in Figure 3.2. The alkaline hydrotalcite is also able to compensate acidity that may occur from the degradation of the polymers.

Properties and characteristics of the hydrotalcites as provided by the supplier are listed in Table 3.2.

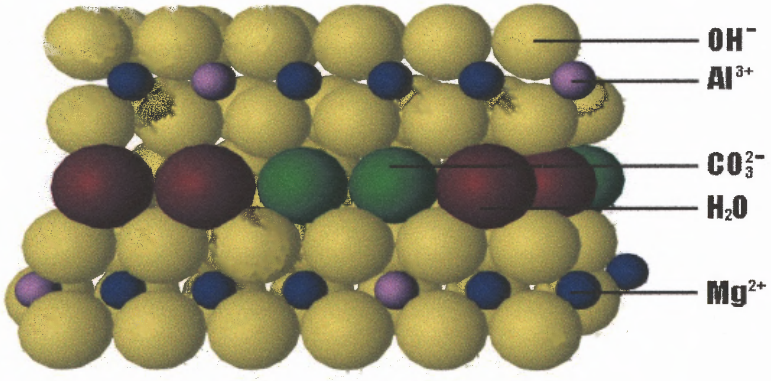

Figure 3.2 Molecular structure of hydrotalcite.

Table 3.2 Characteristics of Minerals

Designation	Chemical Structure	Form	Supplier	Trade Name	Measured pH in water*
HT-U	$Mg_4Al_2(OH)_{12}CO_3.3H_2O$	White Powder (Average Particle Size of 0.4-0.5μm)	Doobon Yuhwa.,Co. Ltd, S. Korea	CLC-120	8.51-8.99 (1wt%-10wt%)
HT-C	$Mg_4Al_2(OH)_{12}CO_3.3H_2O$ with stearate coating	White Powder (Average Particle Size of 0.4-0.5μm)	Doobon Yuhwa.,Co. Ltd, S. Korea	CLC-120 coated	-

* Measured in Polymer Chemistry laboratories.

3.2 Processing

Solution Mixing: Both poly (1, 4-butylene adipate-co-1,4-butylene succinate) and polylactic acid were dissolved in chloroform at room temperature. The addition of each hydrotalcite followed at a polyester / mineral weight ratio of 7:3. The samples were left in the fumehood for five days at room temperature to complete the evaporation of chloroform. After most of the chloroform was evaporated, the remaining solid, was transferred in Pyrex Dishes and put into a vacuum oven for drying overnight.

Extrusion Mixing: A grinder was used to crush PST pellets to a fine powder of variable particle size, but less than 1mm, under liquid nitrogen. Each of the minerals was premixed with the resin at a polyester / mineral weight ratio of 7:3, before feeding the mixture in a co-rotating 15mm twin-screw extruder (APV MP-2015) at 130^0C and 50

rpm. PLLA pellets alone, were also extruded at 220^0 and 100 rpm for producing disc samples.

Compression Molding: All samples obtained from solution and extrusion mixing were compression molded in a PHI press for 2 ½ minutes to form standard test disc specimens with nominal thickness of 0.75mm and diameter of 33mm. Temperatures used were 130^0C and 200^0C for the PST and the PLLA samples, respectively. Designation and composition of compression molded disc samples are shown in Table 3.3.

Table 3.3 Designation of Compression Molded Disc Samples

Sample Designation	**% Hydrotalcite**	**Method of Mixing**
PST-pel	-	-
PST-S1	30(HT-U)	solution
PST-S2	30(HT-C)	solution
PST-melt	-	extrusion
PST-M1	30(HT-U)	extrusion
PST-M2	30(HT-C)	extrusion
PLLA-pel	-	-
PLLA-S1	30(HT-U)	solution
PLLA-S2	30(HT-C)	solution
PLLA-melt	-	extrusion

3.3 Testing and Characterization

Acid Number: Carboxyl Content or Acid Number of the polyesters before processing were determined according to Pohl's method (Pohl 1954) by titrating each solution of the polymer in chloroform with standard KOH in methyl alcohol in the presence of phenolphthalein as an indicator. The Acid Numbers of the polyesters are listed in Table 3.1.

Differential Scanning Calorimetry (DSC): Information on glass transition temperature, melting temperature as well as crystallization effects were obtained by DSC (Perkin - Elmer DSC7). For all samples, scanning heating and cooling rates were 20^0C/min and the final temperatures were 130^0C and 200^0C for the co-polyester and the polylactic acid, respectively.

Isothermal Thermogravimetric Analysis (TGA): Stabilities of the predried polyesters and composite samples as well as those of the inorganic hydrotalcite minerals were studied by TGA (TA instruments, model QA 50) ramp up to 500^0 C with 10^0C/min heating rate under nitrogen blanket for a total time of approximately 62 minutes. During the experiments, weight percentage losses were monitored.

Rheology: Rheological data were collected using a Rheometrics Mechanical Spectrometer (RMS-800) in parallel disc mode under nitrogen. The discs obtained by compression molding were predried in a vacuum oven at room temperature to avoid any possible hydrolytic degradation. The RMS-800 system was programmed for steady shear at $2s^{-1}$ and $5s^{-1}$ shear rates and 130^0C for the PST and its composites and melt viscosity data were obtained.

Degradation: Degradation behavior was followed by immersing discs in triplicate in 30 ml of a Phosphate Buffer Saline (PBS) solution with pH of 7.4 at 37^0C. At predetermined immersion periods (over a total period of three months) the discs were removed from the solution, rinsed with methanol, and were weighted after wiping the excess.

Morphology: The surface structures of the PLLA composites before and after exposure to the buffer solution, as well as the ones for the hydrotalcite minerals were characterized by Scanning Electron Microscopy (LEO Field Emission Gun Digital SEM) at 3keV working voltage.

Elemental Analysis: Inductive Coupled Plasma Analysis (ICP) was performed at QTI Laboratories in order to detect Al and Mg elements that were released from a PLLA composite disc sample to the buffer solution after 139 days of immersion.

CHAPTER 4

RESULTS AND DISCUSSION

This section will provide results from the experiments carried out to elucidate the effects of the hydrotalcites on the properties of the polymer composites. Results for the polymeric matrices alone will also be reported in order to understand the overall structure of the biocomposites. This chapter is divided into three main sections, including a) the composite manufacturing, b) characterization of the composites by Differential Scanning Calorimetry, Thermogravimetric Analysis, and Melt Rheology and lastly, in the third section (c), results of long-term degradation data.

4.1 Composite Manufacturing

As mentioned in the experimental section, two types of polymers, as well as two different processing methods were used to obtain the biocomposites. Both poly (1, 4-butylene adipate-co-1,4-butylene succinate) and polylactic acid were used as polymeric matrices for the composites produced by solution mixing. Both polymers were dissolved in chloroform, and coated and uncoated hydrotalcites were added at a polyester/mineral weight ratio of 7:3. After the evaporation of the chloroform, the materials were left to totally dry in the vacuum oven overnight. The resulting mixtures appeared quite uniform and were compression molded into the desired samples.

The second processing method used was extrusion mixing at a polyester/mineral weight ratio, also, of 7:3. Given the limited quantities available of the polyesters, a small 15 mm twin-screw extruder was used. The major problem during this method was the dry premixing of the polymers with the minerals. Both polyesters were supplied in pellet

form, whereas the fillers were in powder form. It is obvious that it was not easy to obtain good mixing and feeding in the extruder due to segregation and the small size of the feed throat. For these reasons, the polyesters had to be ground. A grinder operating under liquid nitrogen was used to crush the co-polyester PST to a fine powder. This method was not applicable to the polylactic acid, given the high toughness of the material; thus, only melt extruded PLLA was used as control in some characterization experiments, whereas PLLA melt composites were not produced. The designation and composition of the biocomposites are described in Table 3.3.

4.2 Characterization of Composites

4.2.1 Differential Scanning Calorimetry

Table 4.1 contains DSC data for the PLLA and its composites. In the absence of unfilled PLLA sample prepared in solution, one would expect that unprocessed PLLA-pel and perhaps PLLA-melt samples could be used as comparative controls to the PLLA-S1 and PLLA-S2. However, such comparison would be only valid during the second heating scan when the prior thermal history is expected to be substantially erased.

Table 4.1 Thermal Data for PLLA and its Composites

	1st Heating			Cooling	2nd Heating			
Sample Description	T_g (^{0}C)	T_{cc} (^{0}C)	T_m (^{0}C)	T_c (^{0}C)	T_g (^{0}C)	T_{cc} (^{0}C)	T_m (^{0}C)	Heat of fusion* (J/g)
PLLA-pel	63.44	126.33	164.22	-	62.28	-	163.20	0.29
PLLA-S1	60.34	105.18	159.31	-	55.07	118.09	155.03	16.33
PLLA-S2	46.60	80.93	155.01	-	56.26	112.16	158.00	25.91
PLLA-melt	63.90	114.16	164.63	-	61.94	114.95	163.82	26.23

* After normalizing for 30wt% filler content.

During the DSC heating experiments up to 210^{0}C, the decomposition temperature of hydrotalcite has been exceeded and decomposition products such as water may interact with PLLA initiating degradation. This degradation, and molecular weight reduction, may have affected the crystallization characteristics and be responsible for the lower T_g of PLLA in the two composites, during second heating as well as the lower T_m. Coated hydrotalcite seems to increase somewhat T_g and T_m versus its uncoated version and shift the cold crystallization temperature to lower values. The polymer in the coated hydrotalcite sample PLLA-S2 seems to have the same crystallinity as the unfilled melt sample, whereas the uncoated appears to prevent full crystallization of the polymer in sample PLLA-S1. Both unfilled PLLA samples seem to have the same T_g and T_m values, although % crystallinity in the PLLA-pel is much lower suggesting that the thermal history of the pellets may not have been fully erased.

Table 4.2 contains DSC data for PST and its composites. During the DSC first heating experiments up to 120^{0}C, the samples do not appear to have any significant

differences. There are small differences that may be due to the different sample weight at the beginning of the experiment, and to degradation that possibly occurred during sample preparation. It was noted that when the starting weight of the sample was higher than about 3.0 mg, the DSC curve tended to shift to higher peak temperatures.

Table 4.2 Thermal Data For PST And its Composites

	1st Heating			Cooling	2nd Heating			
Sample Description	T_g (^{0}C)	T_{cc} (^{0}C)	T_m (^{0}C)	T_c (^{0}C)	T_g (^{0}C)	T_{cc} (^{0}C)	T_m (^{0}C)	Heat of fusion* (J/g)
PST-pel	-	81.50	96.70	43.25	-	88.00	94.64	45.84
PST-S1	-	80.00	95.84	35.45	-	75.32	94.30	45.21
PST-S2	-	78.48	94.83	38.93	-	76.70	94.36	44.44
PST-melt	37.82	79.50	95.43	39.33	-	76.30	95.76	51.74
PST-M1	51.98	79.66	95.11	39.83	-	76.66	94.92	47.99
PST-M2	40.47	78.95	95.24	39.71	-	76.96	95.26	56.34

*After normalizing for 30wt% filler content.

Similarly to the PLLA samples, after the second heating of the PST samples and their composites the thermal history of the polymers (with the exemption of the T_{cc} value of the unfilled unprocessed PST-pel) appeared to be fully erased. In all cases T_g was not detectable. The type of the hydrotalcite does not affect, in general, the T_{cc} or T_m of the polymer present for either the solution, or the melt prepared samples. The heat of fusion for samples PST-S1 and PST-S2 does not change significantly. Coated hydrotalcite in the melt-processed samples appears to enhance crystallization producing even higher crystallinity than the unfilled PST-melt. In conclusion, no major changes in the properties of all PST samples could be detected by the DSC experiments.

The DSC thermograms for all the polymers and composites can be found in Appendix A.

4.2.2 Thermogravimetric Analysis

Figures 4.1, 4.2 and 4.3 show the results of the TGA experiments, whereas Table 4.3 summarizes the results for all the samples used during these experiments. Both uncoated and coated hydrotalcites show a very similar degradation between losing first bound water and then water and CO_2 up to 500^0C, where a predominantly Al/Mg silicate residue is remaining, according to information provided by Kyowa Chemical Industry Co., Ltd. With respect to PLLA (Figure 4.1), at 200^0C the unfilled polymer and its composites seem to be very stable, although for the PLLA-S2 composite there is a trend for more degradation than for the PLLA-S1. This trend seems to be confirmed at 300^0C where the coated hydrotalcite appears to affect the thermal/hydrolytic degradation of PLLA more than the uncoated one. At 300^0C both composites suffer severe weight losses not corresponding to the observed lesser weight losses of their individual compounds at the same temperature. Finally, at 500^0C the presence of the uncoated hydrotalcite appears to promote less weight loss to the composite than the coated one.

With respect to PST (Figures 4.2 and 4.3), at 200^0C unfilled polymer and both melt and solution composites seem to be very stable. By contrast to the PLLA composites, PST composites suffer much less weight loss at 300^0C. At 300^0C, the uncoated hydrotalcite appears to catalyze slightly more than the coated one the thermal degradation of both types of PST composites. This is not confirmed at 500^0C, where the trends for the two hydrotalcites in the PST composites, appear to be reversed.

At this temperature both the polymeric matrices have been totally degraded and the residue is, in most cases, consistent with the inorganic components remaining in the hydrotalcites. In the absence of detailed information on the type and amount of stearate coating, and the method of its applications, it is difficult to speculate on the observed different effects of the two grades of hydrotalcite on the TGA results.

Table 4.3 TGA Weight Change Data at 200^{0}C, 300^{0}C and 500^{0}C

	Weight Change (%)		
	200^{0}C	300^{0}C	500^{0}C
PLLA-pel	99.77	98.87	1.140
PLLA-S1	96.19	41.61	22.05
PLLA-S2	92.69	34.62	19.71
PST-pel	99.78	99.23	0.69
PST-S1	98.97	88.93	31.41
PST-S2	99.07	90.25	21.80
PST-melt	99.77	99.07	0.29
PST-M1	99.08	88.88	26.89
PST-M2	99.32	92.38	18.79
HT-U	92.95	81.32	59.90
HT-C	93.87	81.80	59.02

In summary, the presence of hydrotalcites in the PLLA matrix promotes significant polymer weight losses in the temperature region 200-300^{0}C; this is in contrast to the small weight losses of the PST composites in the same temperature region, which correspond to a large extent to the weight losses of the individual compounds. This may be partly due to the higher hydrolytic stability of the PST, presumably resulting from its chain extended block copolymer structure. The effect of the degradation products on the hydrotalcite on such a structure appears to be less pronounced than in the case of PLLA.

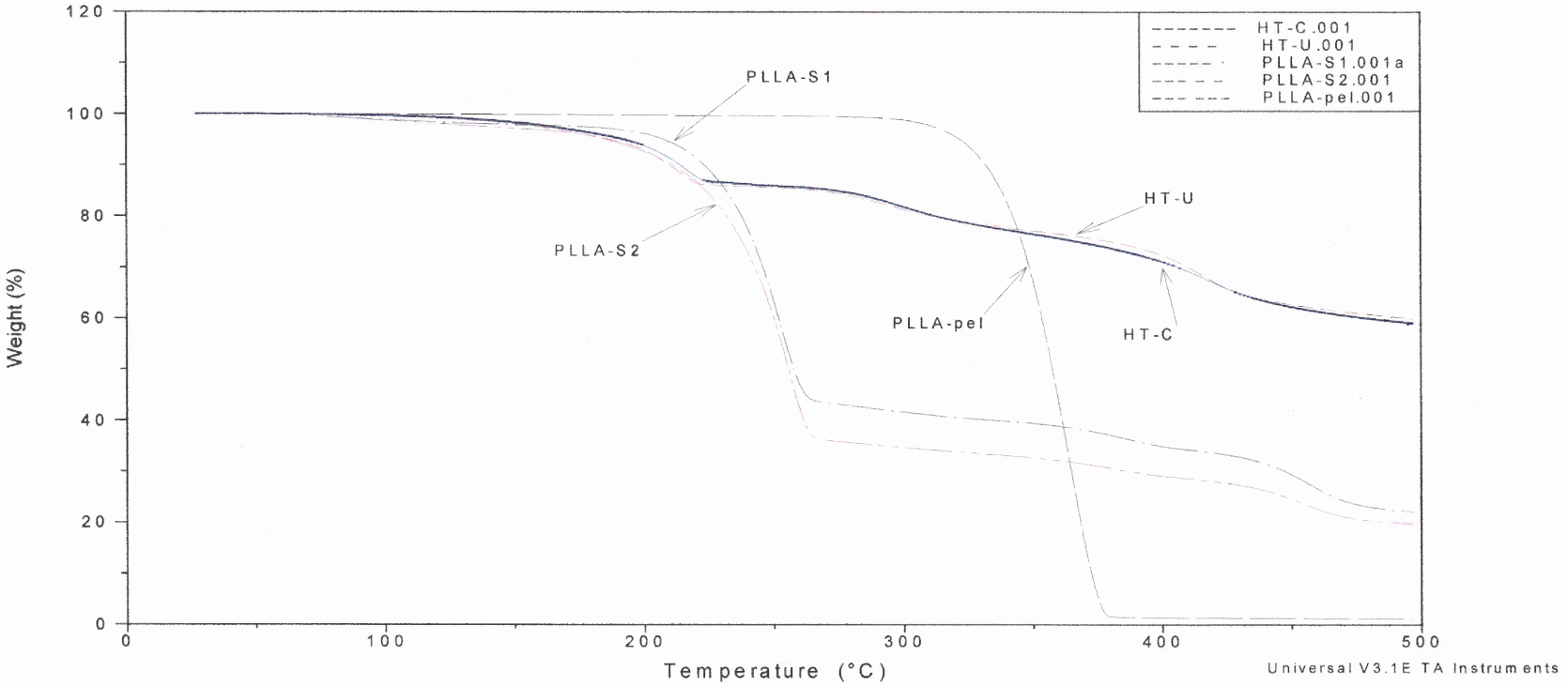

Figure 4.1 Combined TGA curves of hydrotalcite fillers, PLLA pellets, and composites prepared by solution mixing, at 10^0C/min under nitrogen.

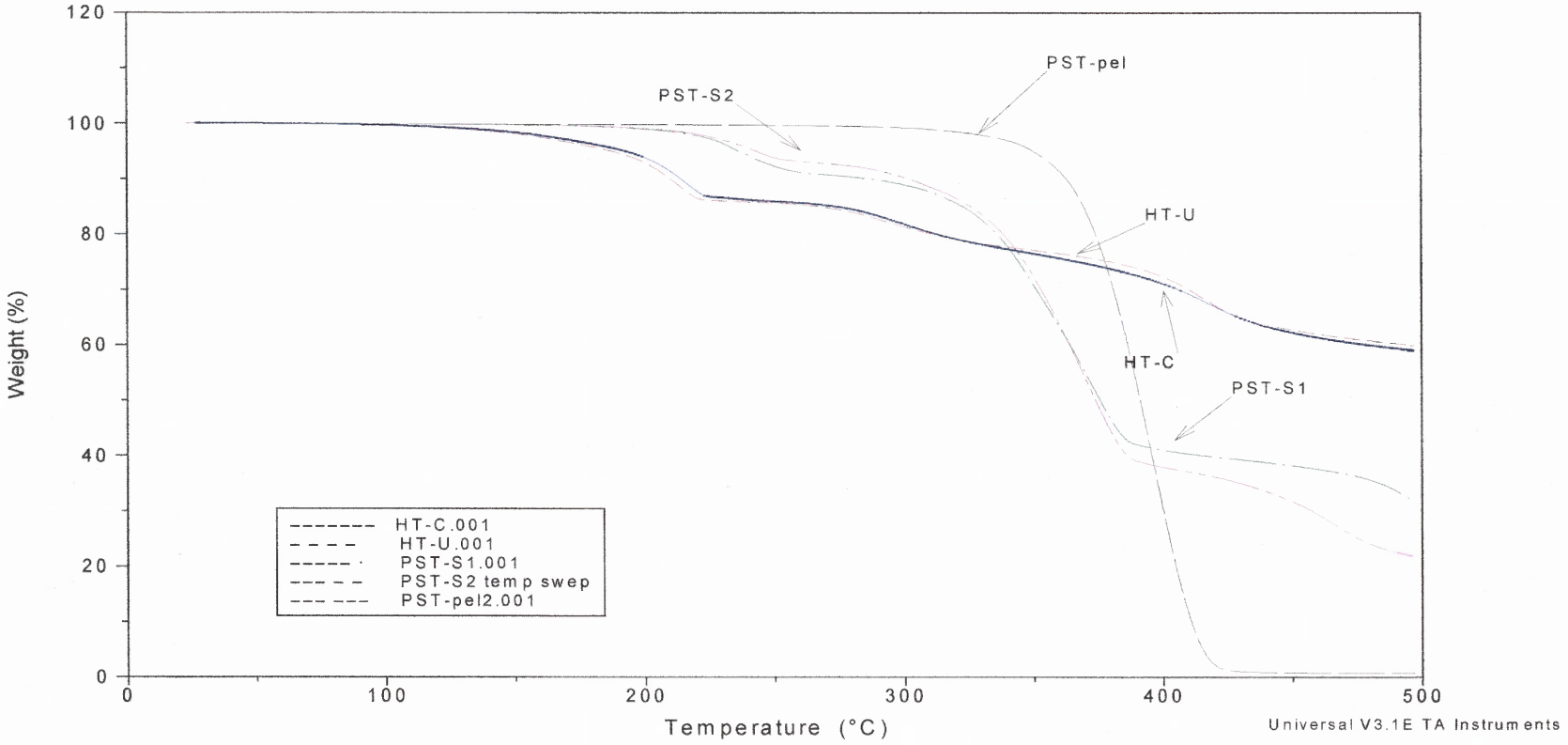

Figure 4.2 Combined TGA curves of hydrotalcite fillers, PST pellets, and composites prepared by solution mixing, at 10^0C/min under nitrogen.

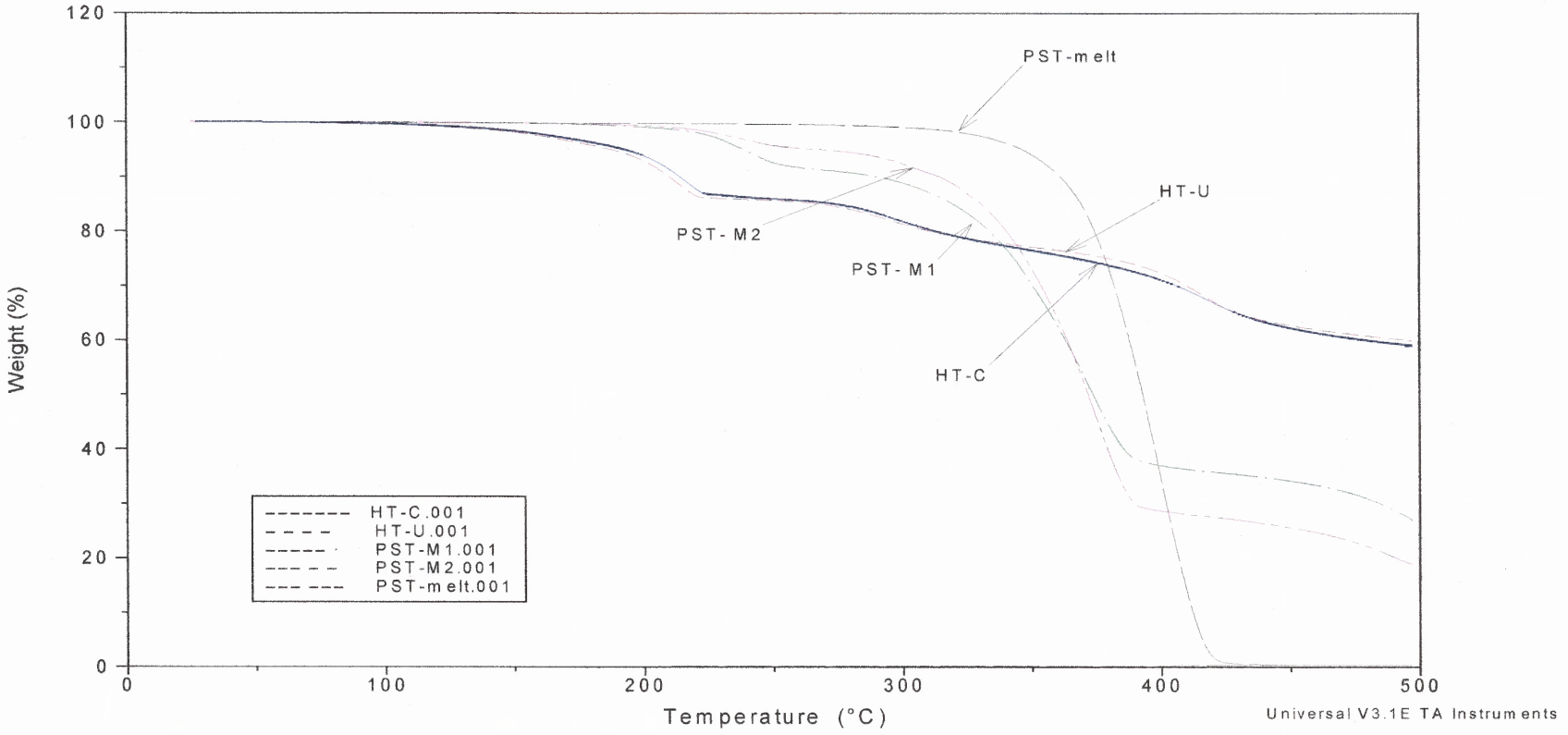

Figure 4.3 Combined TGA curves of hydrotalcite fillers and PST polymer and composites prepared by melt processing, at 10^0C/min under nitrogen.

4.2.3 Melt Rheology

Melt rheology data were obtained only for PST and its composites. There was an attempt to obtain melt rheology data for PLLA and its composites, but this could not be accomplished since PLLA samples did not have a stable torque over time, possibly due to their continuing degradation.

The rheology experiments for PST samples were initiated with a shear rate sweep at 130^0C. The ones that resulted to a relatively stable torque were those run at shear rates of $2s^{-1}$ and $5s^{-1}$. The resulting graphs can be found in Appendix B. After all the rheology data were collected for the PST samples, statistical analysis appeared to be necessary due to time dependent variations. Values for Coefficient of Variation (CV) were necessary, in order to measure reliability of the measurements. More than 29 values for the viscosity, during the first 100 sec of the experiment were used to calculate the average value (AVR) and standard deviation (STDEV), as follows:

$$STDEV = \sqrt{\frac{n\sum x^2 - (\sum x)^2}{n(n-1)}} \qquad (4.1)$$

The values for CV were calculated by the following equation:

$$CV = \frac{STDEV}{AVR} \times 100 \qquad (4.2)$$

Table 4.4 contains melt viscosity data of PST and its composites at two different shear rates, $2s^{-1}$ and $5s^{-1}$. All polymer composites are typically non-Newtonian with the melt processed PST-M2 showing higher shear sensitivity. Polymer alone does not seem to degrade at all during measurements, as shown by the very low CV values. The inorganic minerals increase at about 3.5 to 4 times the melt viscosity of the matrix, as expected theoretically and shown experimentally by many authors. At these low shear rates flake orientation is not expected; such orientation could bring the viscosity of the filled system closer to that of the matrix. There is no significant difference between the PST-S1 and PST-S2 in terms of viscosity values, although there is a trend for the melt viscosity of PST-S2 to be higher than that of PST-S1, at both shear rates. For the unfilled system, PST- melt has a lower (4.5%) viscosity than PST-pel as anticipated, based on possible slight thermomechanichal and hydrolytic degradation expected to occur during extrusion in the absence of nitrogen blanket. It also appears, based on statistical analysis, that PST-M2 is less stable than PST-S2, during the steady shear measurements.

Table 4.4 Melt Viscosity Data for PST and its Composites at Different Shear Rates

Sample Designation	**Melt Viscosity at 130^0C (Pa · s)**	
	$2s^{-1}$	**$5s^{-1}$**
PST-pel	-	615 (CV=1.0%)
PST-S1	3136 (CV=11.5%)	2140 (CV=9.5%)
PST- S2	3513 (CV=10.0%)	2542 (CV=10.3%)
PST- melt	-	589 (CV =1.8%)
PST-M2	2643 (CV=17.4%)	1557 (CV=20.3%)

4.3 Long Term Degradation Studies

The degradation experiments were performed *in vitro* in the presence of a phosphate buffered saline solution, and the results were compared with structural and chemical changes from the short-term characterization tests. All samples of unfilled polymers and their composites were tested in triplicate, and graphs of percentage weight change versus time were obtained. The percentage weight change is given by the following equation:

$$\%\Delta W = \frac{W_t - W_0}{W_0} \times 100 \qquad (4.3),$$

where W_t, is the sample weight at time t and

W_0, is the initial sample weight

In addition, pH measurements were taken to determine if the minerals had any acid neutralizing capacity towards the acidic low molecular weight fragments formed during the polyester hydrolytic degradation. Furthermore, the buffer solution after 139 days immersion of one of the PLLA composites was analyzed for Al and Mg content by Inductive Coupled Plasma Analysis, ICP, to examine if elements had passed from the hydrotalcite composites to the buffered solution. Lastly, for observation of any morphological changes on the surface of selected composites, SEM microphotographs were taken before and after 21 days immersion in the phosphate buffered solution.

4.3.1 Physical and Chemical Changes

It is well known that the molecular weight of the polymer plays an important role to its swelling. There are also other significant parameters such as the method of polymer processing, and the thermal history of the disc samples, which may change the molecular weight or the molecular weight distribution of the polymer. The existence of monomers or oligomers in the polymer sample, which may be responsible for the flexibility of the chain and the higher hydrophilicity of the polymer, is also important. Lastly, the carboxyl groups present in the polymer matrix catalyze the hydrolysis reaction.

According to Zhang et al. (1993) and Ming et al. (1990), the swelling development of an unfilled polymer follows two stages. During the first stage, the disc samples swell as a result of water penetration, and hydrolysis of the ester bonds takes place. When the first stage is over, hydrolysis involves additional penetration. The water acts as a plasticizer and the polymeric chains become more flexible, which result to a lower glass transition temperature. In this way, the discs are more sensitive to degradation. In particular, their surface becomes more prone to degradation than their nucleus. Carboxyl groups, which are present on the polymer surface, promote hydrolysis, so degradation rate rises and molecular weight decreases. The diffusion rate of degradation by-products that are formed inside the system is slower, and as a result they become entrapped into the sample. Consequently, more carboxyl groups exist in the center of the system and the hydrophilicity of the matrix is higher, resulting to higher water absorption. In addition to lower molecular weight, molecular weight distribution is broader and a second peak of lower molecular weight fragments may appear. As a result of the second swelling stage, the rate of swelling increases again.

Generally, after the initial swelling stage of the unfilled polymers and their composites (during which each sample has a different degree of swelling) a pseudo-equilibrium takes place for a limited time period, where the rate of swelling and the degradation rate become equal. After that, the degradation rate is high in both the surface and the nucleus. The polymeric matrix does not have the same structural characteristics as before, and a significant change to the molecular weight and the molecular weight distribution appears. Finally, the weight loss due to erosion prevails over the weight increase due to swelling, resulting in the overall sample weight loss.

It is worth mentioning that degradation behavior would also depend on the shape and the size of the disc, the pH of the solution and the temperature. The temperature used in this work is 37^0C, since composites for tissue engineering applications are investigated; in general, an increase in temperature would lead to higher degradation rates of the polymeric matrices.

In the case of the composites, shown in Figures 4.4 and 4.5, swelling and swelling rate are significantly higher, than those of the unfilled polymers. Figure 4.4 shows the degradation behavior of PLLA and its composites. An average value for $\%\Delta W$ of each sample, at every specific time was taken in order to obtain the degradation graph. It is evident that during the first days of the experiment, water uptake takes place, which leads to the swelling of the disc samples. This would result to the hydrolysis of the ester linkage and the subsequent degradation of the samples.

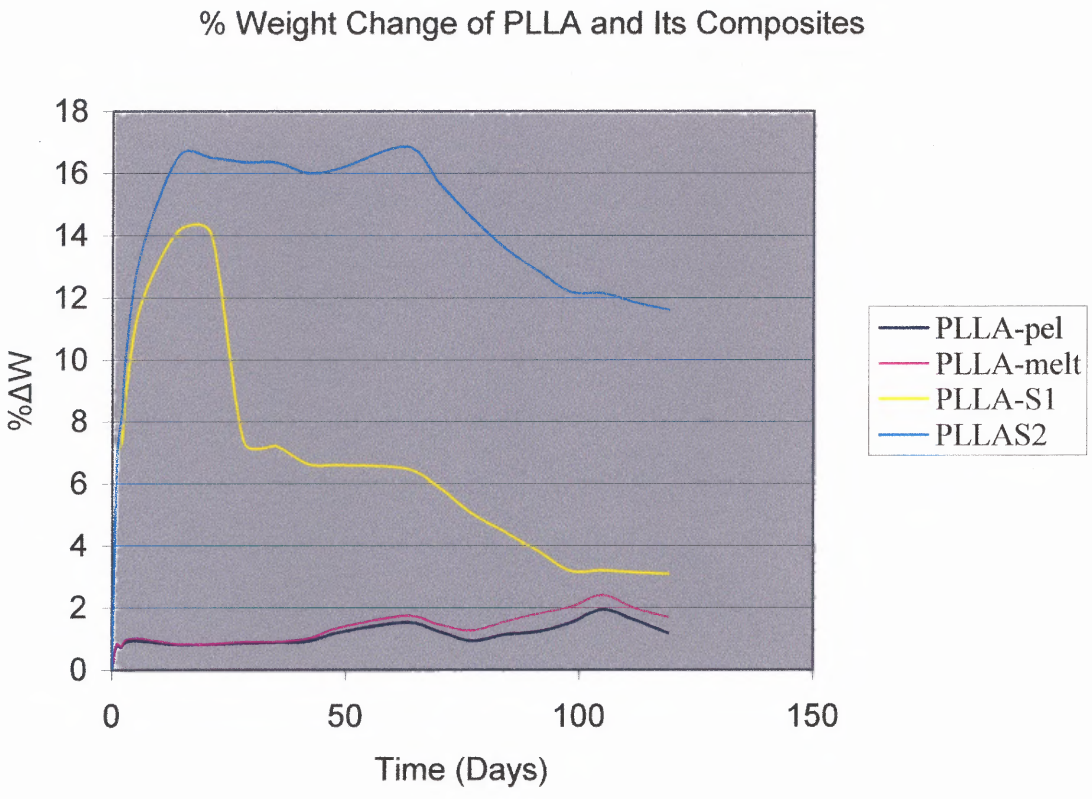

Figure 4.4 %Weight Change versus time for PLLA-pel, PLLA-melt and its composites produced by solution mixing.

Both unfilled PLLA samples appear to be fairly stable compared to the filled ones. There is some water uptake for the polymers alone, which after a long period of time (approximately 110 days) is followed by a downswing corresponding to the onset of hydrolytic degradation. The melt-processed sample appears to swell slightly more than the sample from the unprocessed pellets. This will lead to earlier degradation, as expected, since the extrusion process may have led to prior degradation and as a result to lower molecular weight samples. What is of a great interest though, is the behavior of the composites. Both PLLA-S1 and PLLA-S2 have high water uptake ability. The composites discs swell up to 17%, and according to Ming et al. (1990), water acts as a plasticizer and hydrolysis of the ester linkage of polylactic acid is dominant. It seems that

the coated hydrotalcite "attracts" water (in spite of its higher hydrophobicity due to the presence of stearate coating) which is being trapped to the system and consequently leads to swelling followed by degradation. It is of interest to note that the downswing of the curves for the PLLA-S2 composites, indicating the onset of matrix disintegration, occurs at about 75 days. At that time, the PLLA-S1 composite is undergoing its second significant downswing (the first having taken place after about 20 days).

Since PLLA samples appeared to degrade more than the PST ones, as will be shown below, it was considered important to further analyze one of the PLLA composites. A sample containing uncoated hydrotalcite was selected, due to the mineral apparent ability to enhance degradation. Elemental analysis showed that after 139 days of immersion in the PBS solution 225ppm of Mg were released from the disc to the solution. The amount of Al element that was released to the solution was less than 1 ppm. This does not correspond to the initial ratio of Mg and Al (4.0-5.0) in the hydrotalcite, and may be due to differences in the solubility of the acetate and phosphate salts in the analyzed fluid. The release of Mg may be beneficial since bioactive glass no. 13-93 used by Kellomäki et al. contained 5% MgO. Based on these results though, it is not possible to speculate on the possible formation of apatite type minerals that are known to be required for bone growth in tissue engineering applications.

A pH reading of the PBS solution taken after the same time period of 139 days showed a value of 6.94. If one considers that the initial pH of the PBS solution is 7.4 and during degradation, lower molecular weight acidic fragments could lower that significantly, the value of 6.94 may still be considered as very neutral. This is very

important for tissue engineering applications, where the pH has to remain in the physiological region of the human organism to avoid toxic effects.

Figure 4.5 shows % weight change of the unfilled PST samples and their composites after immersion in the PBS solution. Again the unfilled systems are the ones showing less weight change. However, the weight changes for the PST composites are much less than in the case of the PLLA composites. Hydrotalcite containing samples have relatively higher water uptake but their downswing behavior showing the onset of matrix degradation appears to occur after about the same time period (105 days) as for the unfilled matrix. Among the composites minor differences in weight changes are observed. The melt-processed composite containing the uncoated hydrotalcite, PST-M1, seems to swell a little more and also to have a steeper curve in the degradation regions compared to the others. In summary, PST samples did not show any significant degradation weight change, and as a result no further investigations were performed with respect to pH changes and release of elements in the PBS solution.

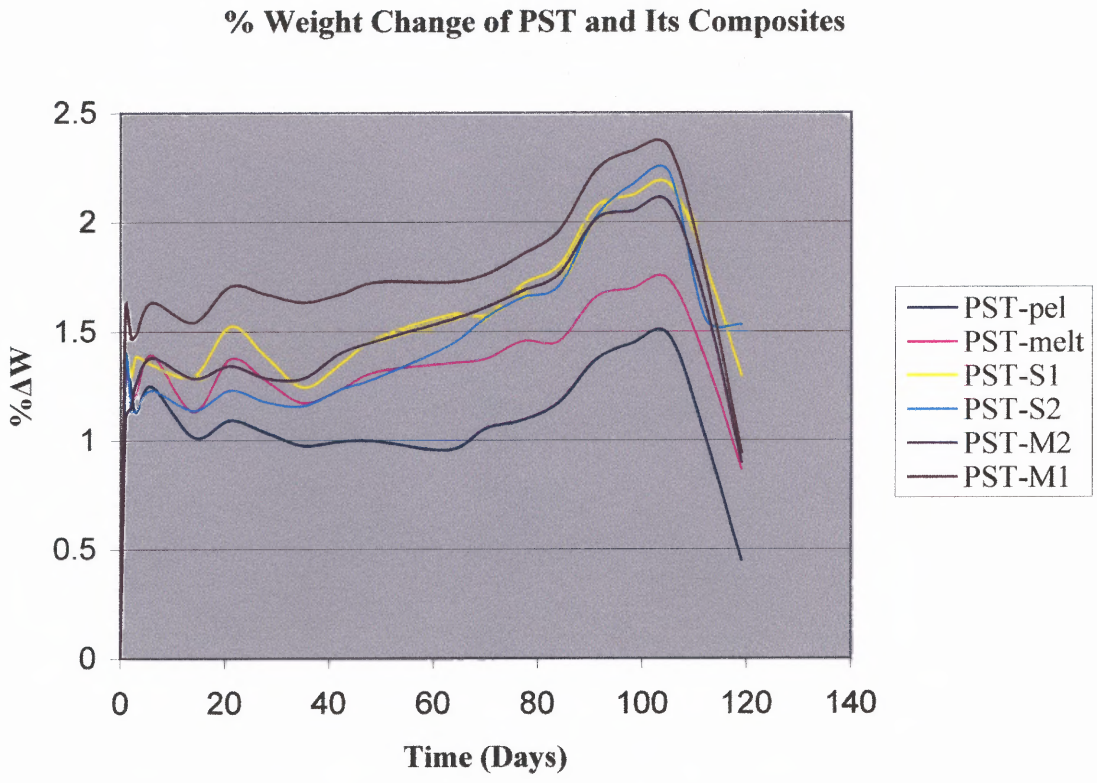

Figure 4.5 % Weight Change versus time for PST-pel, PST-melt and its composites produced by solution and melt mixing.

4.3.2 Morphological Changes

For reasons mentioned above, it was considered essential to observe morphological changes only for the PLLA composite samples, which appear to degrade more significantly than the PST ones. Therefore, SEM microphotographs were only taken for PLLA-S1.

Figures 4.6 to 4.11 are SEM microphotographs of PLLA-S1 before and after 21 days of exposure to the PBS solution. It is obvious that there is a significant difference in the surface morphology of the samples. Surface roughness is developed at certain locations in the composite that has been immersed in the buffer solution. Due to the

polymer water uptake ability, simultaneous degradation phenomena occurring in the polymeric matrix at other surface locations lead to the exposure of hydrotalcite particles to the solution. Hydrotalcite particles can clearly be observed in Figures 4.10 and 4.11, among degrading regions of PLLA, characterized by fibrillar morphology. It is believed that this fibrillar morphology is due to PLLA, but however, further analysis has to be done through elemental mapping. For comparison, Figures 4.12 and 4.13 show the morphology of hydrotalcite particles prior to their incorporation in the polymeric matrix. Both micrographs show lamellar structure of low aspect ratio. Exfoliation could produce flakes of much higher aspect ratio, comparable to those found in montmorillonite nanoclays.

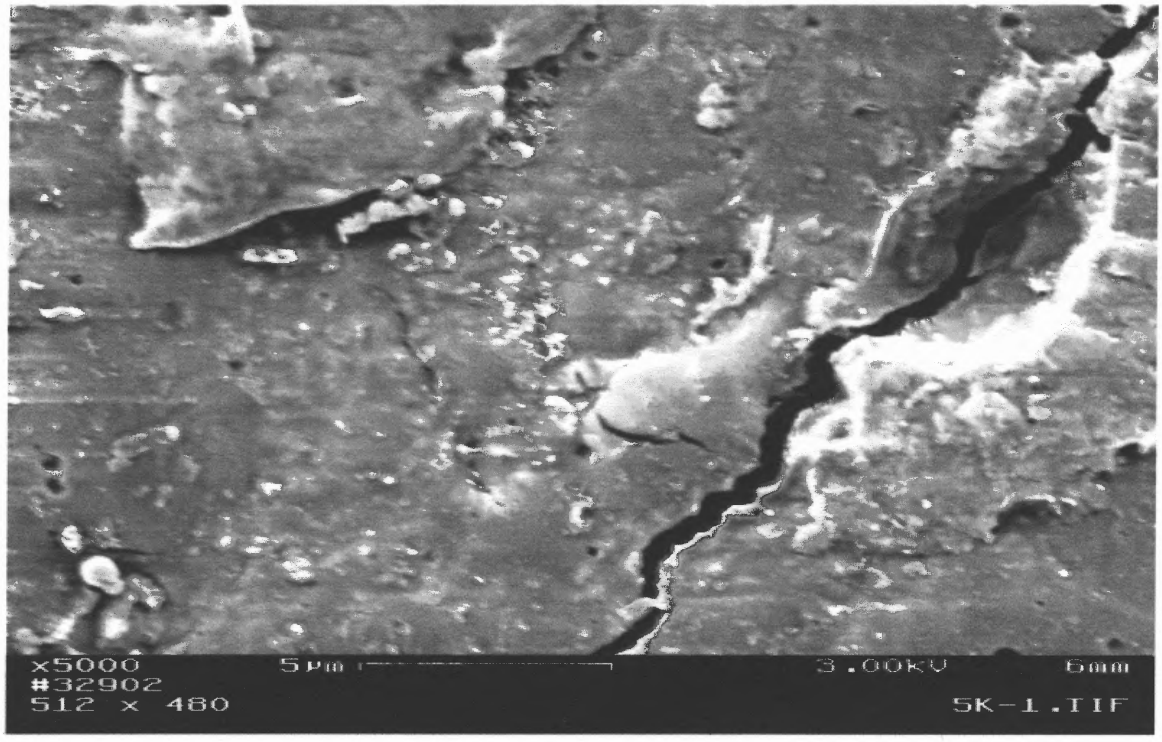

Figure 4.6 SEM micrograph of a PLLA-S1 sample surface before immersion in the PBS solution × 5000.

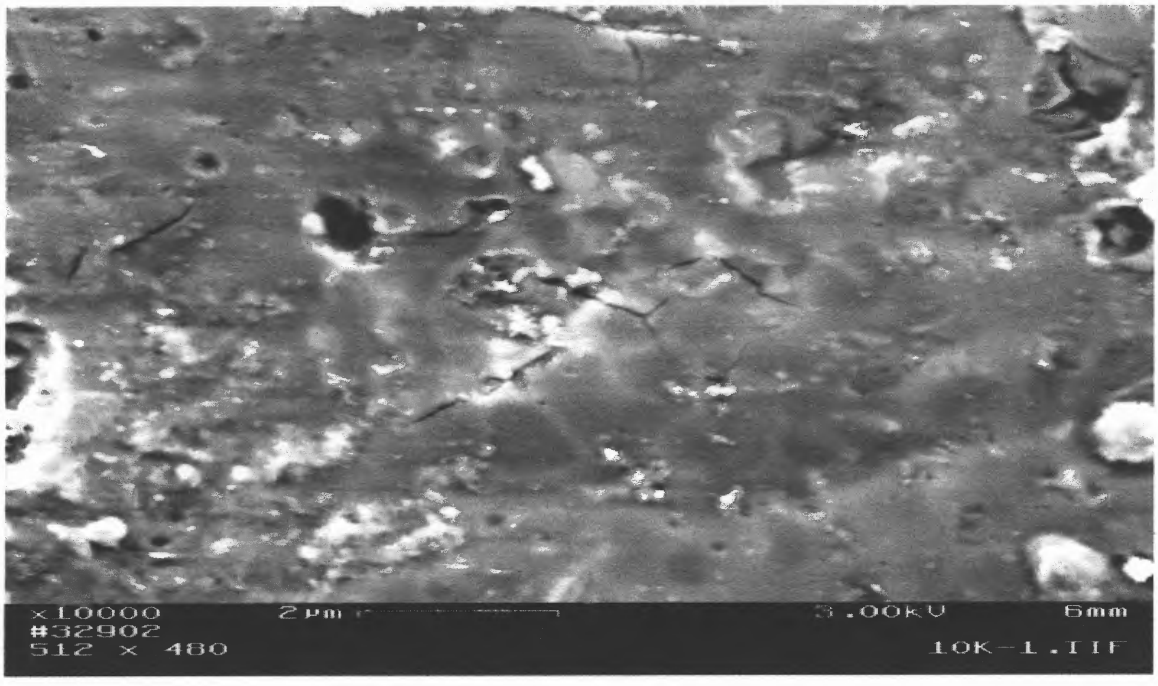

Figure 4.7 SEM micrograph of a PLLA-S1 sample surface before immersion in the PBS solution × 10,000.

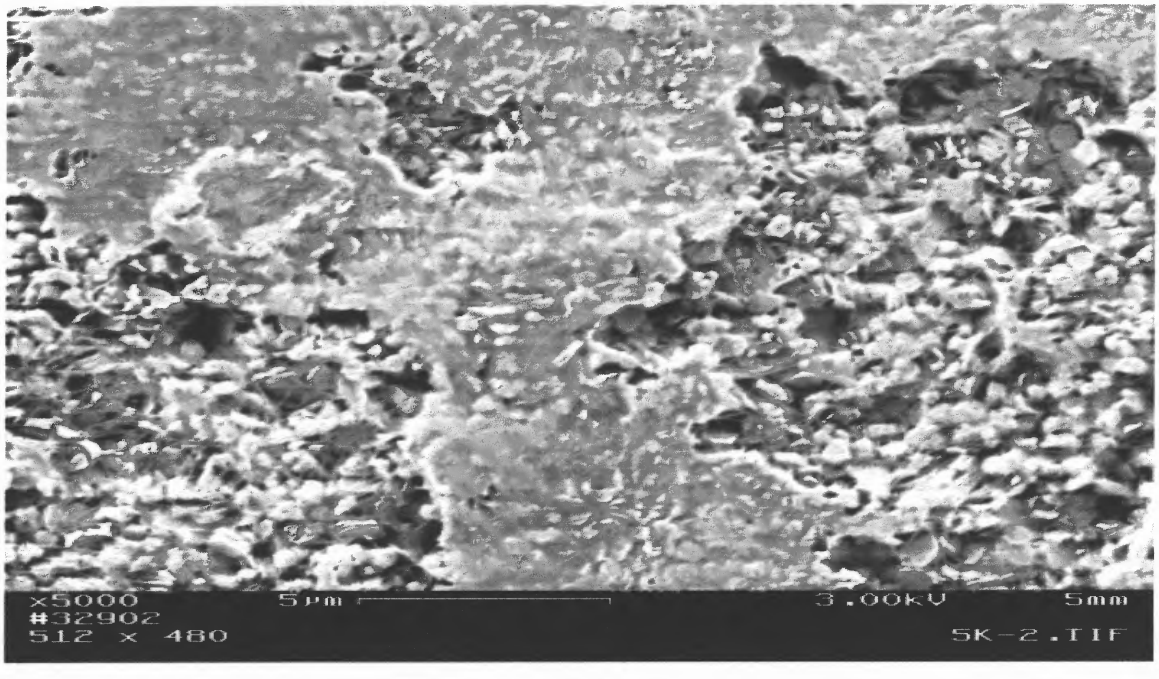

Figure 4.8 SEM micrograph of a PLLA-S1 after 21 days immersion in the PBS solution × 5,000.

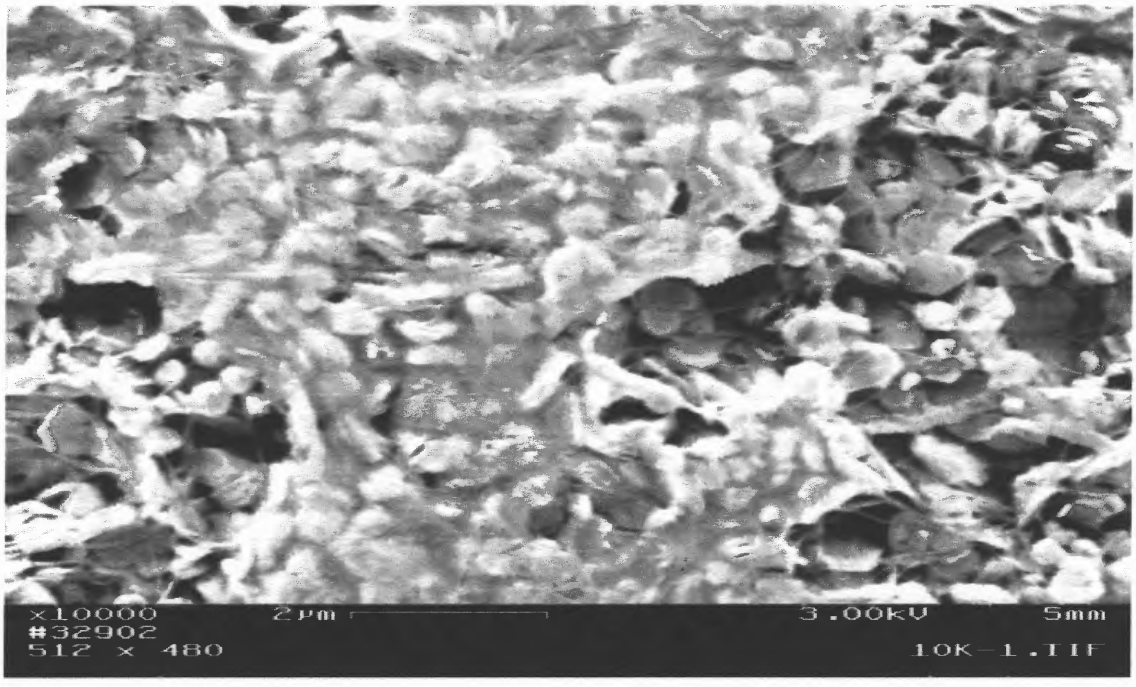

Figure 4.9 SEM micrograph at a higher magnification of the sample in Fig. 4.8 after 21 days of immersion in the PBS solution × 10,000.

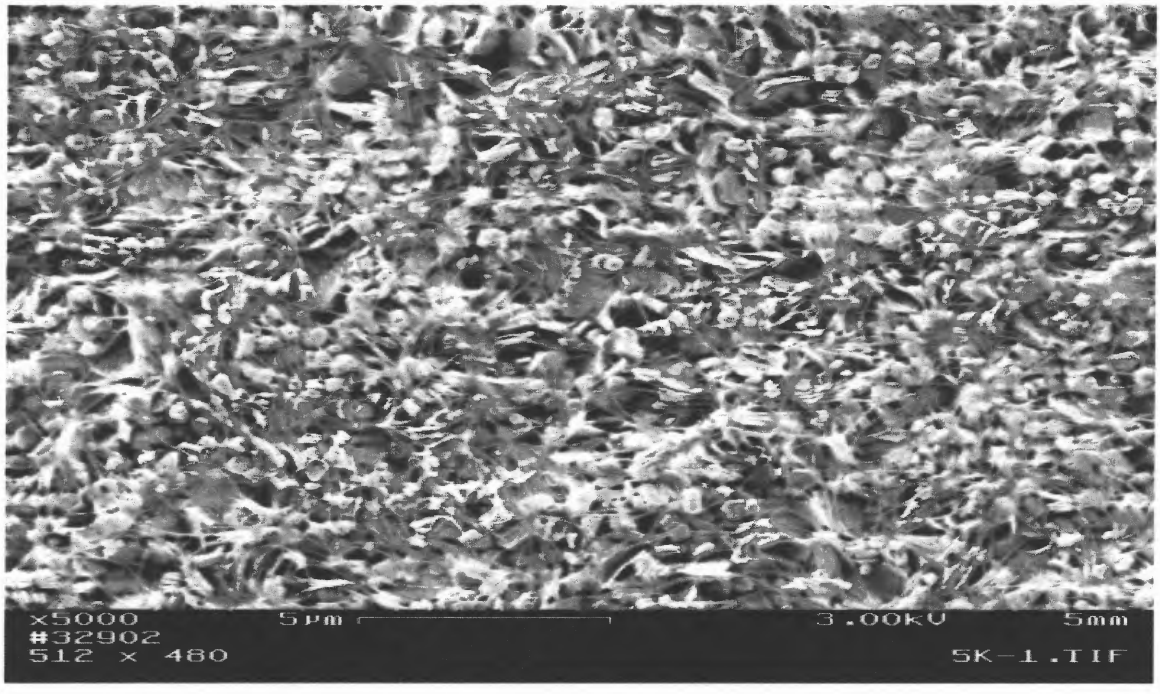

Figure 4.10 SEM micrograph of a different region of the sample in Fig. 4.8 after 21 days of immersion in the PBS solution × 5,000.

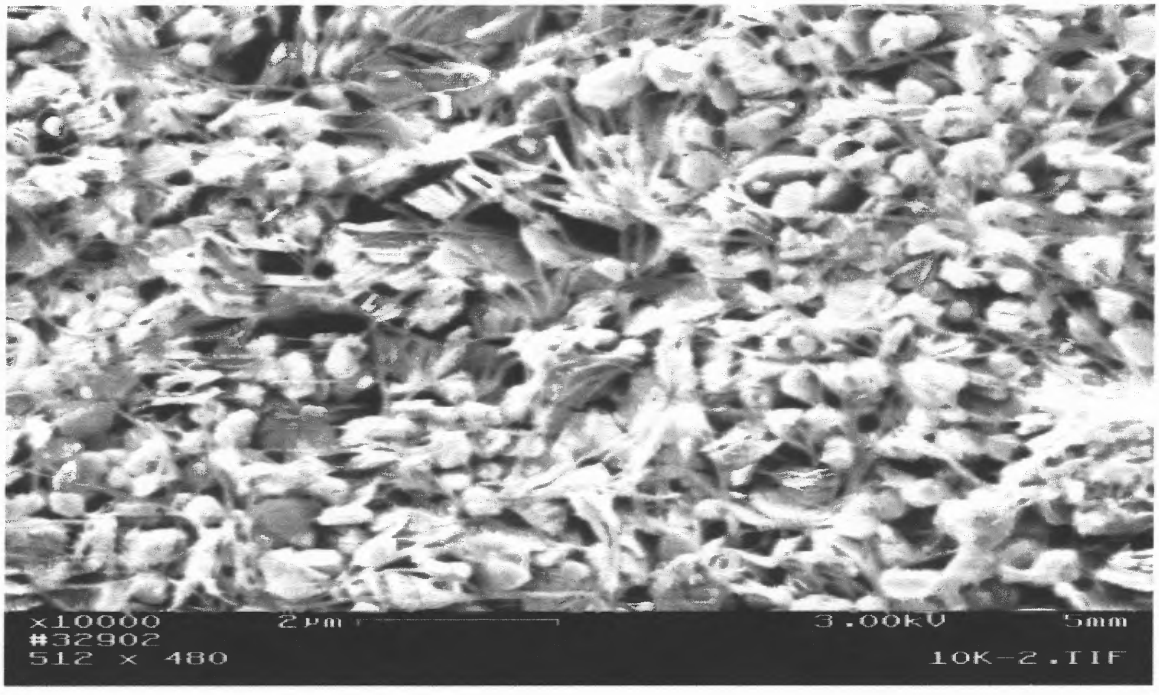

Figure 4.11 SEM micrograph of a different region of the sample in Fig. 4.8 after 21 days of immersion in the PBS solution at a higher magnification × 10,000.

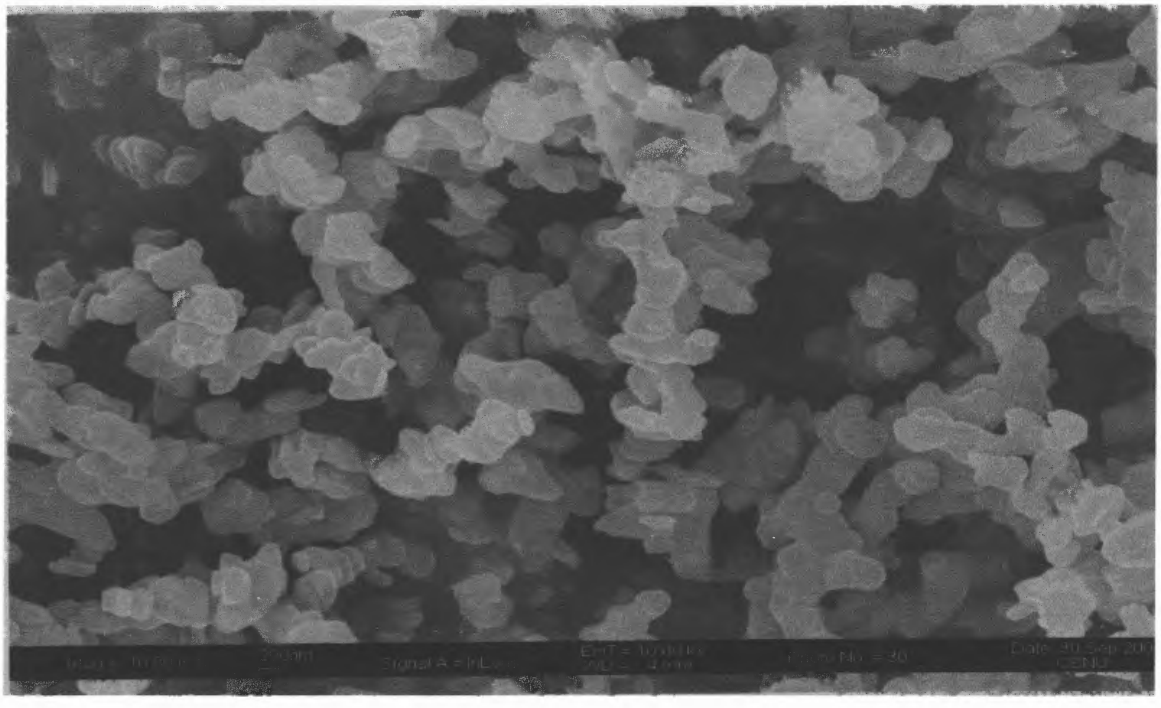

Figure 4.12 SEM micrograph of hydrotalcite particles × 10,000.

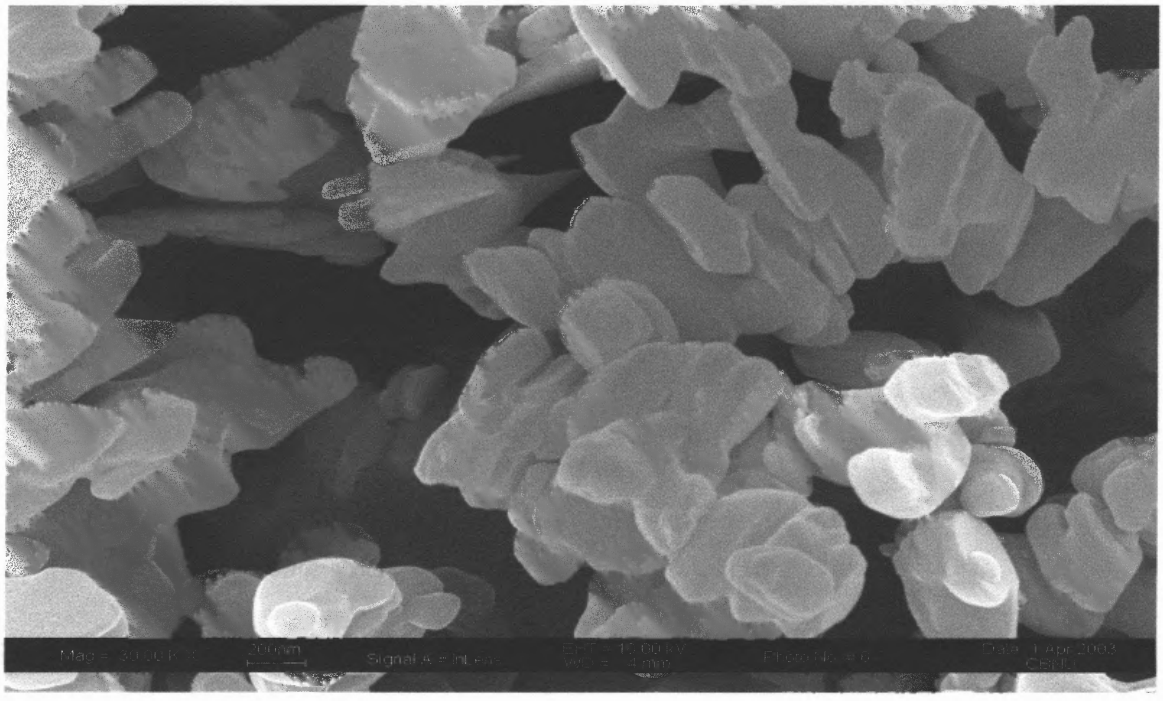

Figure 4.13 SEM micrograph of hydrotalcite particles × 30,000.

CHAPTER 5

CONCLUSIONS

The present work was initiated to explore the preparation and characteristics of a category of biomaterials used in tissue engineering applications, i.e. bioactive composites based on biodegradable polyesters reinforced with inorganic fillers. During the past two decades, significant interest has been developed in the area of such biocomposites. Systems based on biodegradable polymeric matrices and a variety of organic or inorganic fillers such as starch, glass ceramics, calcium phosphate salts and hydroxyapatite have been investigated by researchers. The necessity for improved and precise solutions in tissue engineering applications has led to biomaterials with improved mechanical properties, controlled degradation characteristics and bioactive capability. The latter refers to the ability of the biocomposites to promote an interfacial bond with the tissue that supports its regeneration, and is mostly related to the type of filler used.

The idea of using a synthetic inorganic mineral based on hydrated magnesium/aluminum carbonate, known as hydrotalcite, arose from results of the bioactivity shown by hydroxyapatite and certain glass ceramics. The intent was to provide alternative bioactive fillers in biodegradable composites that were to be used for bone growth and orthopedic applications. In addition to its reinforcing characteristics prior to the onset of polymer degradation, the inherent acid neutralizing capacity of hydrotalcite was expected to provide pH control during the stage of polymer degradation, which is usually accompanied by the formation of acidic low molecular weight components.

Two biodegradable polymers were used for the production of the composites, namely a thermoplastic polyester based on butylene adipate/succinate and polylactic acid. Two types of hydrotalcite fillers were used and compared in the present study; stearate surface coated and uncoated hydrotalcite. Composites were produced by solution and melt mixing techniques at a 30 wt% filler level. Unfilled polymer samples were also obtained for comparison studies. A 15 mm twin-screw extruder was used for melt mixing of the composites. It was not possible to obtain composites with polylactic acid by melt mixing because of difficulties in grinding PLLA pellets to a fine powder feed for the extruder and the lack of process stability of the polymer at the relatively high melt temperatures.

Significant differences were noted following characterization of the composites by DSC, TGA and melt rheology. Results varied depending on the type of polymer and hydrotalcite materials and the choice of processing methods. Long-term degradation experiments *in vitro* in the presence of a phosphate buffered saline (PBS) solution were performed, in order to compare any structural and chemical changes with results from the short-term characterization tests.

During the heating scans in the DSC experiments up to 210^0C for the unfilled PLLA and its composites, the decomposition temperature of hydrotalcite has been exceeded and decomposition products as water may have interacted with PLLA initiating degradation. This degradation may have affected properties such as T_g and T_m that appeared to be lower in the two composites during the second heating. In general, comparison between PLLA samples is only valid during the second heating scan when their prior thermal history has been substantially erased. The polymer with the coated

hydrotalcite seemed to have the same crystallinity as the unfilled melt sample; this is in contrast to the uncoated one in which the filler appeared to prevent full crystallization. In the absence of detailed information on the type and amount of stearate coating, and the method of its application, it is difficult to speculate on the observed different effects of the two grades of hydrotalcite on the DSC results.

Similar behavior of the PLLA composites was also observed in the TGA experiments. Up to 200^0C, both unfilled and filled PLLA systems were very stable, whereas starting at 300^0C, the hydrotalcites appear to catalyze thermal/hydrolytic degradation of the matrix. Composites appear to suffer severe weight losses compared to the unfilled systems, with only slight weight loss differences between the samples containing the coated and the uncoated minerals.

In the long-term degradation studies polylactic acid composites show higher % weight change than the unfilled samples. Unfilled PLLA samples show some swelling, but compared with the composites this is insignificant. Hydrotalcite promotes much higher swelling, hydrolysis and consequently degradation; this confirms the above short term results on its catalytic role on degradation due to its bound water and alkalinity. Additional studies in a composite PLLA sample, showed that 225 ppm of Mg and less than 1 ppm of Al were released from the disc sample to the PBS solution. Further investigation is needed to understand the release mechanisms of the hydrotalcite elements, as well as further *in vivo* studies to speculate on the formation of the apatite type minerals needed for bone growth applications. A pH reading equal to 6.94, after 139 days of immersion in the PBS solution, confirmed the expected neutralizing ability of the hydrotalcite, which is toxicologically desirable for tissue engineering applications. SEM

microphotographs were taken before and after 21 days of immersion in the PBS solution, showed significant degradation of the polymer with exposed hydrotalcite particles to the solution. The morphology of the surface was significantly different, as it appeared rough and fibrillar.

By contrast to the PLLA samples, PST samples did not show, in general, any remarkable degradation results and were not investigated to the point that the PLLA ones had. The type of hydrotalcite during DSC scans does not appear to affect the matrix properties in either the solution or the melt-processed samples. During TGA analysis, PST samples suffer much less weight losses compared to the PLLA ones and these mostly correspond to those of the individual compounds. Although reliable melt rheology data of PLLA composites are not available, PST composites show little or no degradation at short times (less than 100sec) at the low temperatures of 130^0C used. No significant differences were observed among coated and uncoated hydrotalcite containing composites. As far as long-term degradation studies are concerned, all samples showed a slight degradation in the PBS solution. Weight changes in the composites is not higher than 2.5%, which is very low compared to the 17% changes observed for the PLLA composites.

In summary, hydrotalcite minerals appear to be promising fillers in PLLA biocomposites with potential uses in tissue engineering applications, where degradation kinetics and good mechanical properties need to be coupled. Further *in vivo* experiments are recommended in order to investigate the bioactivity of the mineral as related to the release mechanism of Al and Mg and the formation of apatite type structures necessary for bone growth. In any case, the resulting composite materials could also be used for

other applications, where high rates of degradation are important, such as drug release applications.

APPENDIX A

DIFFERENTIAL SCANNING CALORIMETRY THERMOGRAMS

In this Appendix, DSC thermograms for all the unfilled polymers and their composites are presented.

Figures A.31 to A.36 present the DSC thermograms for samples PST-SN1 and PST-SN2. These samples were prepared the same way as the solution mixed ones with the difference that a 0.1 N methanolic KOH solution was added to the solution before the hydrotalcite. The concentration of the alkali was calculated based on the acid number of the resins. After several days, the resulting composites appeared to have degraded significantly as shown by the multiple peaks in DSC Figs A.31 to A.36. As a result no further investigation was performed.

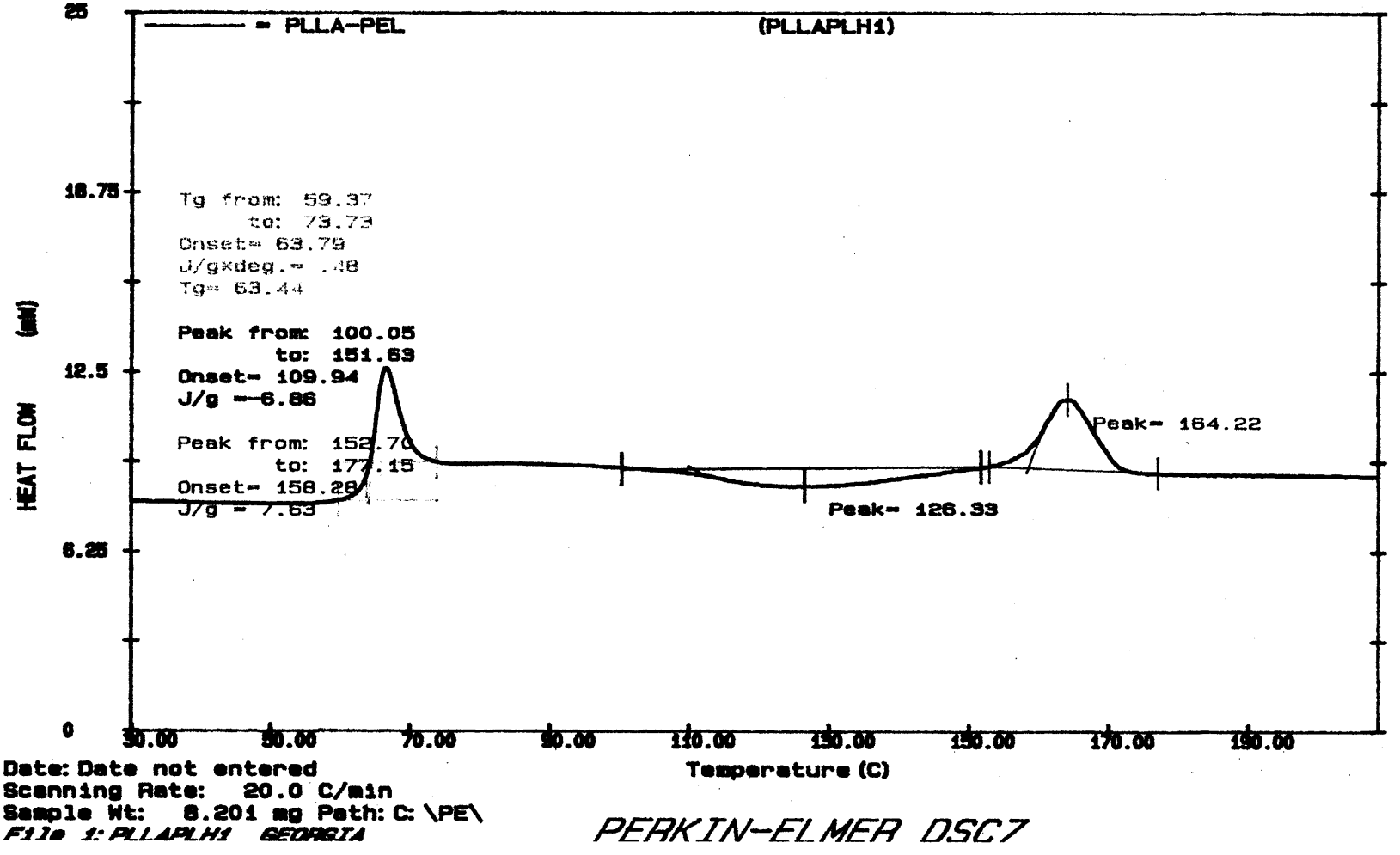

Figure A.1 DSC thermogram of PLLA pellets during the first heating scan.

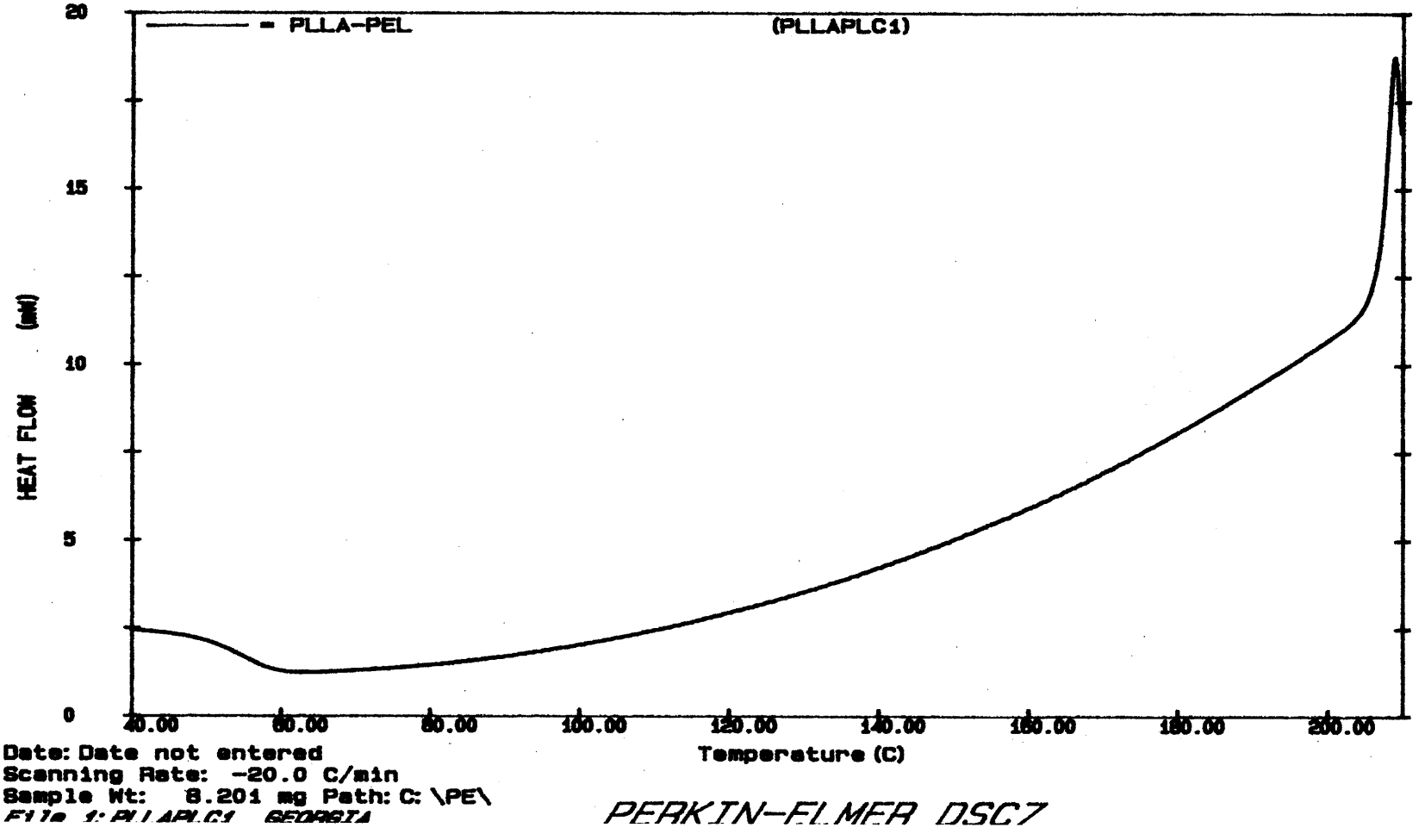

Figure A.2 DSC thermogram of PLLA pellets during the cooling scan.

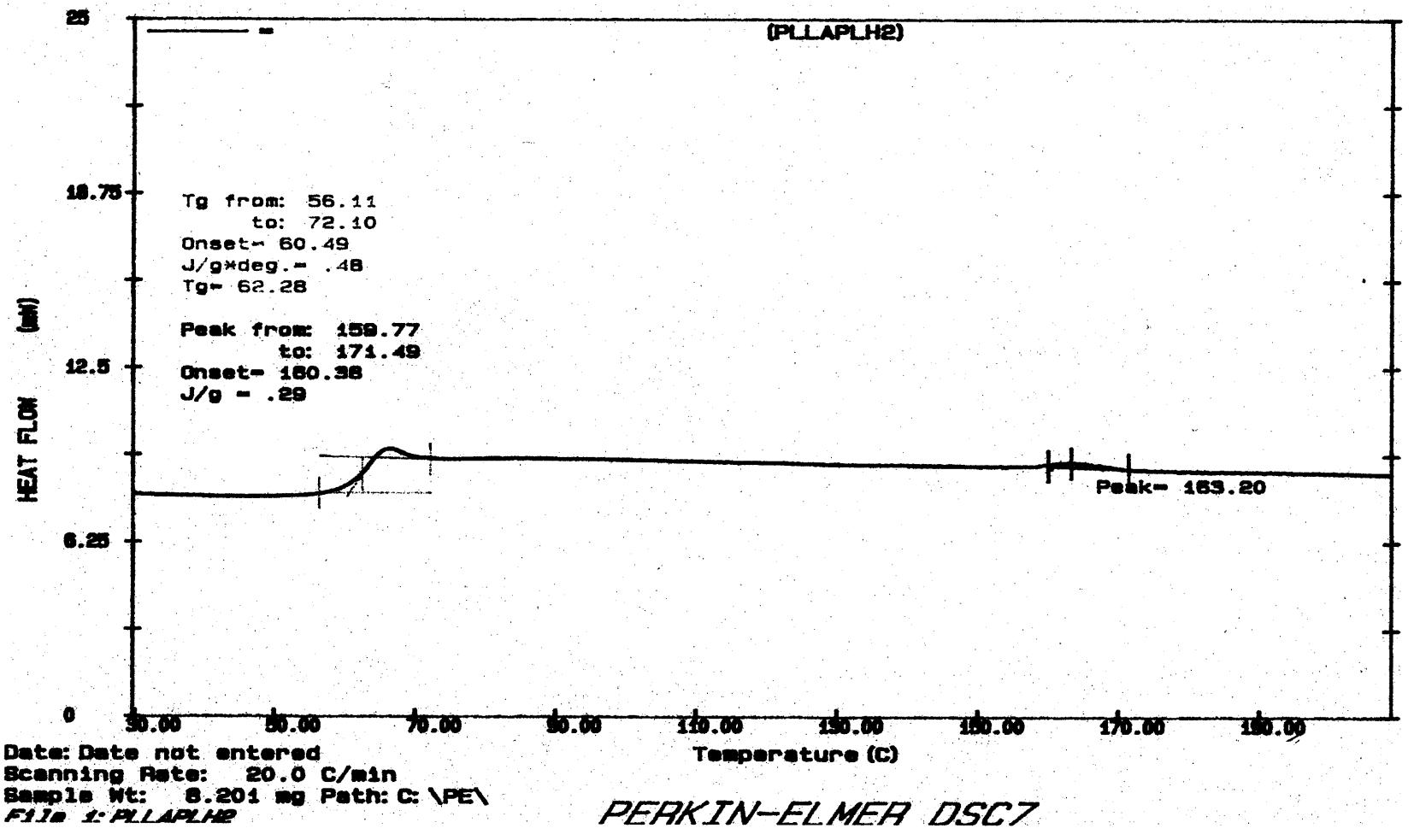

Figure A.3 DSC thermogram of PLLA pellets during the second heating scan.

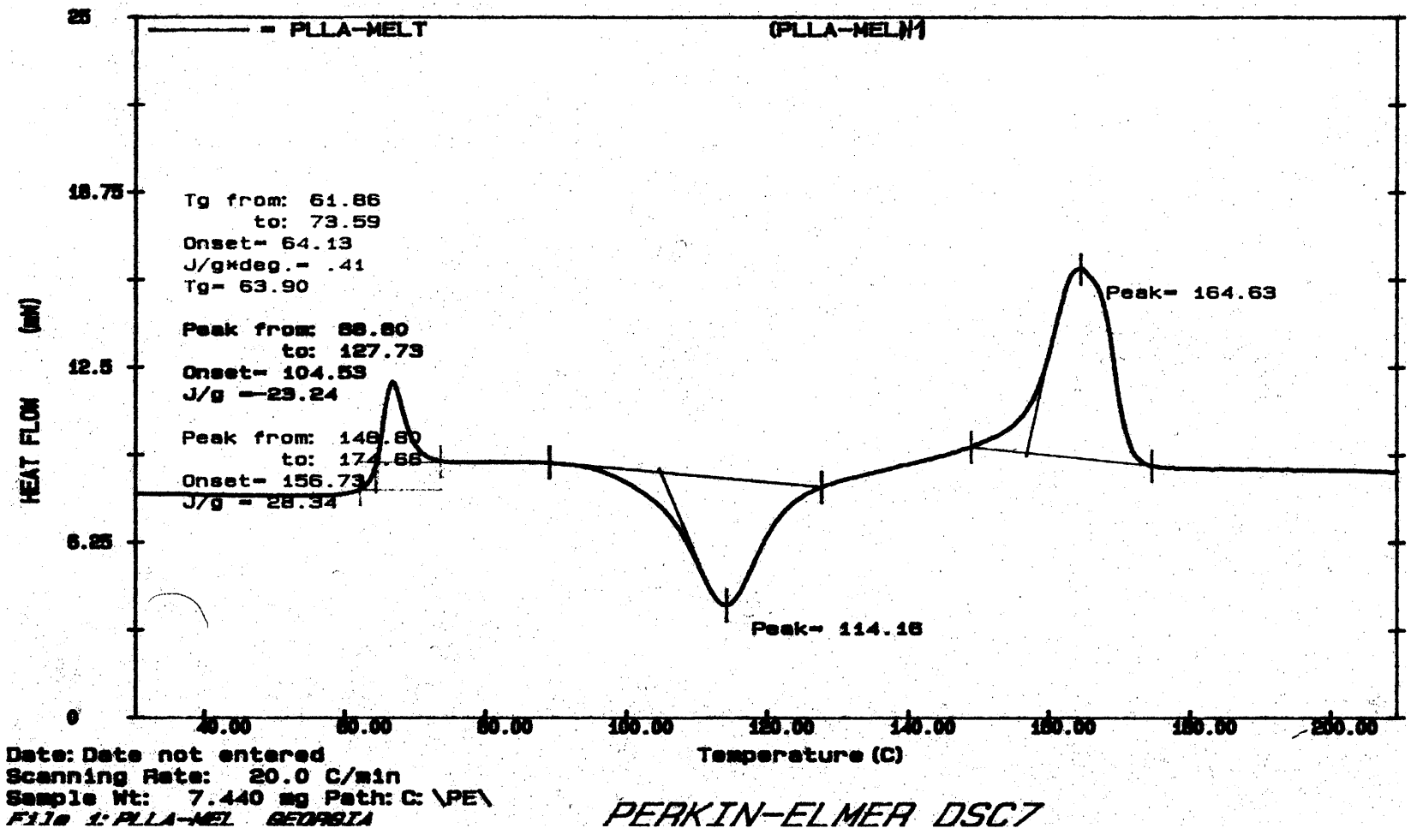

Figure A.4 DSC thermogram of PLLA-melt during the first heating scan.

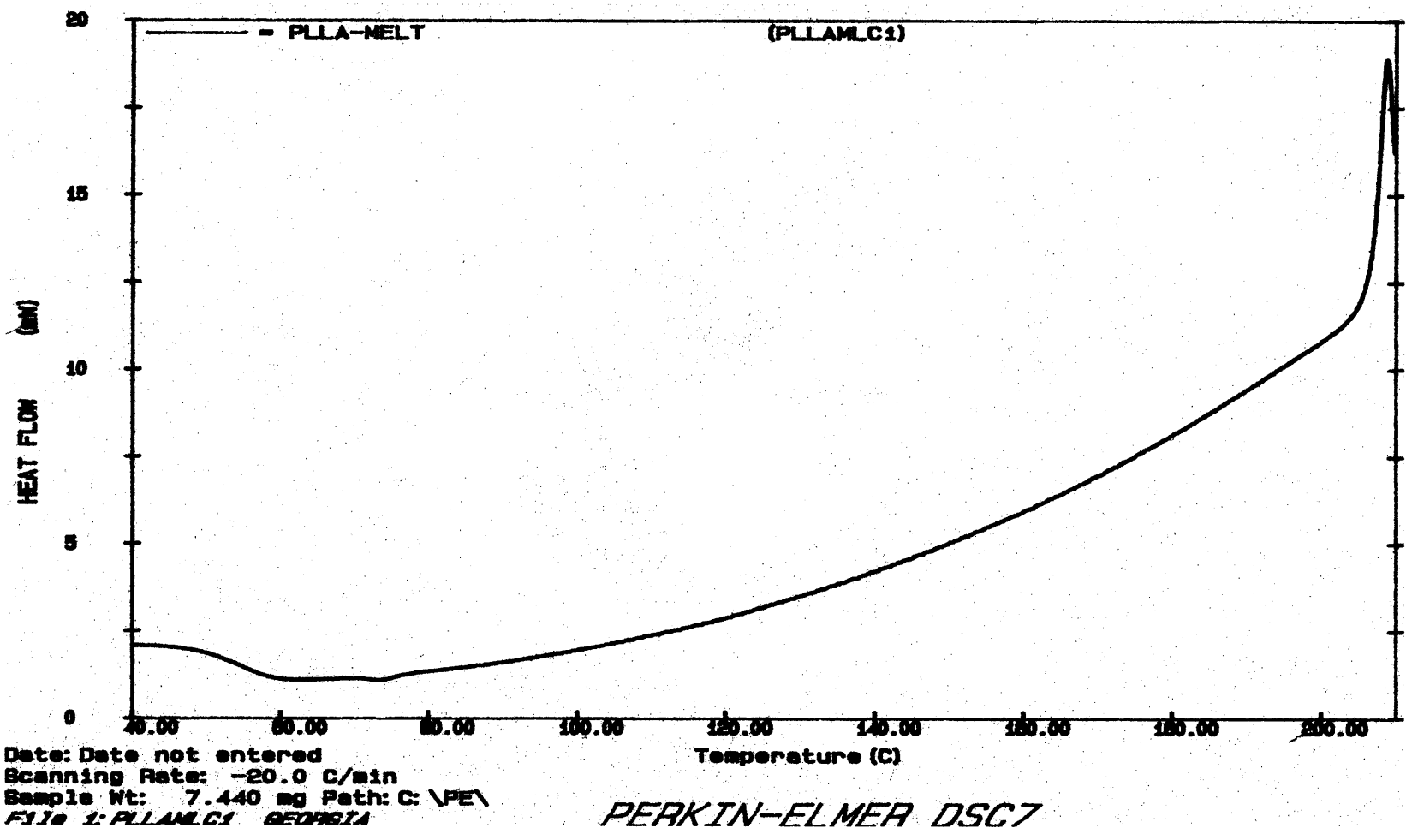

Figure A.5 DSC thermogram of PLLA-melt during the cooling scan.

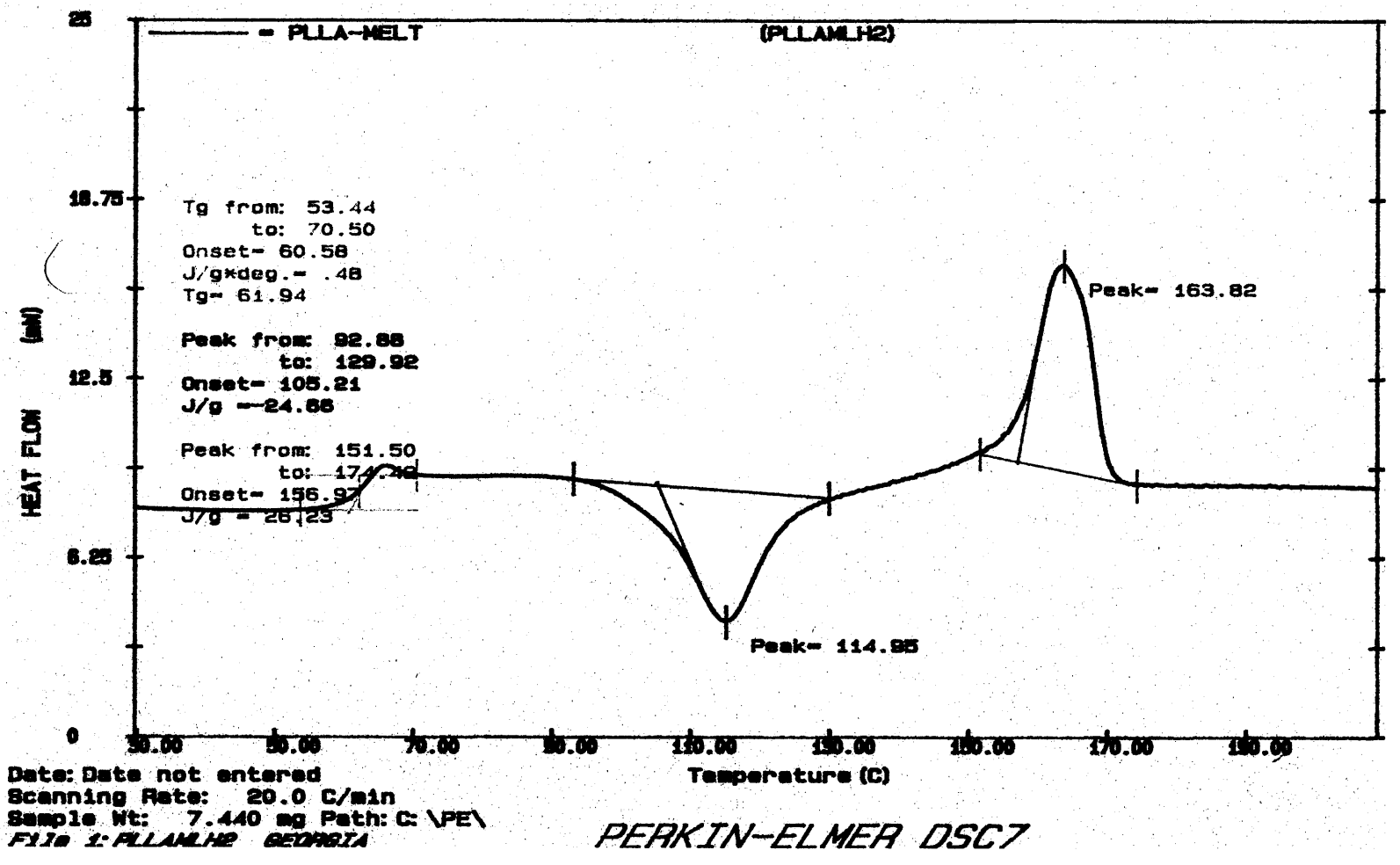

Figure A.6 DSC thermogram of PLLA-melt during the second heating scan.

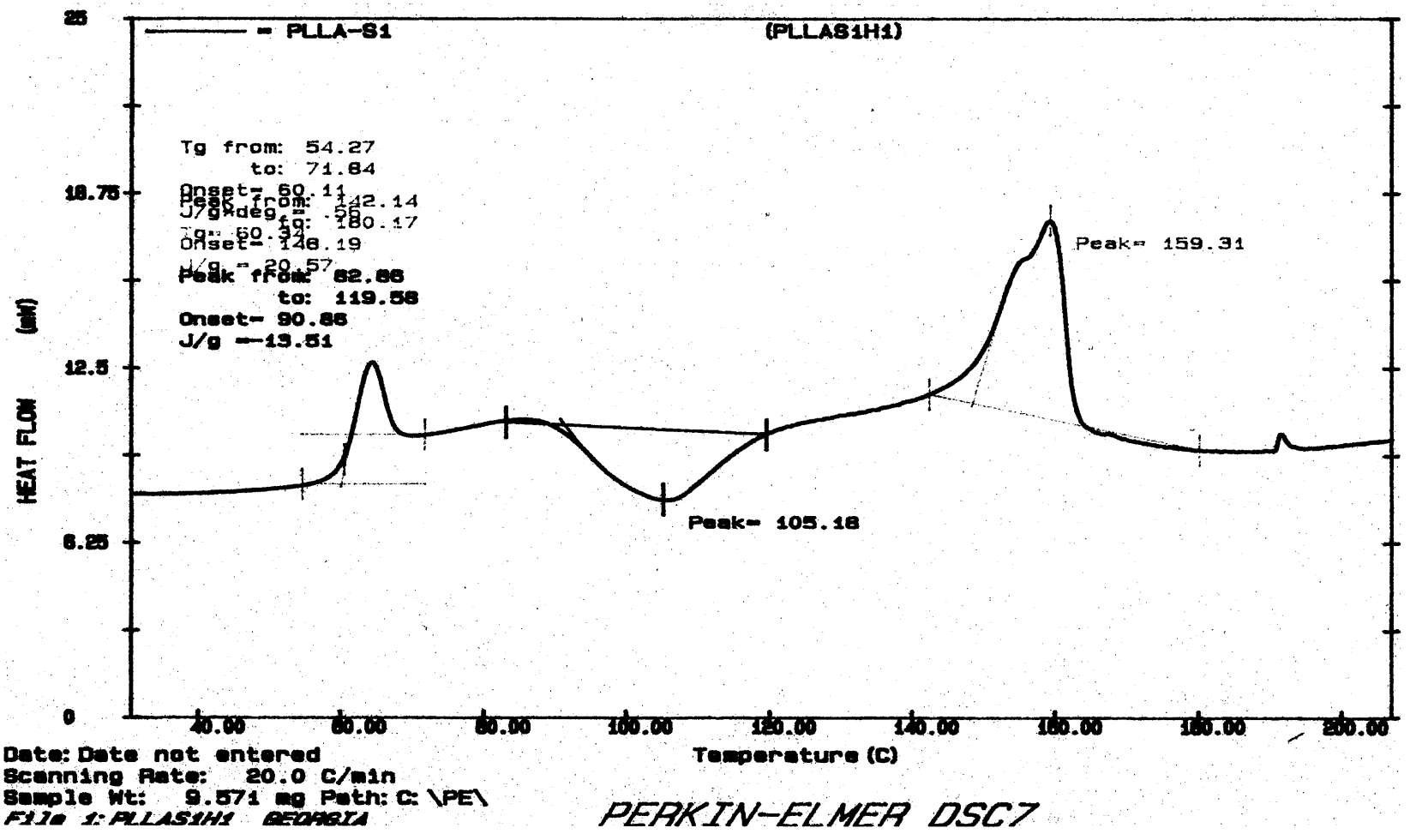

Figure A.7 DSC thermogram of PLLA/uncoated hydrotalcite composite, prepared by solution mixing, during the first heating scan.

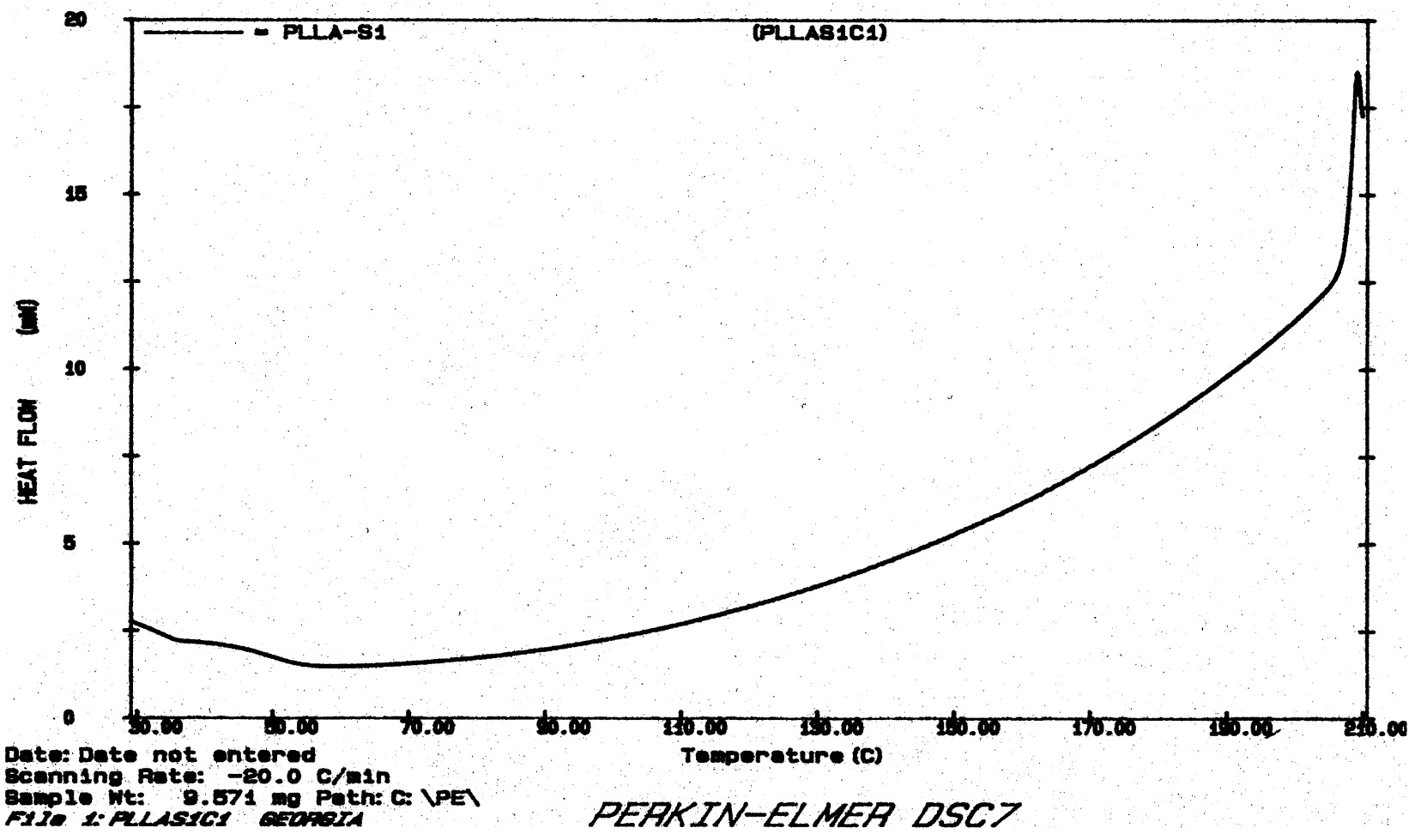

Figure A.8 DSC thermogram of PLLA/uncoated hydrotalcite composite, prepared by solution mixing, during the cooling scan.

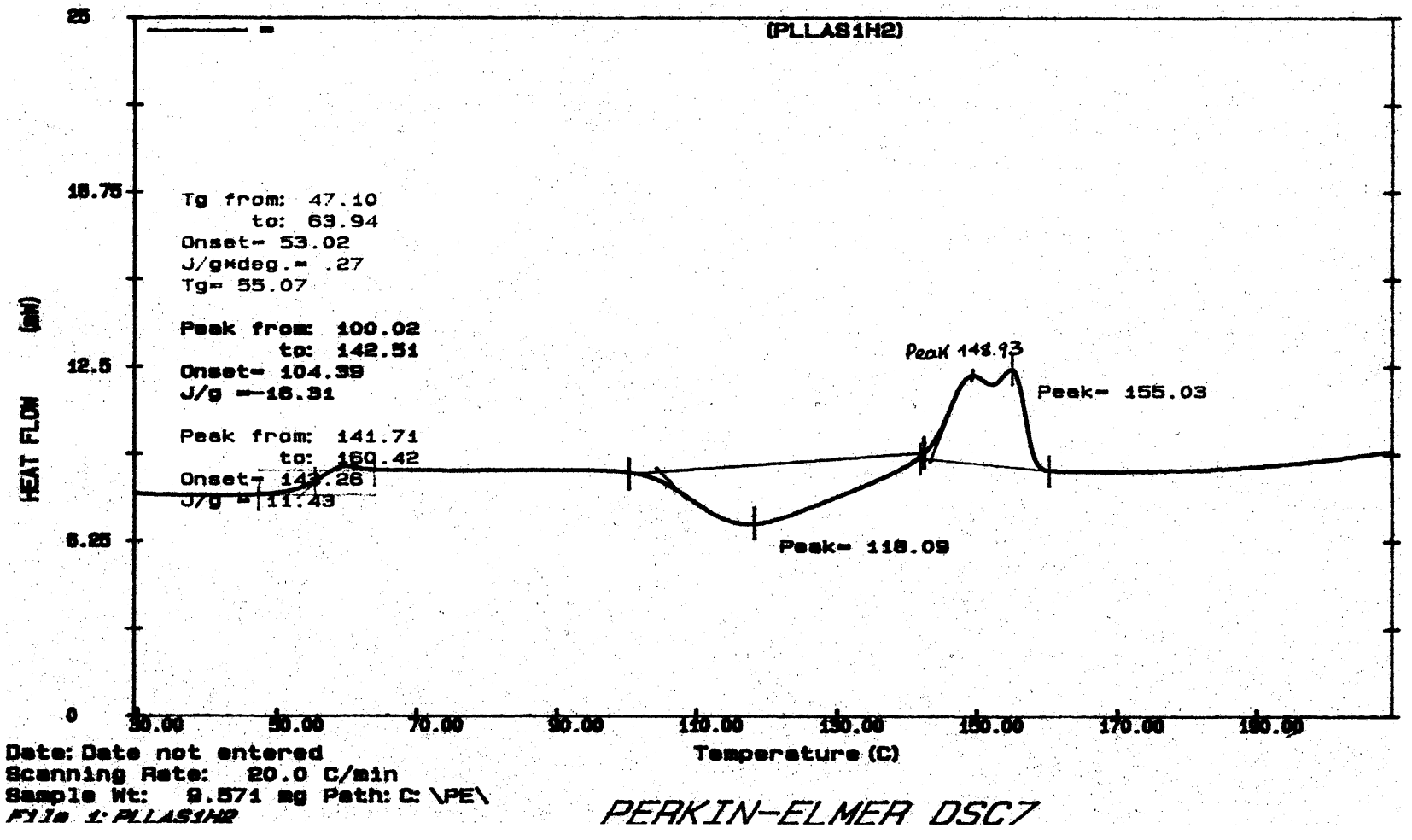

Figure A.9 DSC thermogram of PLLA/uncoated hydrotalcite composite, prepared by solution mixing, during the second heating scan.

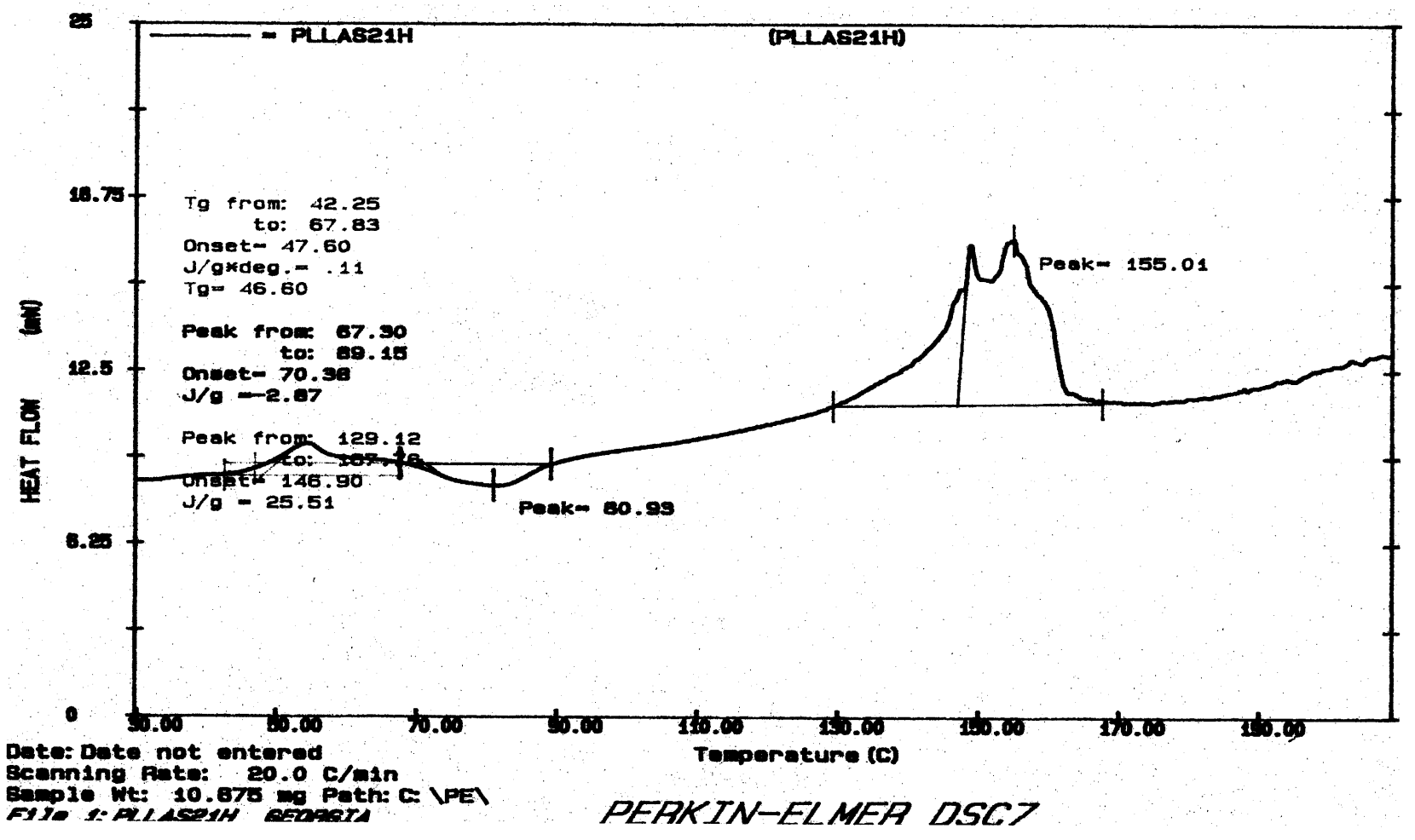

Figure A.10 DSC thermogram of PLLA/coated hydrotalcite composite, prepared by solution mixing, during the first heating scan.

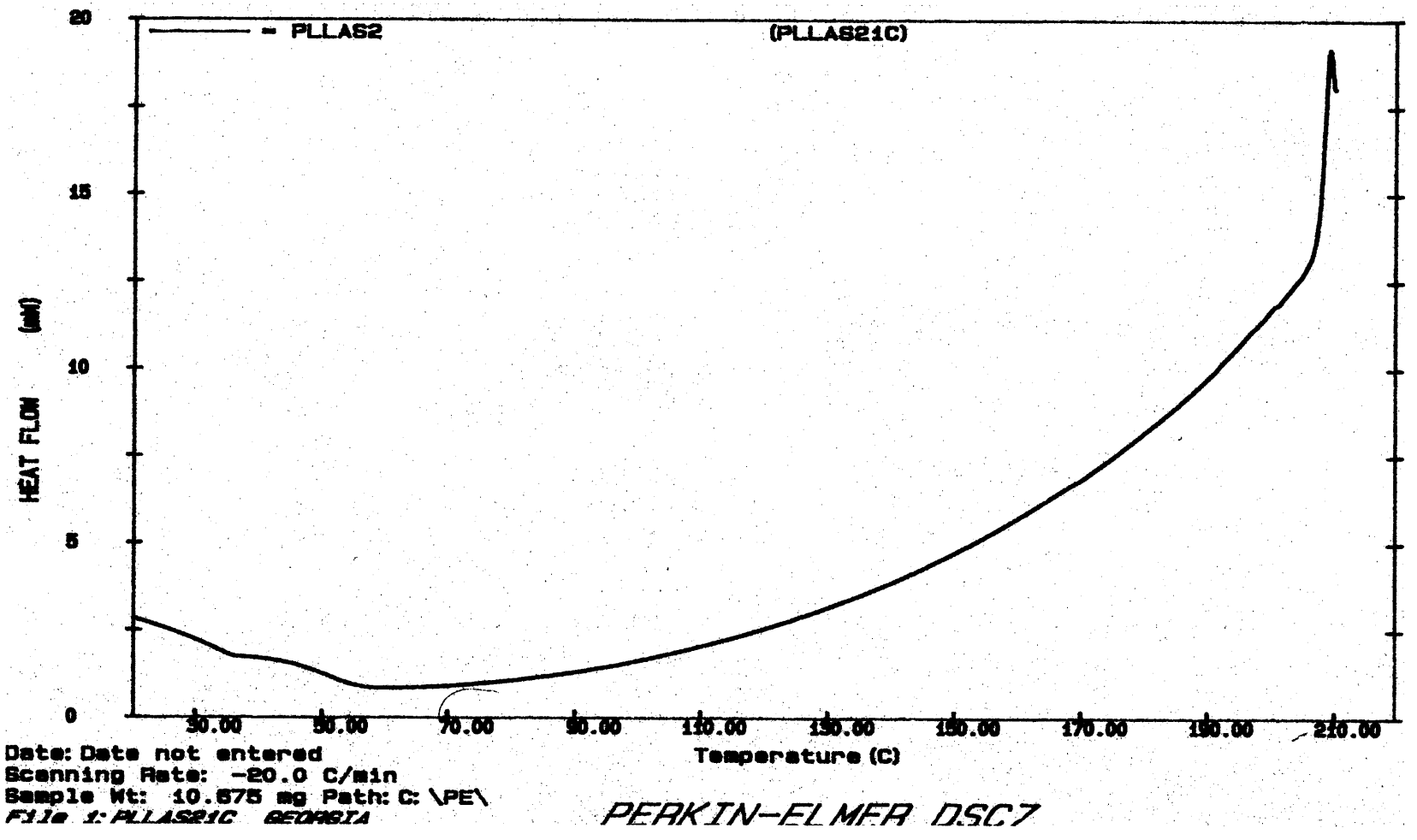

Figure A.11 DSC thermogram of PLLA/coated hydrotalcite composite, prepared by solution mixing, during the cooling scan.

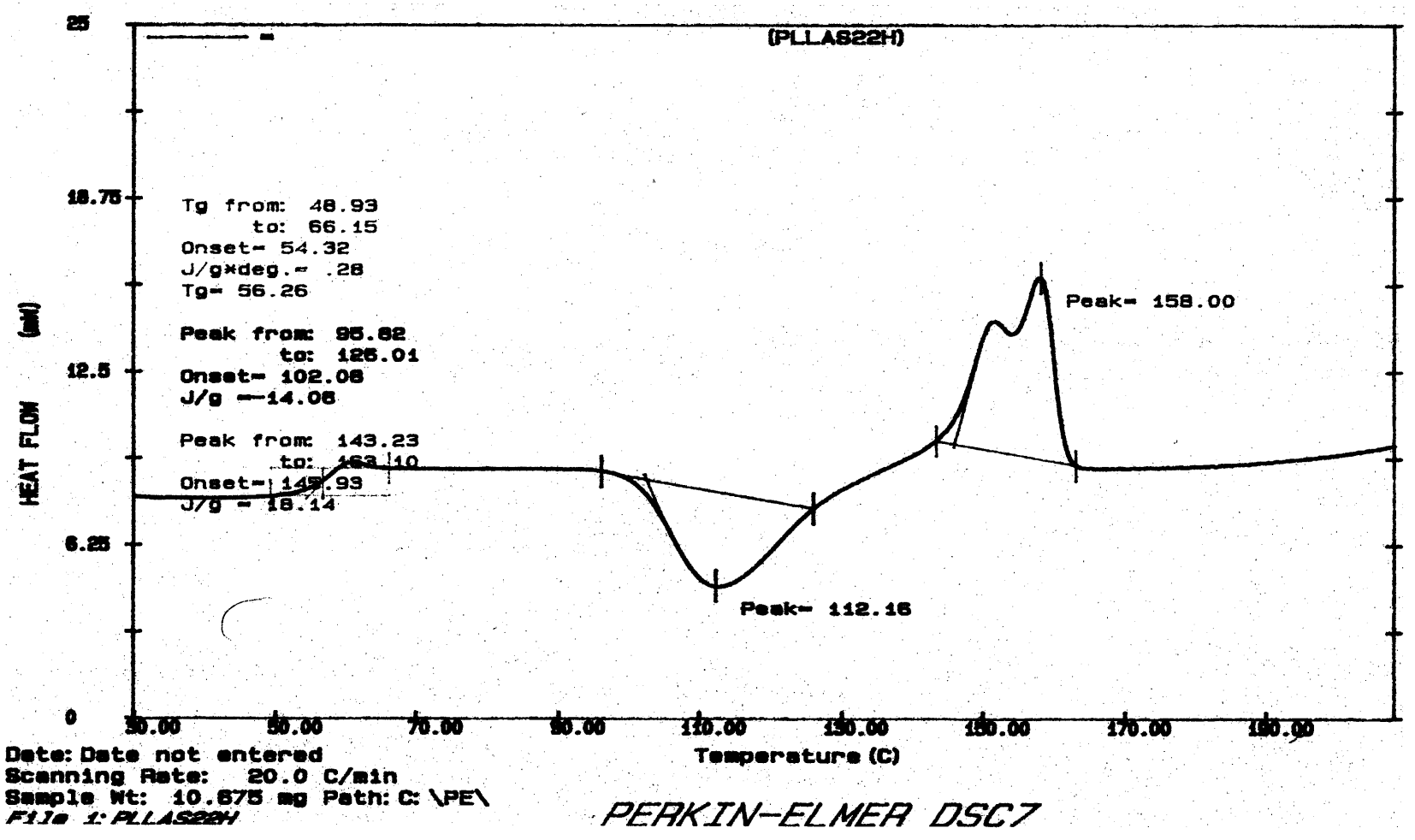

Figure A.12 DSC thermogram of PLLA/coated hydrotalcite composite, prepared by solution mixing, during the second heating scan.

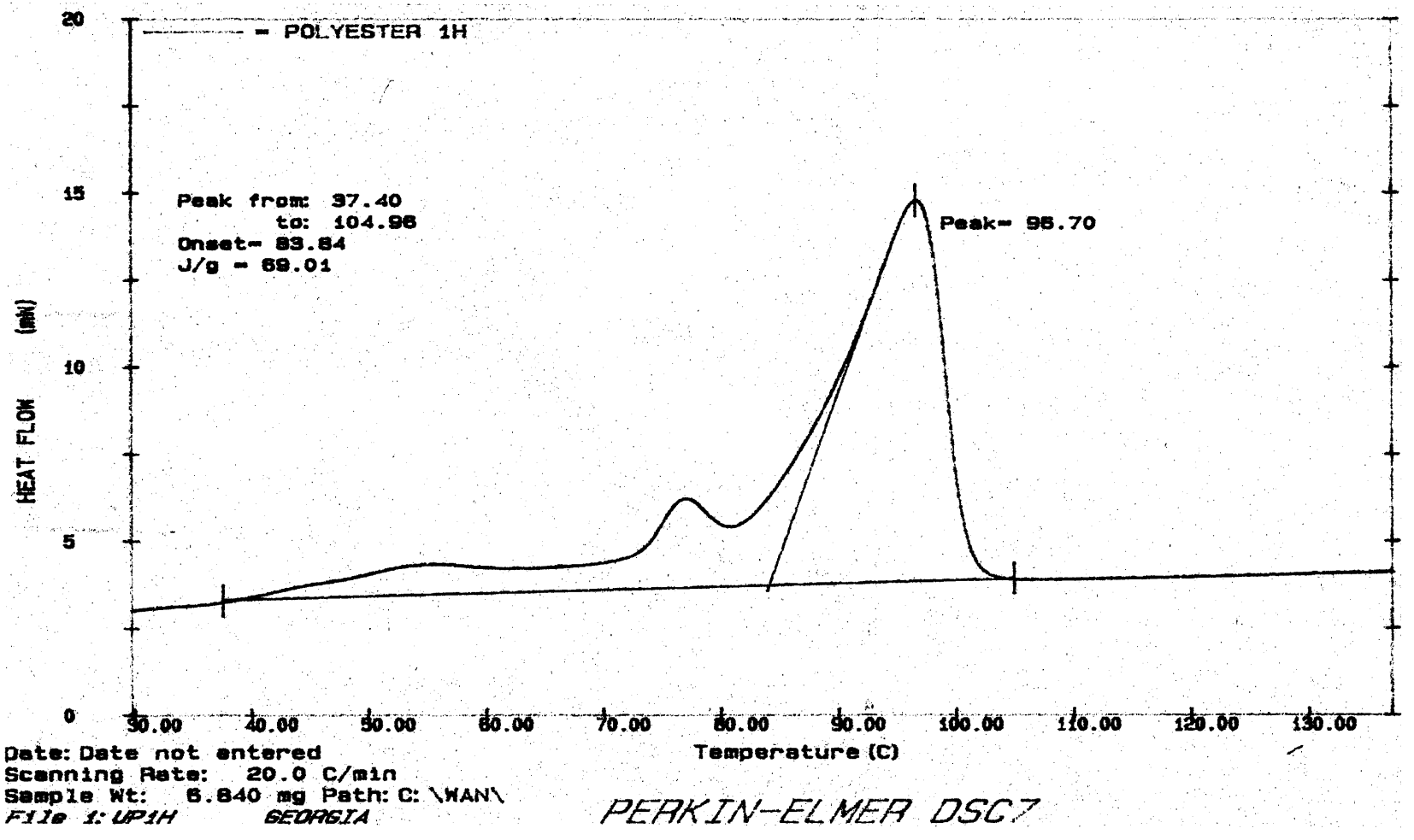

Figure A.13 DSC thermogram of PST pellets during the first heating scan.

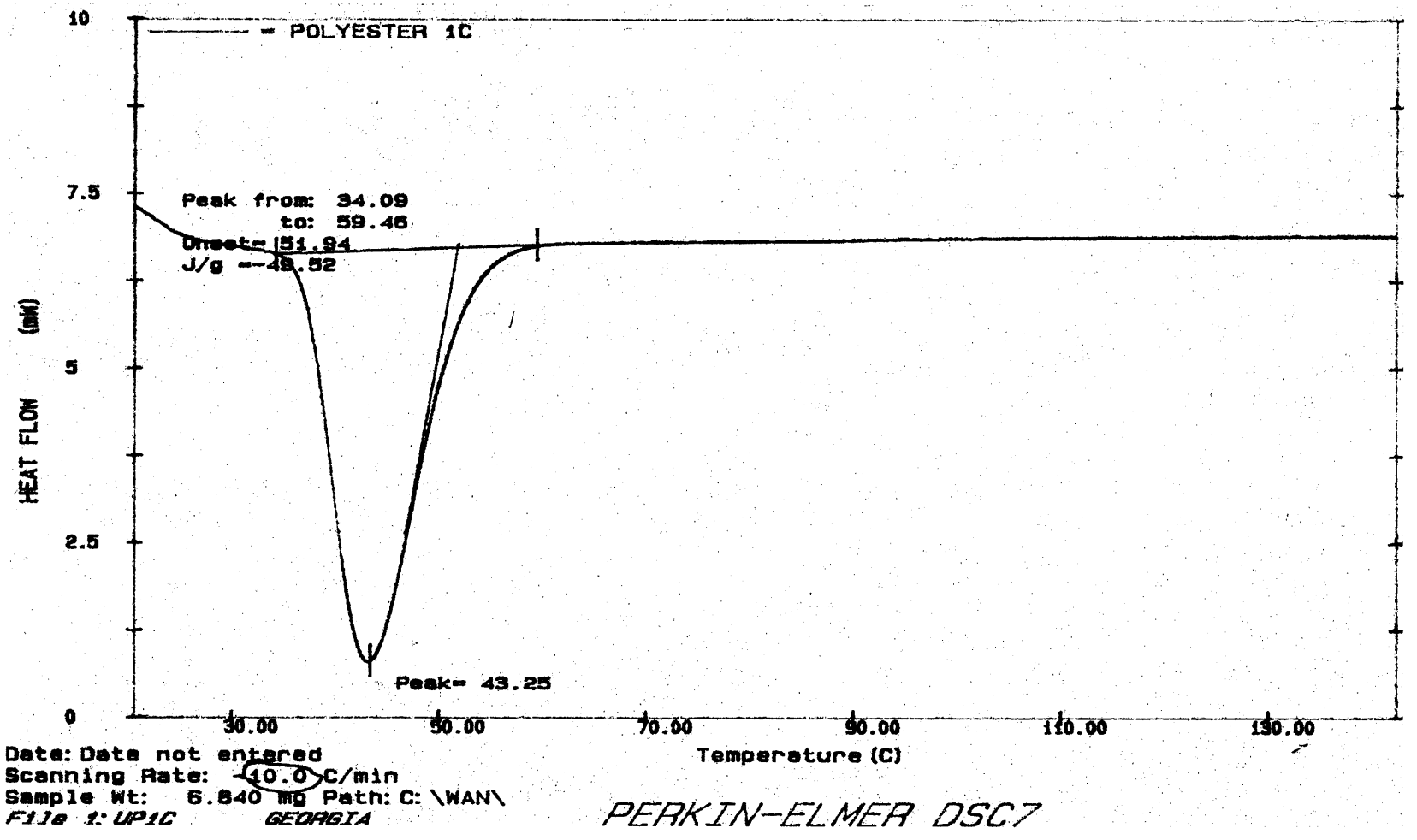

Figure A.14 DSC thermogram of PST pellets during the cooling scan.

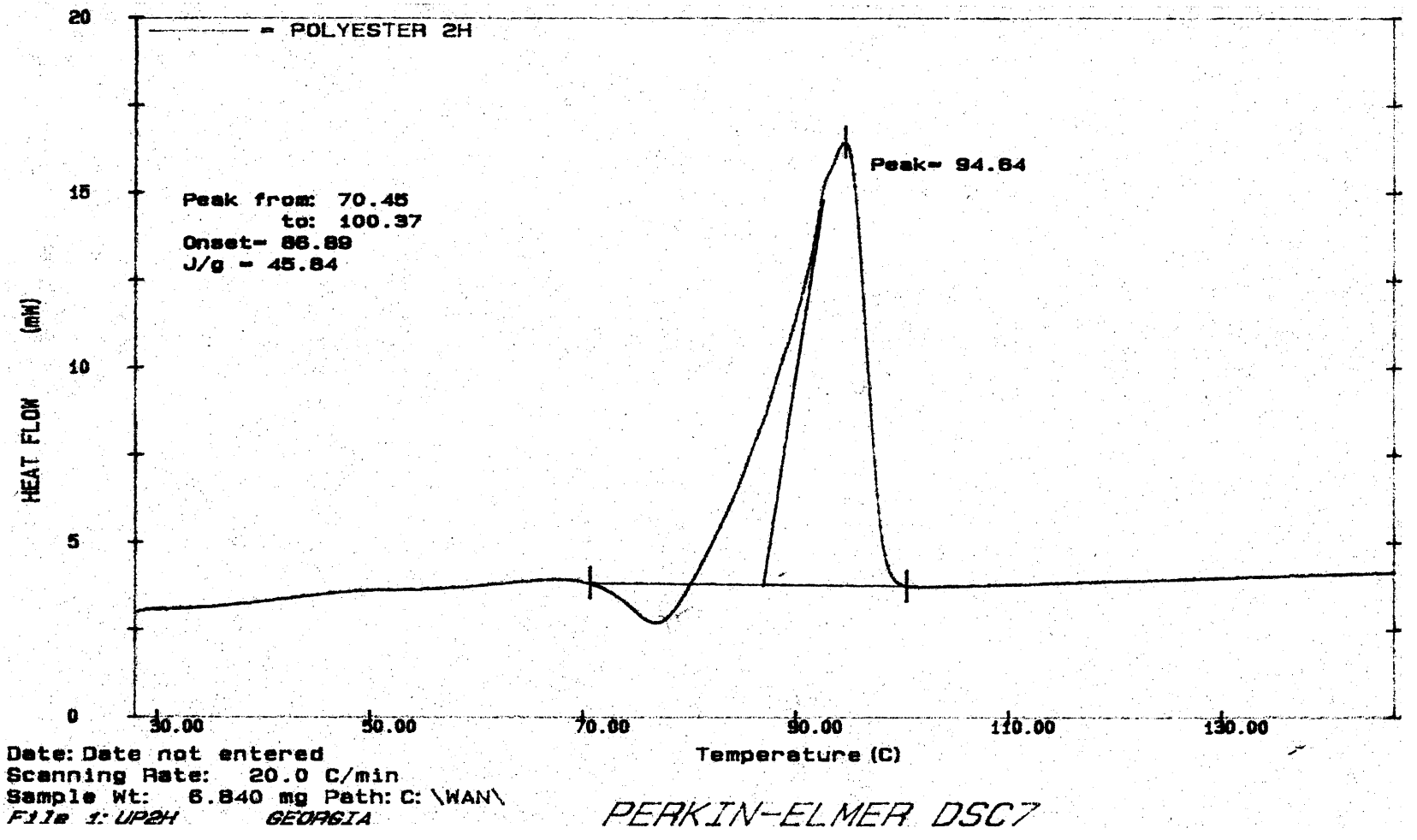

Figure A.15 DSC thermogram of PST pellets during the second heating scan.

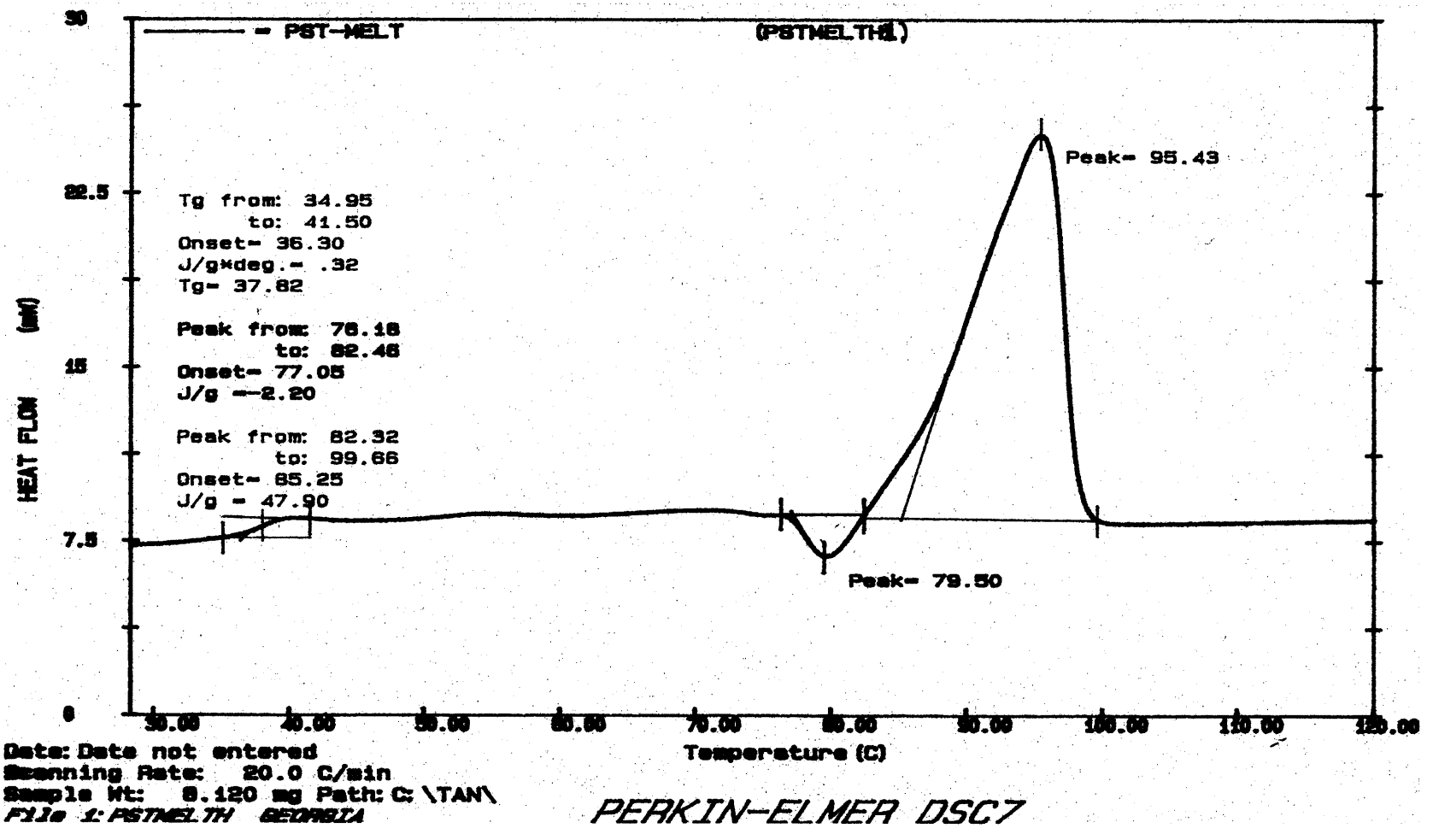

Figure A.16 DSC thermogram of PST - melt during the first heating scan.

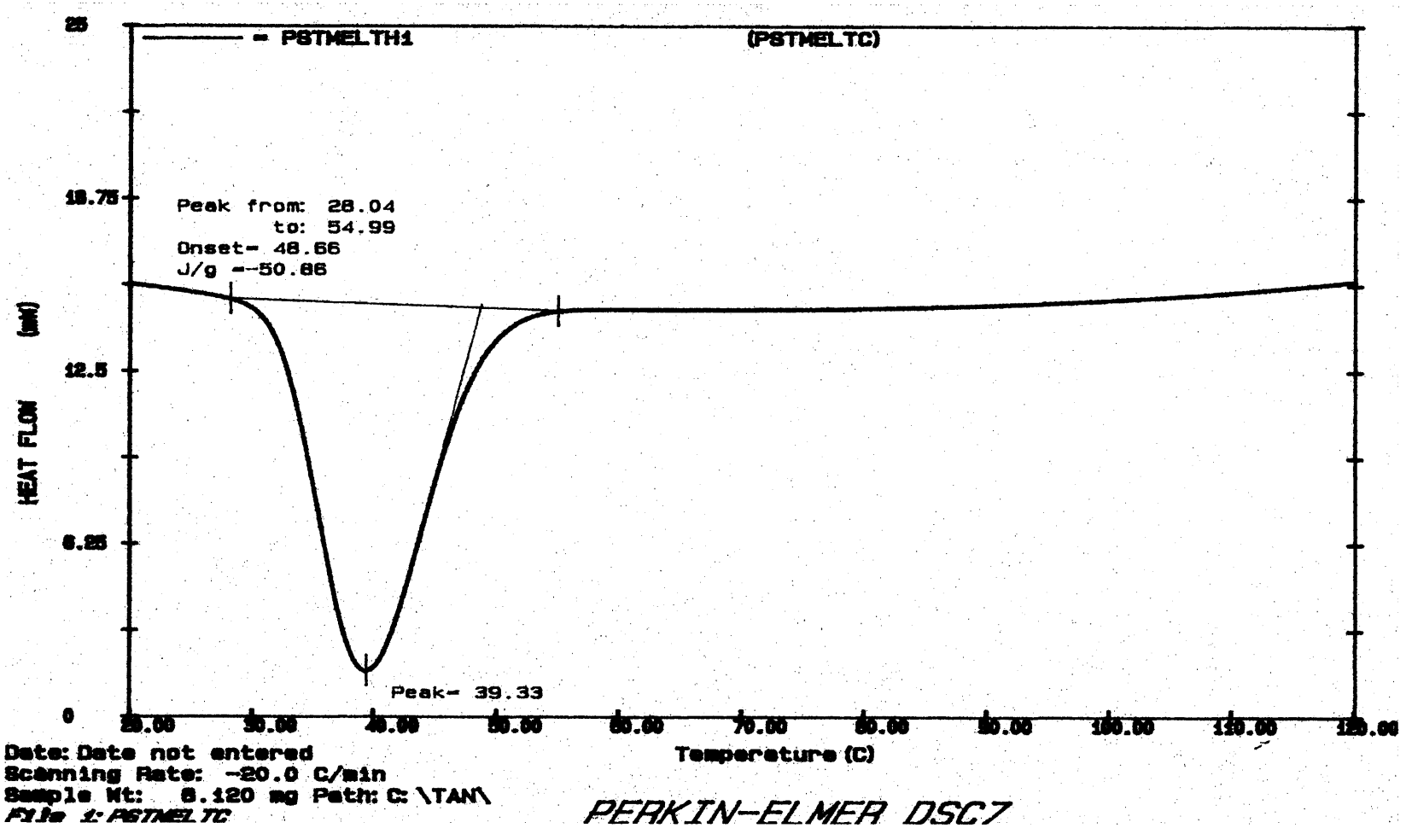

Figure A.17 DSC thermogram of PST - melt during the cooling scan.

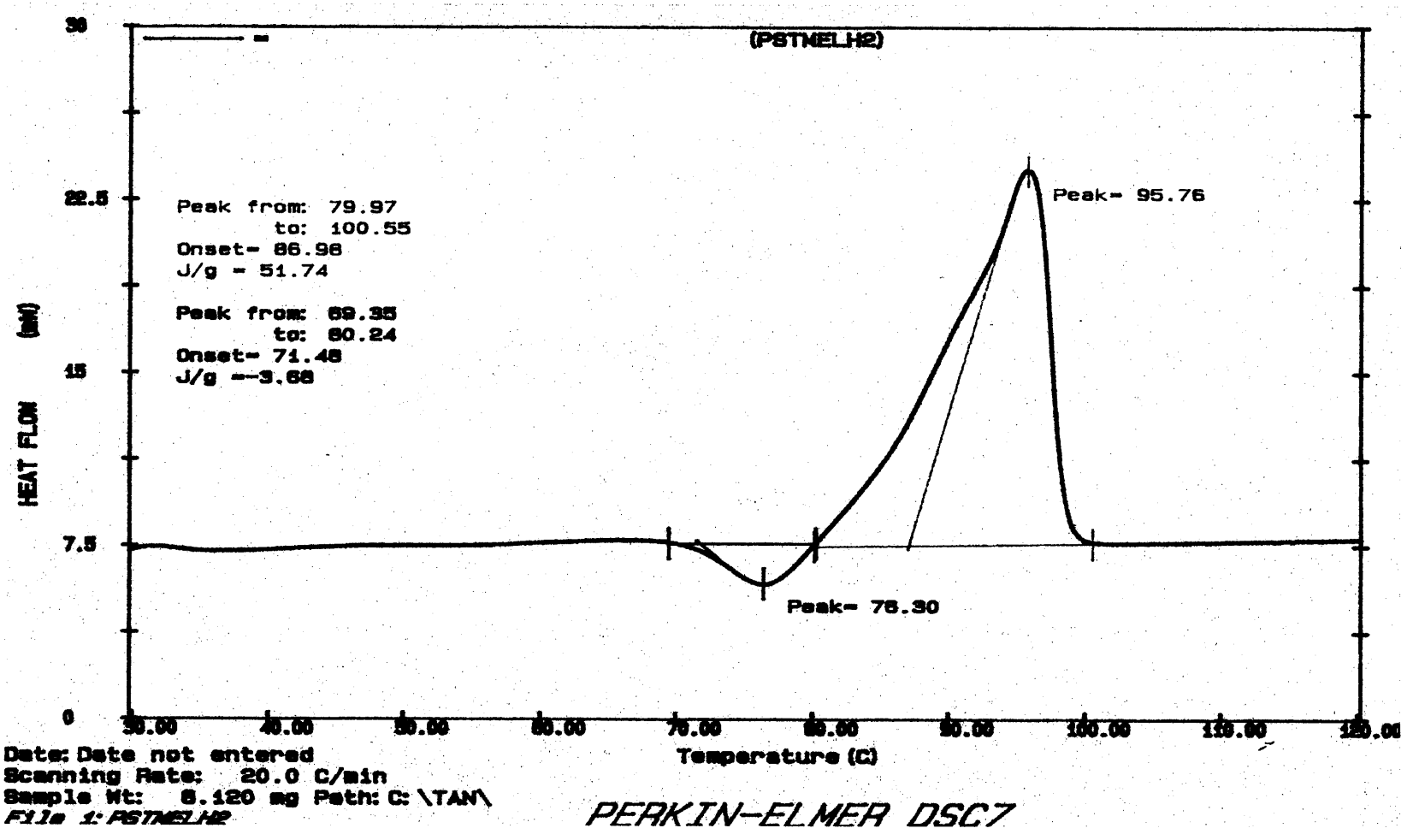

Figure A.18 DSC thermogram of PST - melt during the second heating scan.

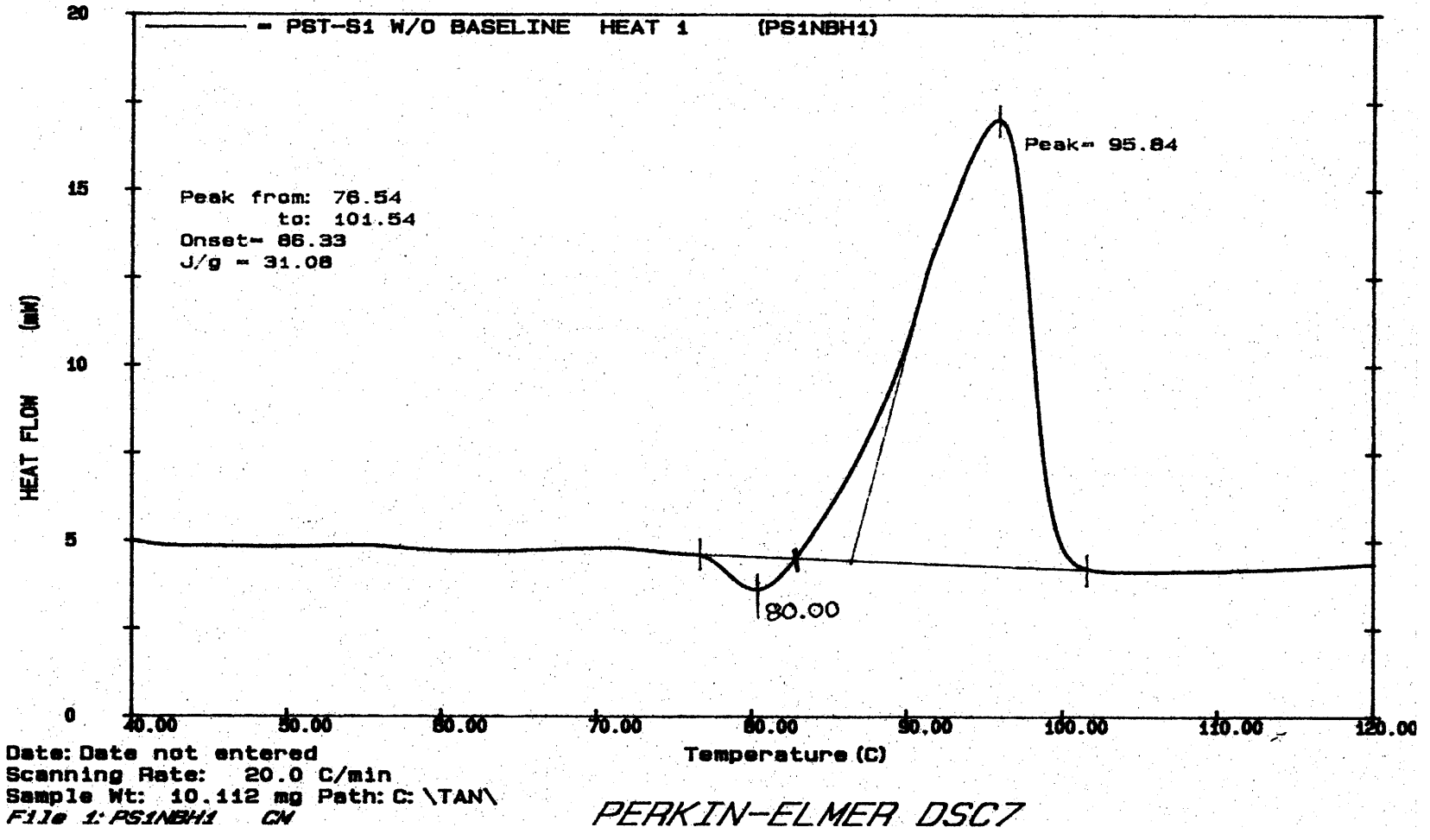

Figure A.19 DSC thermogram of PST/uncoated hydrotalcite composite, prepared by solution mixing, during the first heating scan.

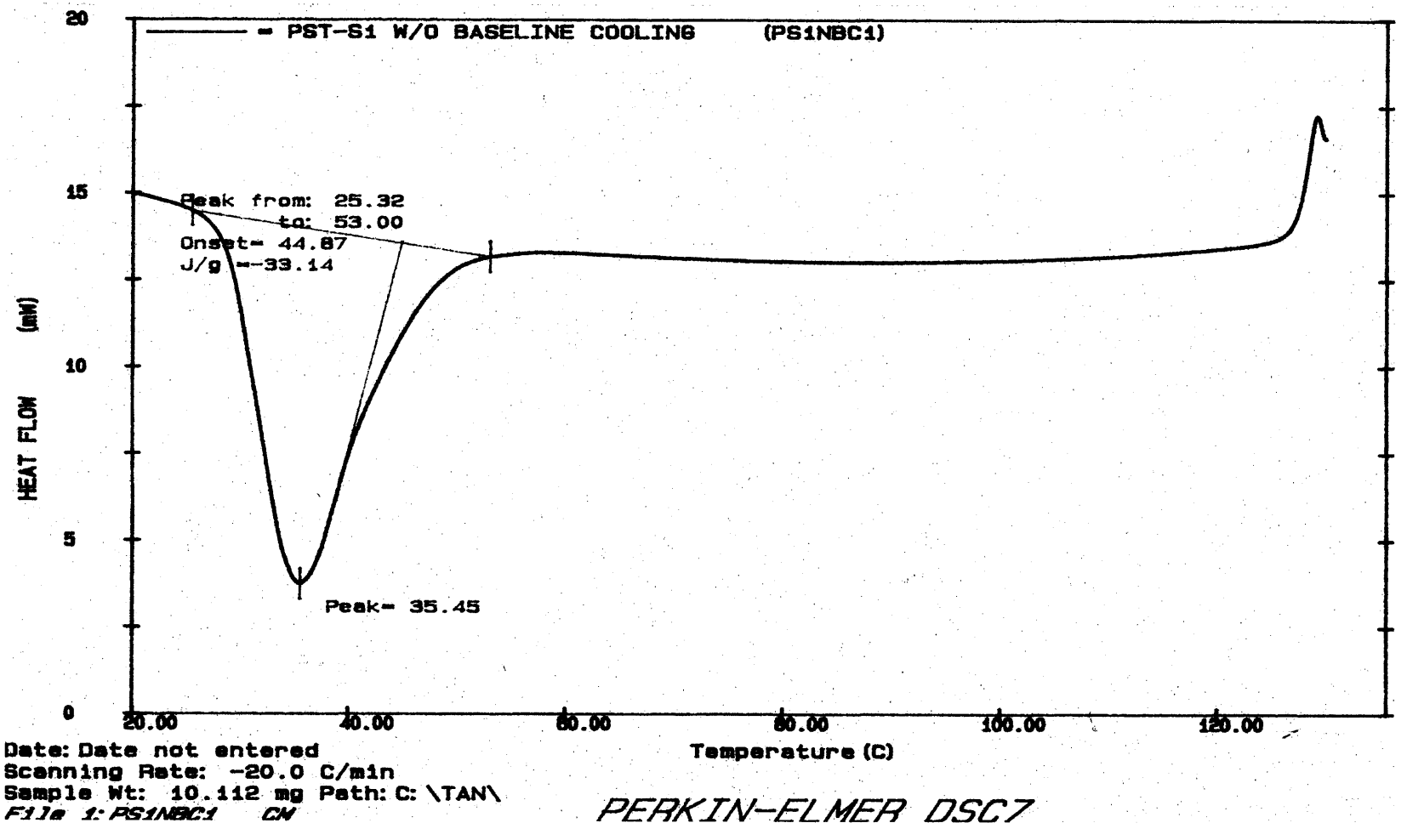

Figure A.20 DSC thermogram of PST/uncoated hydrotalcite composite, prepared by solution mixing, during the cooling scan.

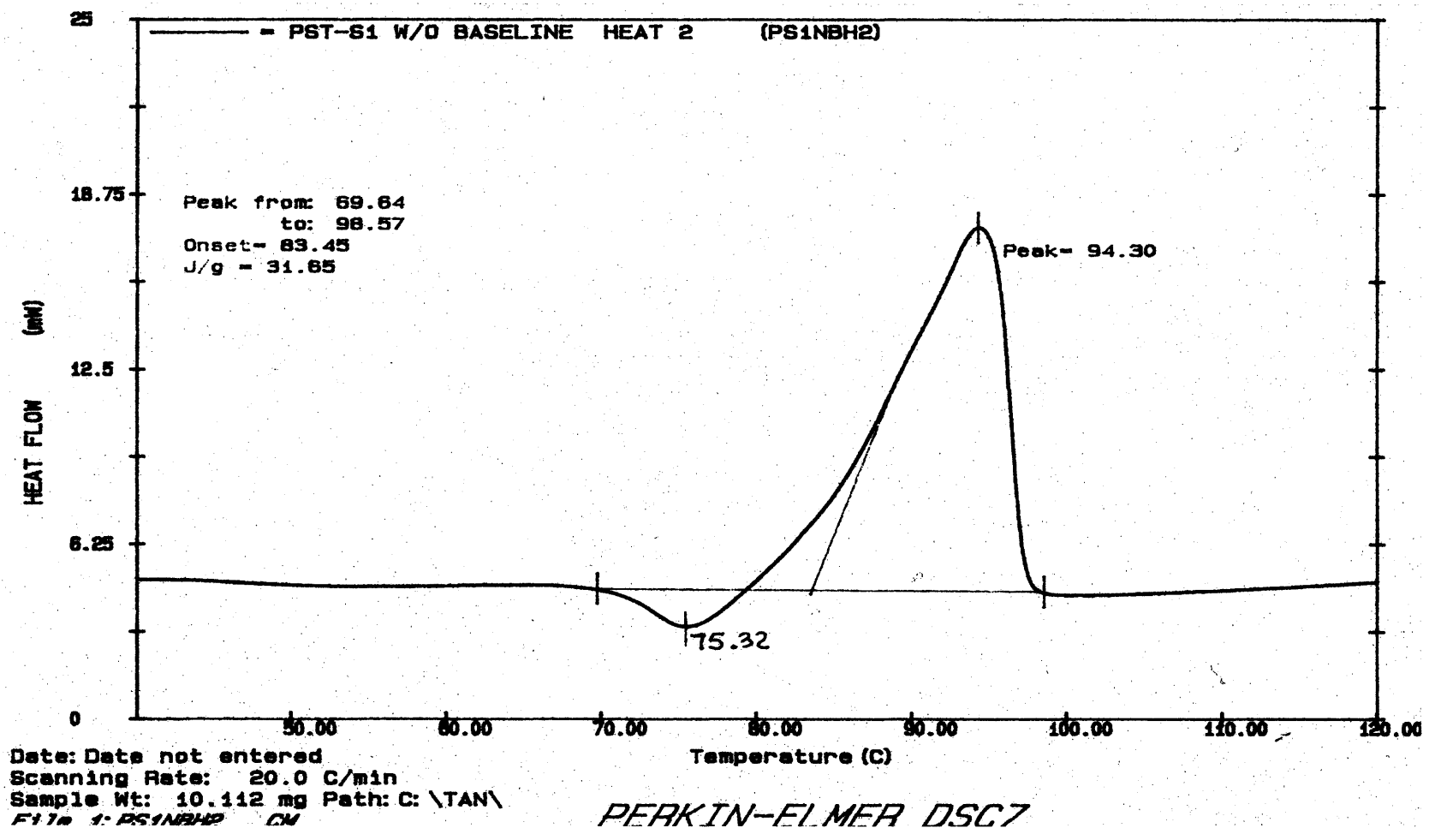

Figure A.21 DSC thermogram of PST/uncoated hydrotalcite composite, prepared by solution mixing, during the second heating scan.

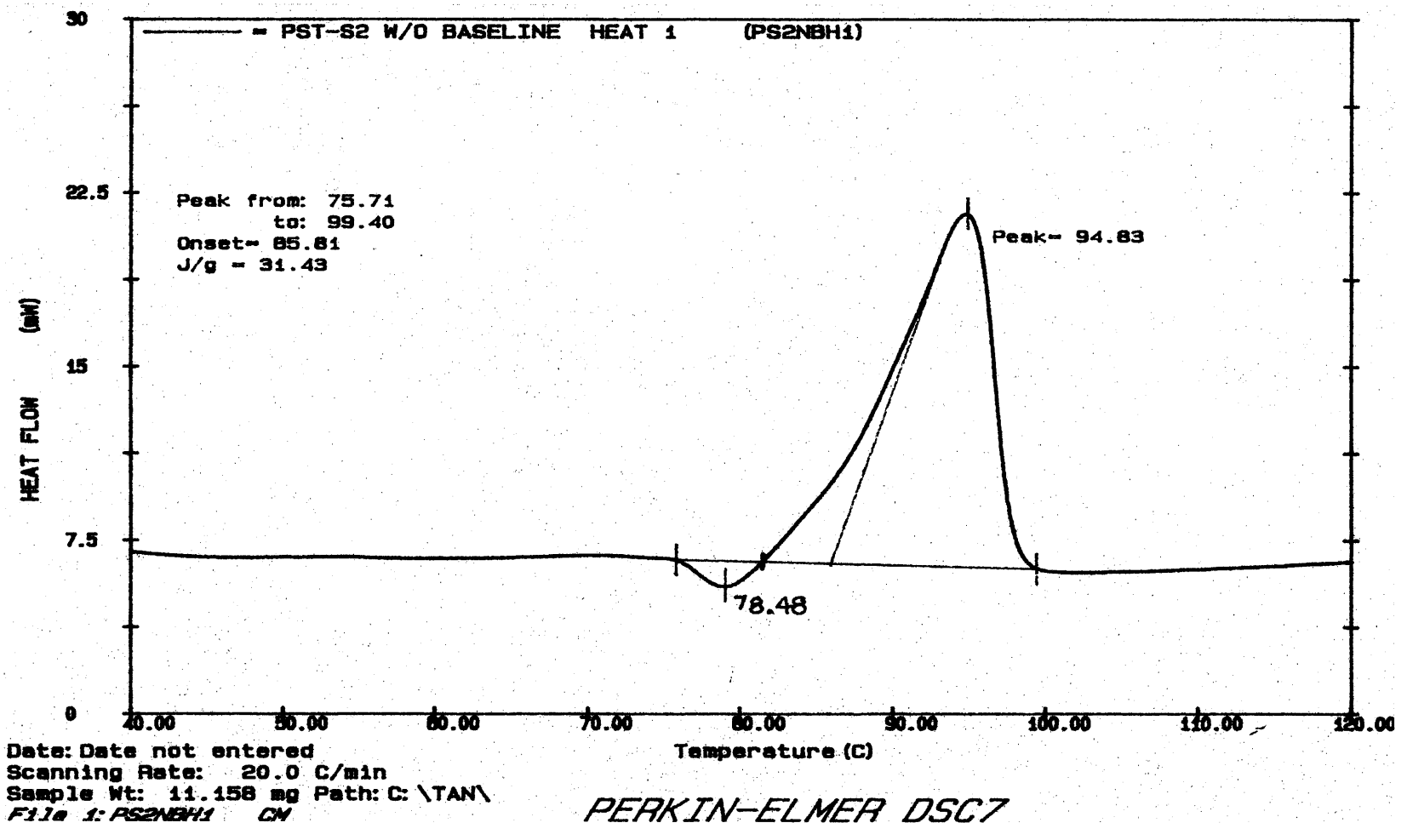

Figure A.22 DSC thermogram of PST/coated hydrotalcite composite, prepared by solution mixing, during the first heating scan.

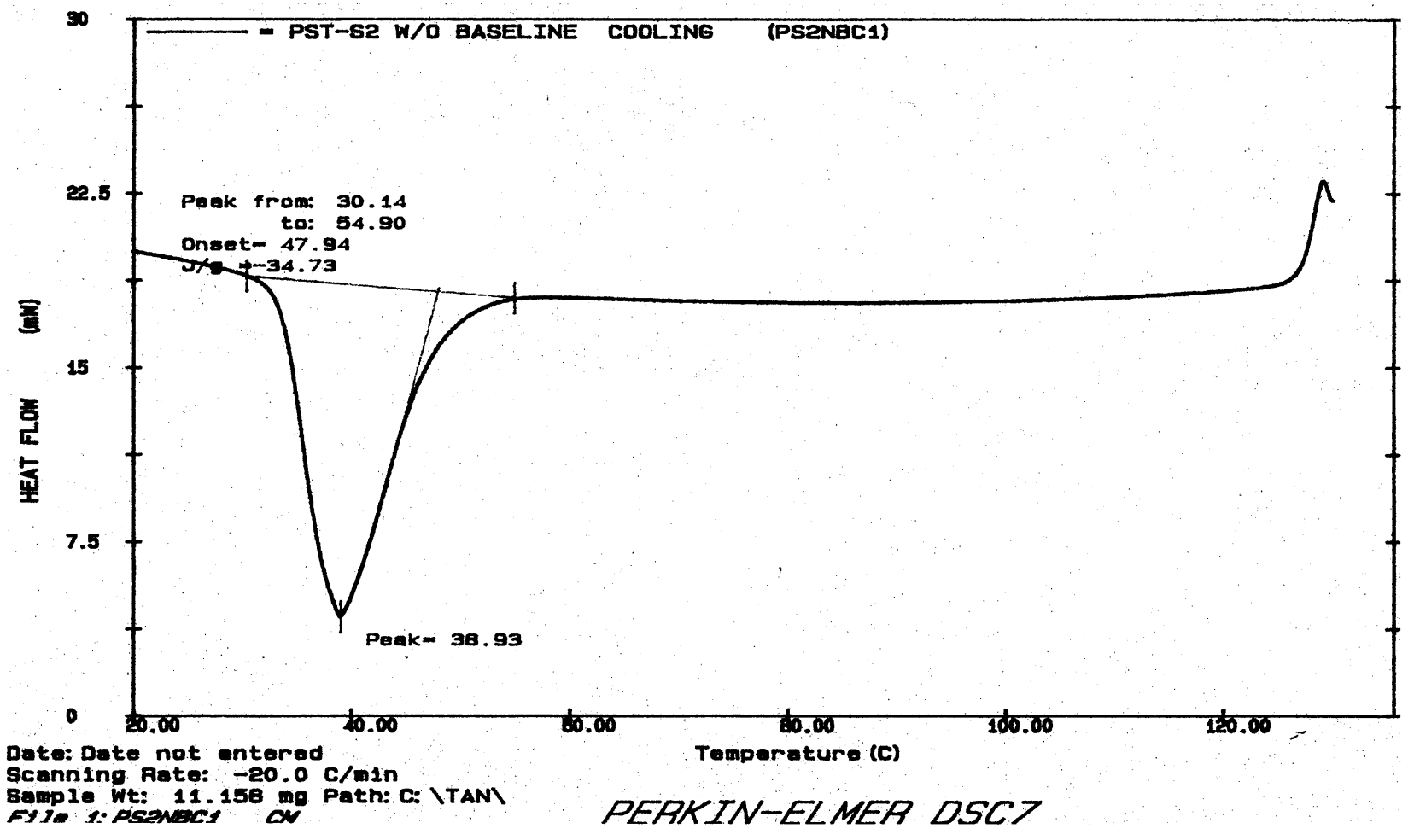

Figure A.23 DSC thermogram of PST/coated hydrotalcite composite, prepared by solution mixing, during the cooling scan.

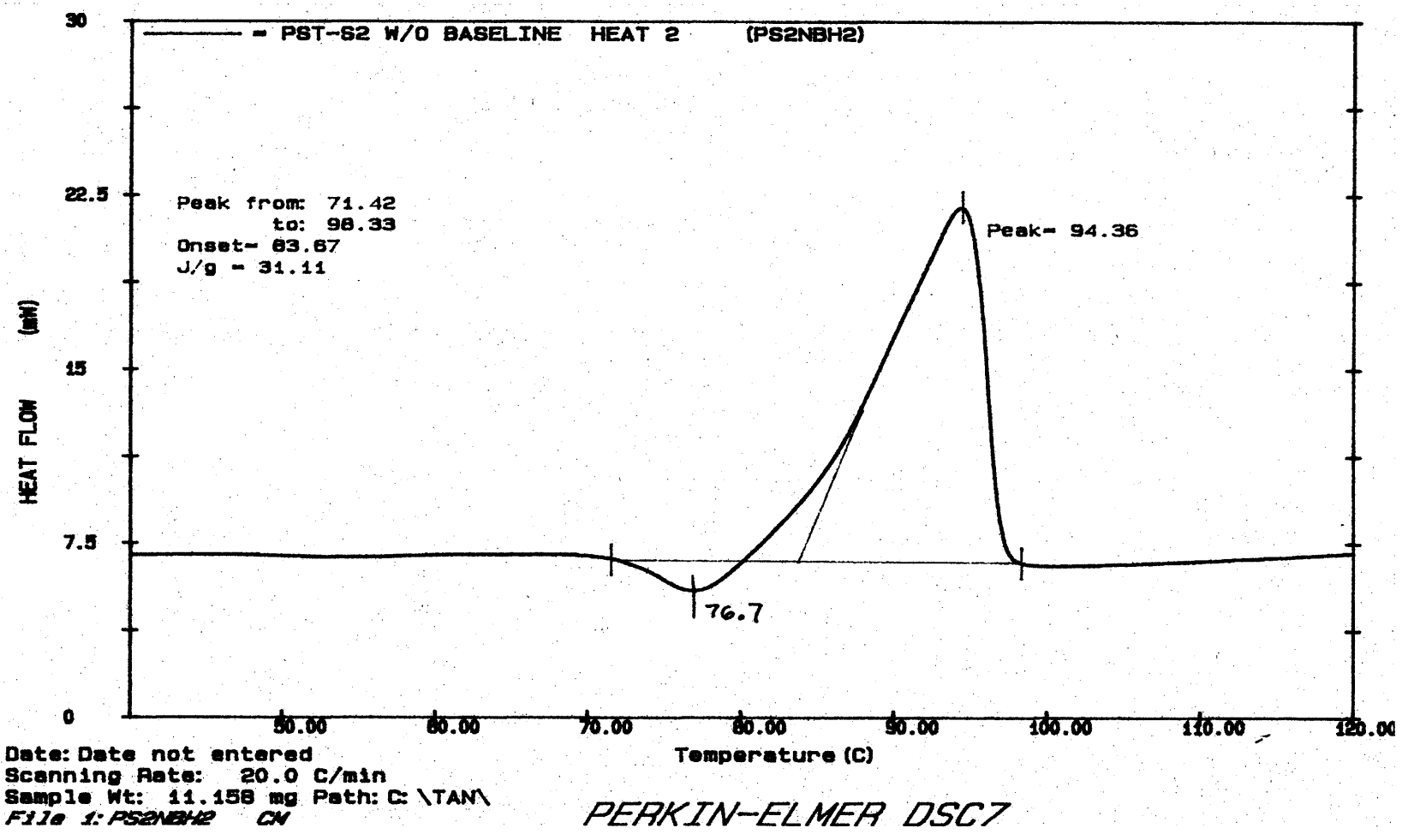

Figure A.24 DSC thermogram of PST/coated hydrotalcite composite, prepared by solution mixing, during the second heating scan.

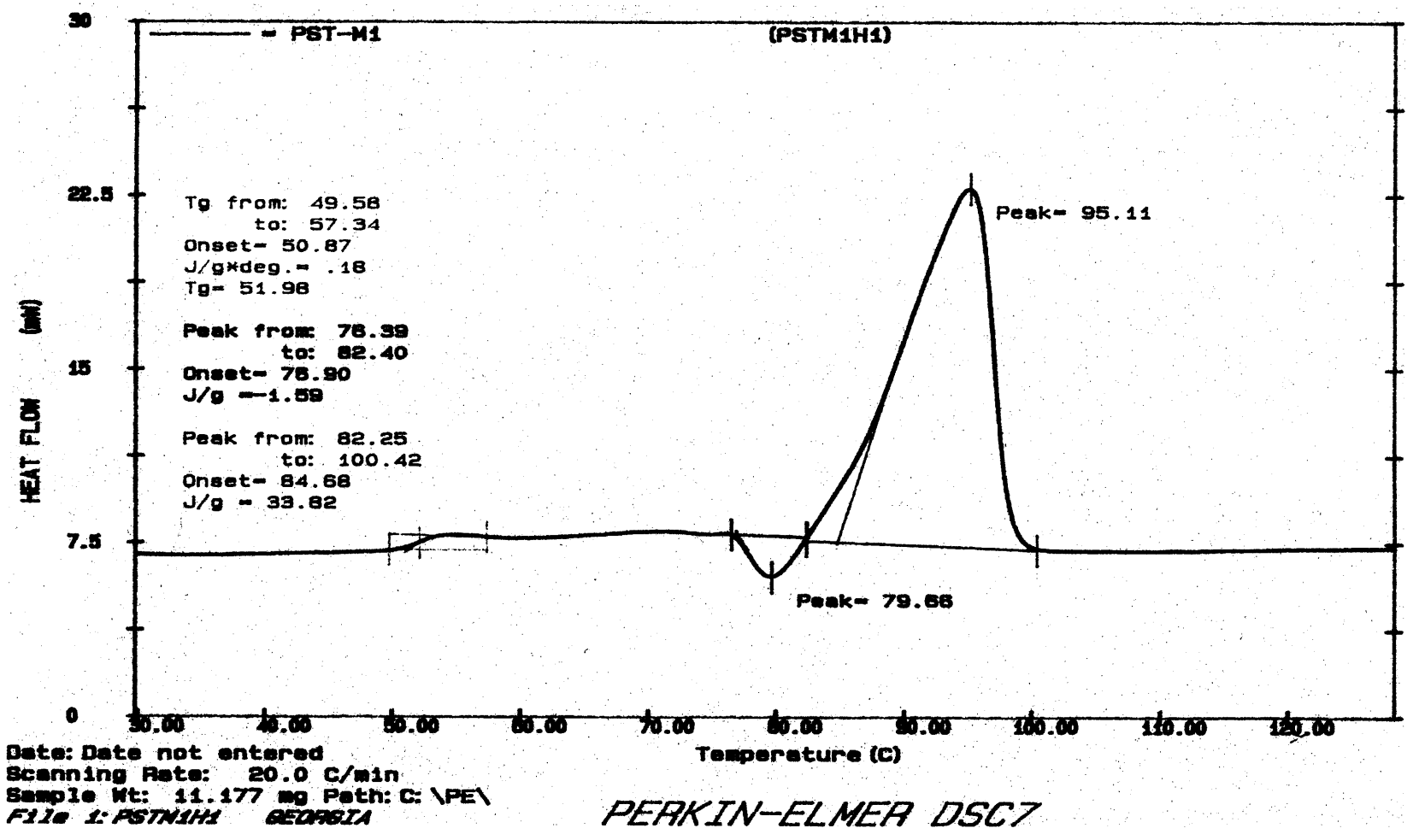

Figure A.25 DSC thermogram of PST/uncoated hydrotalcite composite, prepared by melt processing, during the first heating scan.

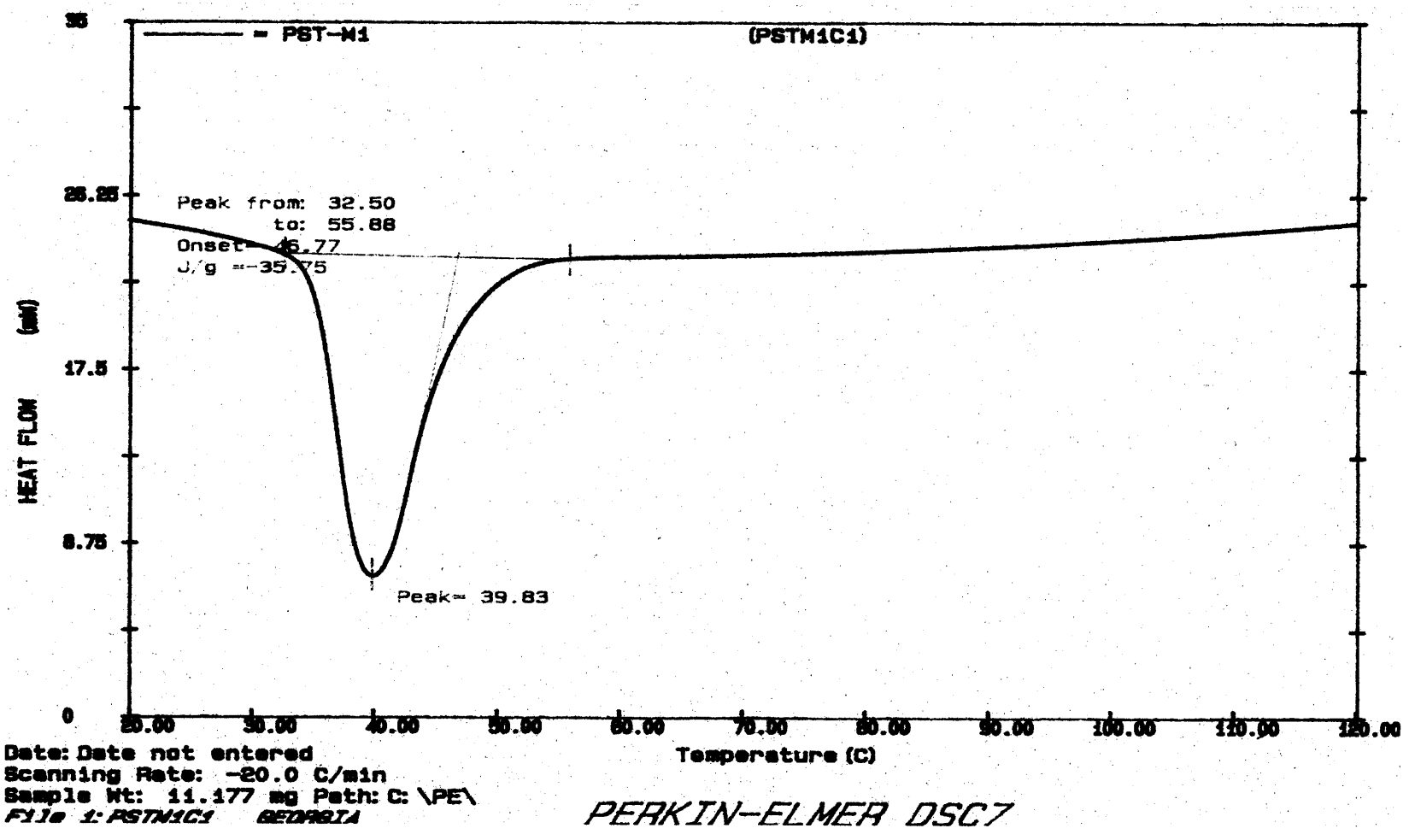

Figure A.26 DSC thermogram of PST/uncoated hydrotalcite composite, prepared by melt processing, during the cooling scan.

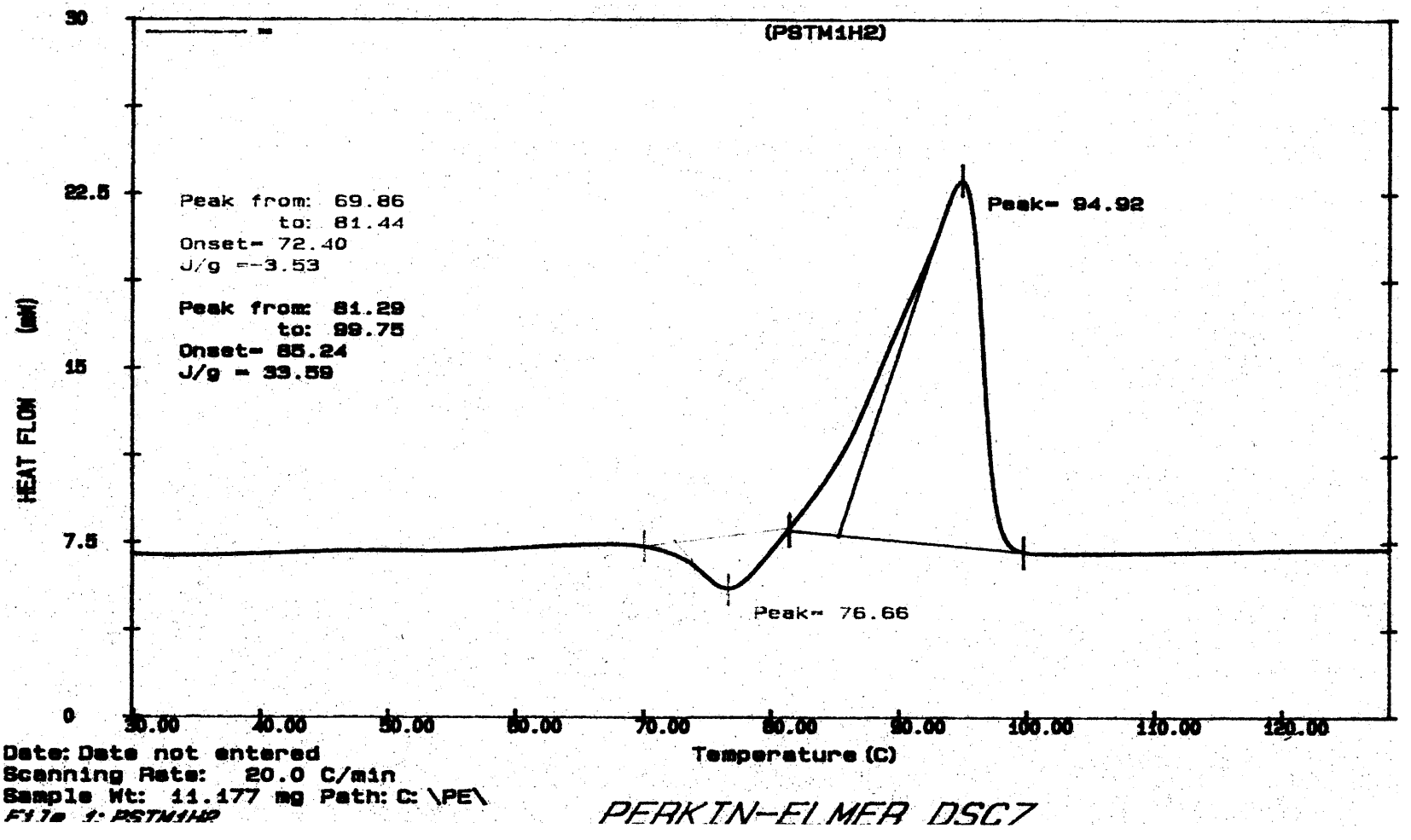

Figure A.27 DSC thermogram of PST/uncoated hydrotalcite composite, prepared by melt processing, during the second heating scan.

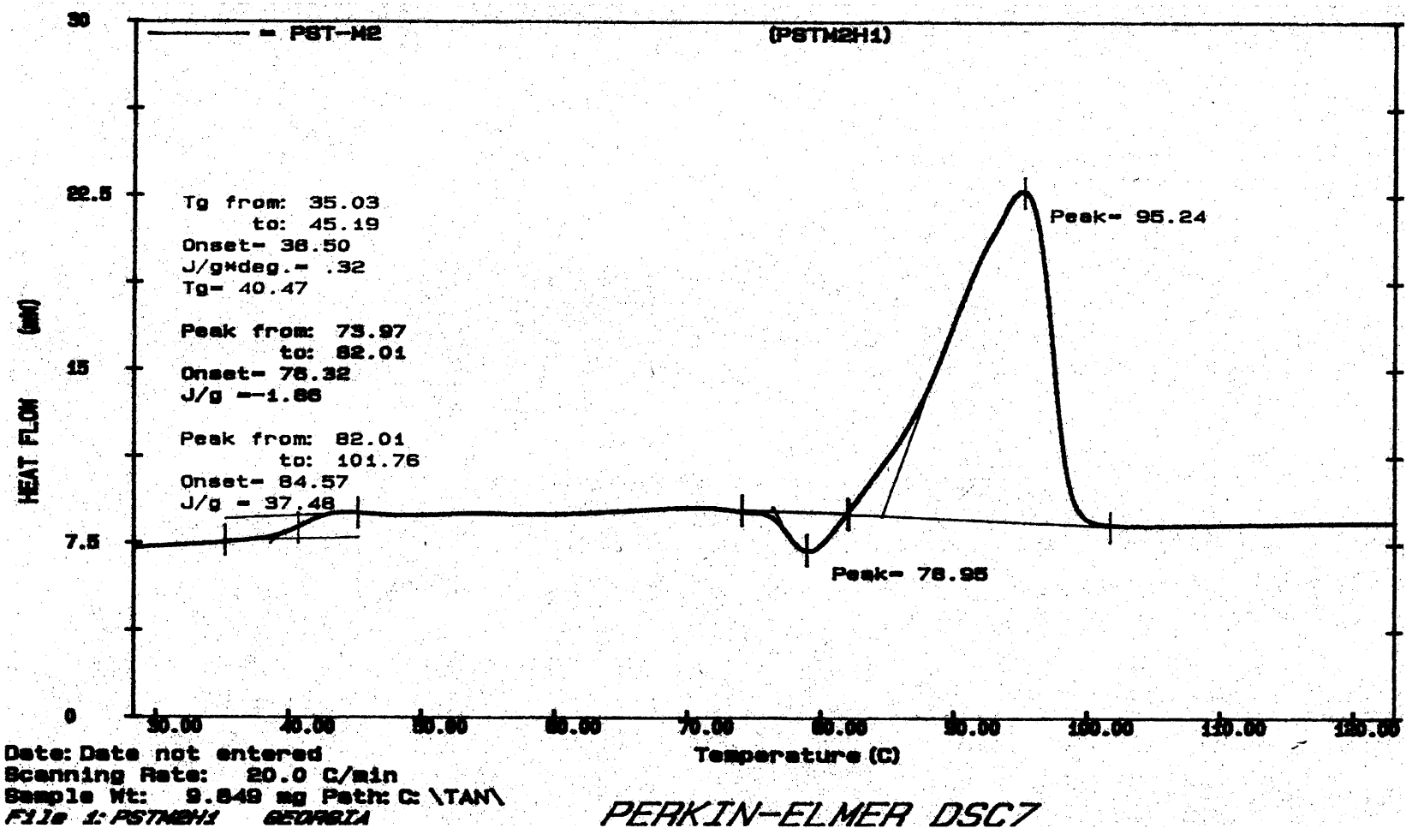

Figure A.28 DSC thermogram of PST/coated hydrotalcite composite, prepared by melt processing, during the first heating scan.

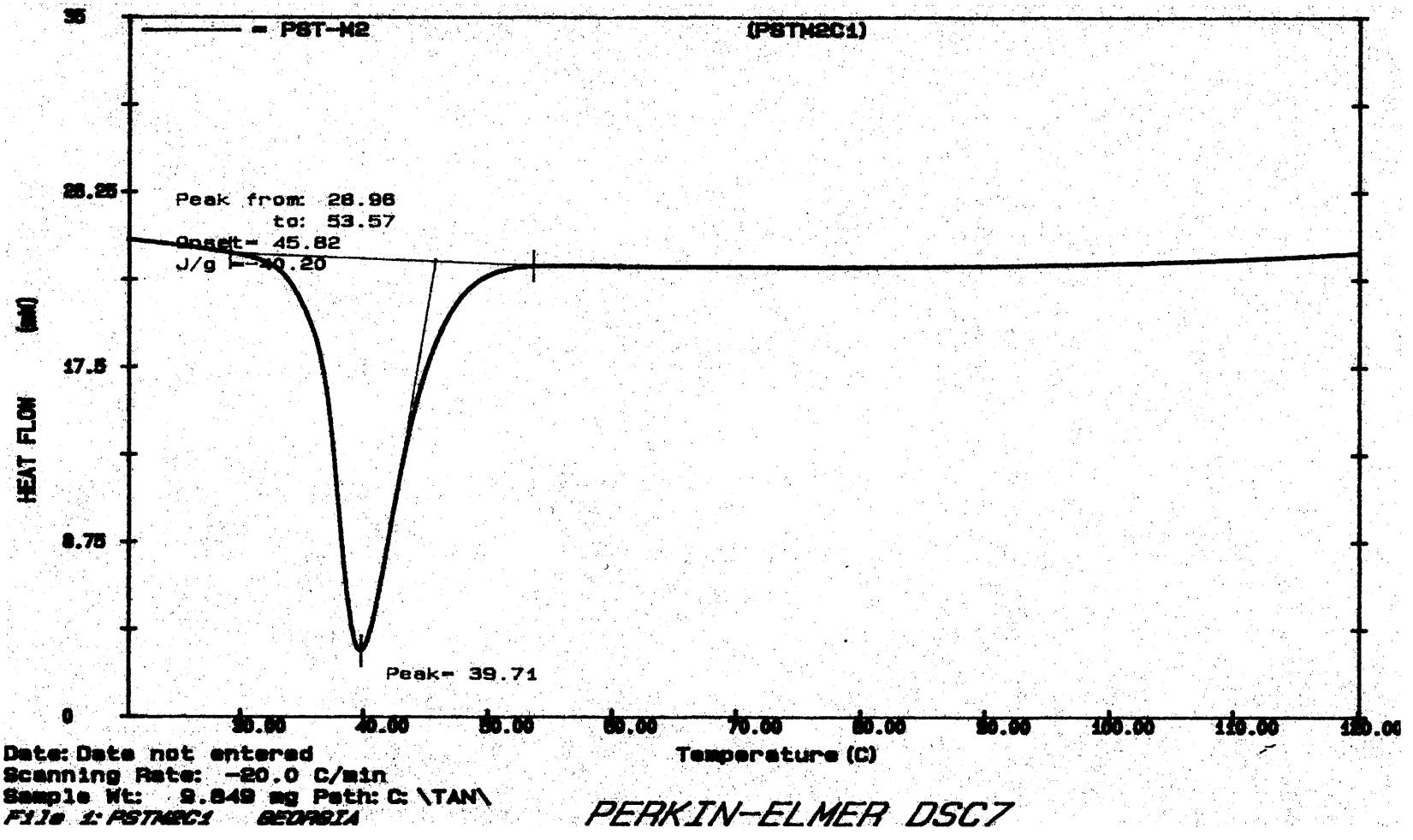

Figure A.29 DSC thermogram of PST/coated hydrotalcite composite, prepared by melt processing, during the cooling scan.

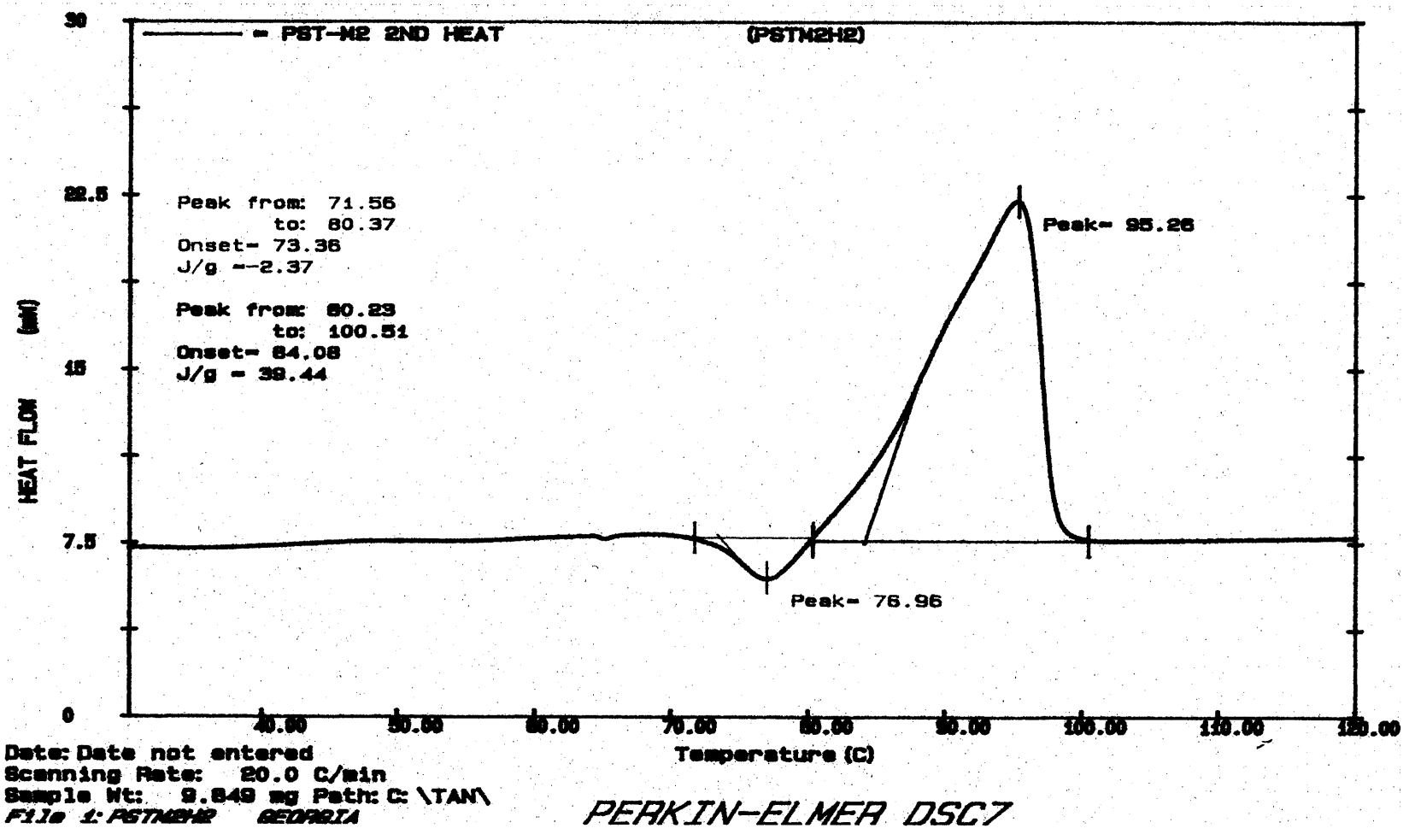

Figure A.30 DSC thermogram of PST/coated hydrotalcite composite, prepared by melt processing, during the second heating scan.

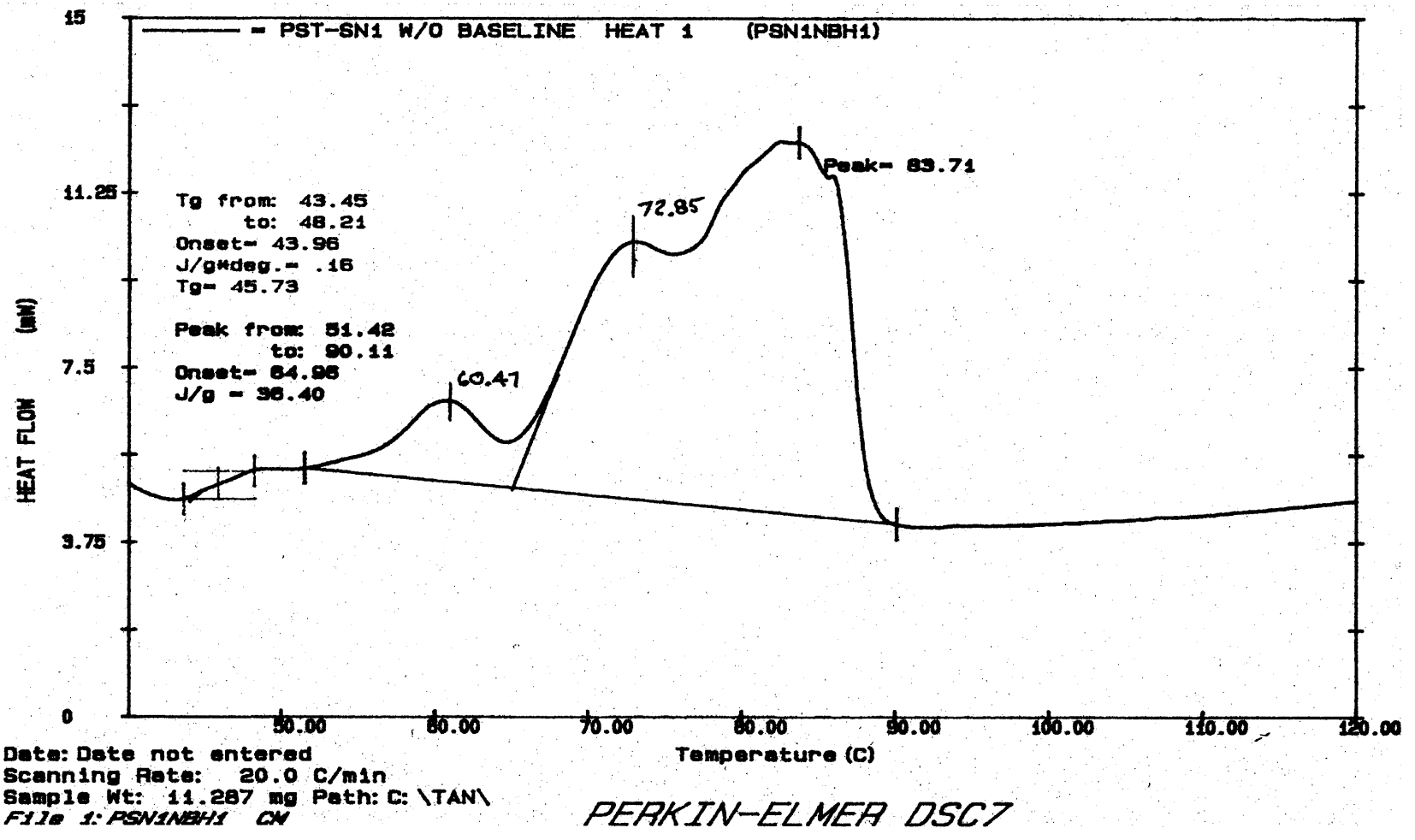

Figure A.31 DSC thermogram of neutralized PST/uncoated hydrotalcite composite, prepared by solution mixing, during the first heating scan.

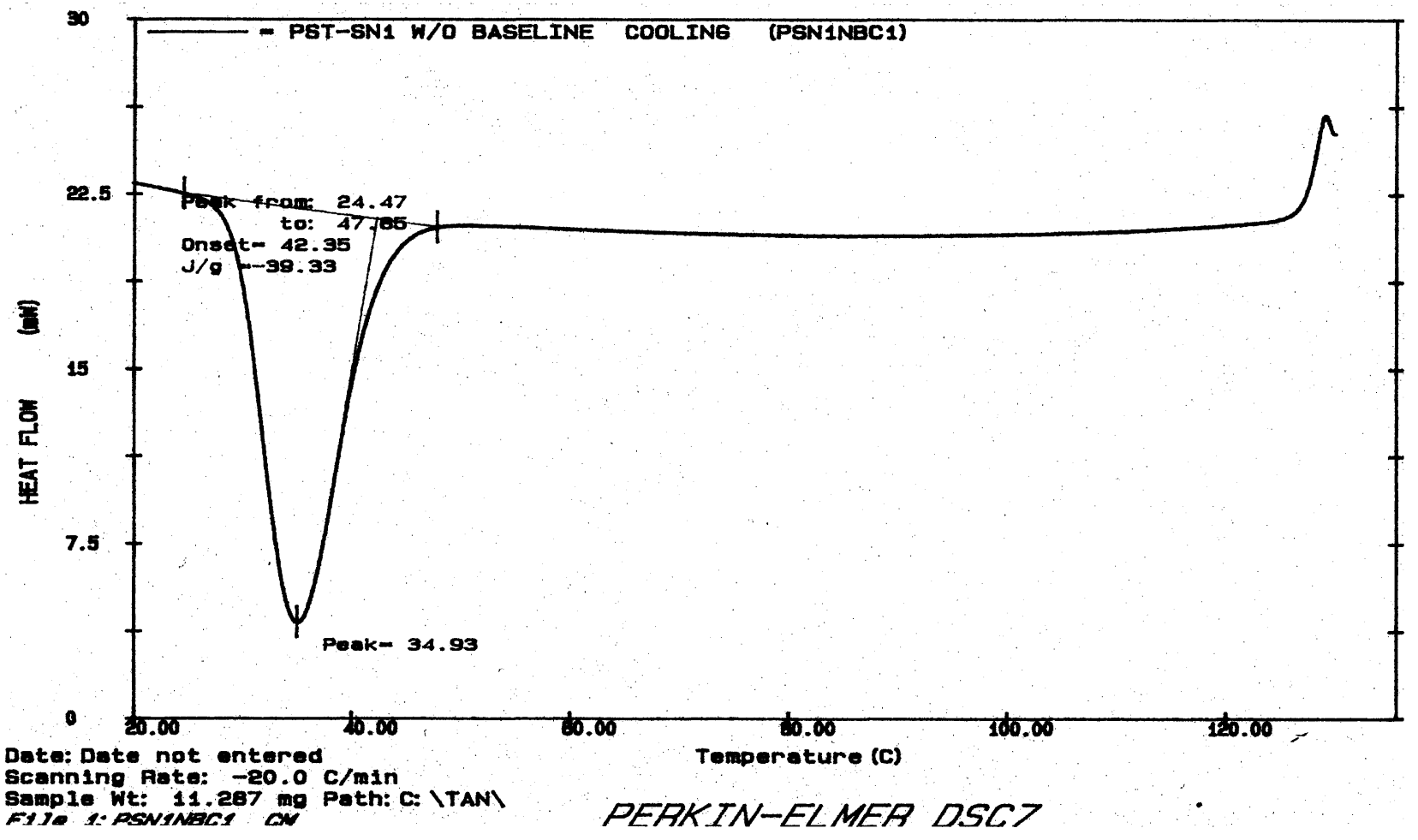

Figure A.32 DSC thermogram of neutralized PST/uncoated hydrotalcite composite, prepared by solution mixing, during the cooling scan.

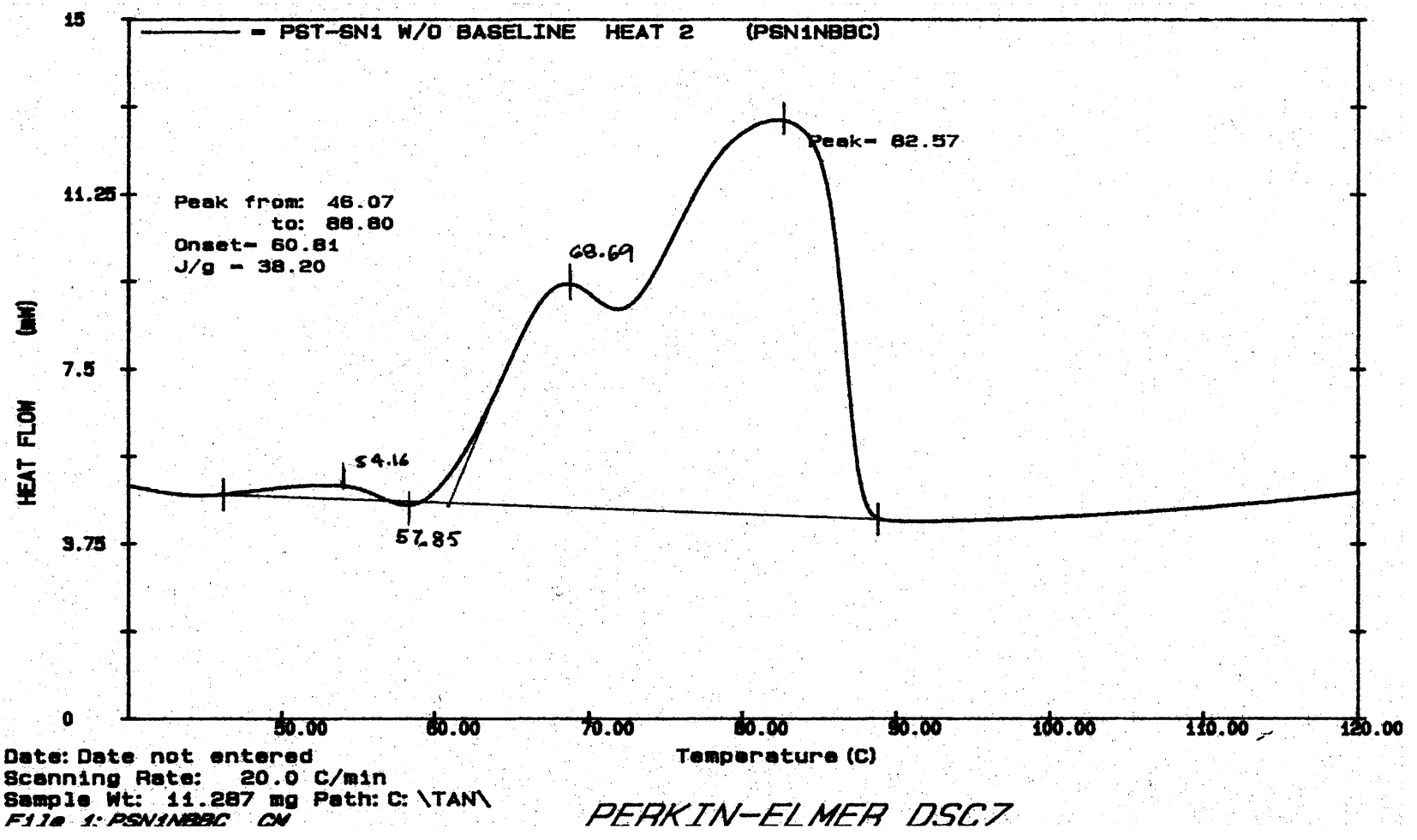

Figure A.33 DSC thermogram of neutralized PST/uncoated hydrotalcite composite, prepared by solution mixing, during the second heating scan.

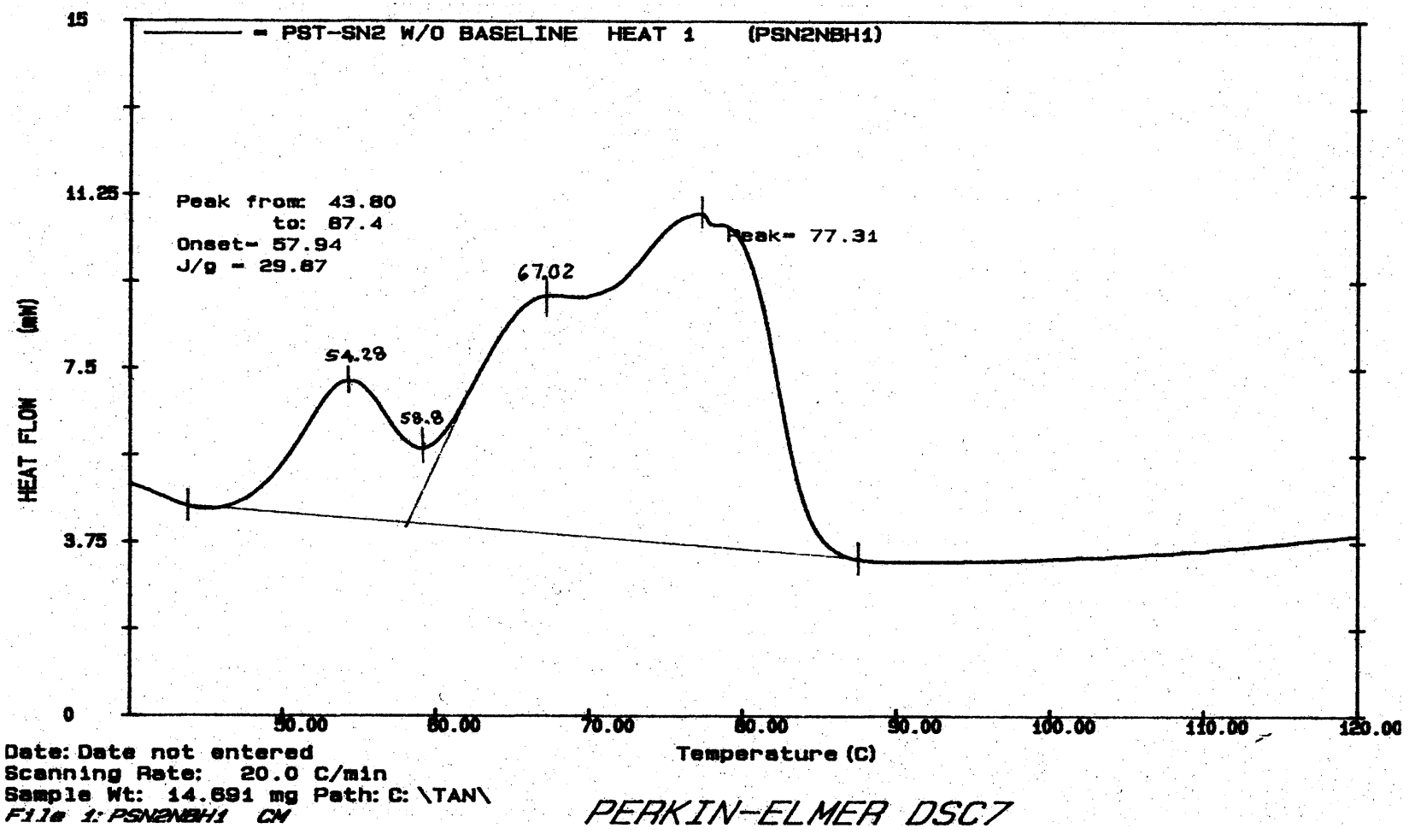

Figure A.34 DSC thermogram of neutralized PST/coated hydrotalcite composite, prepared by solution mixing, during the first heating scan.

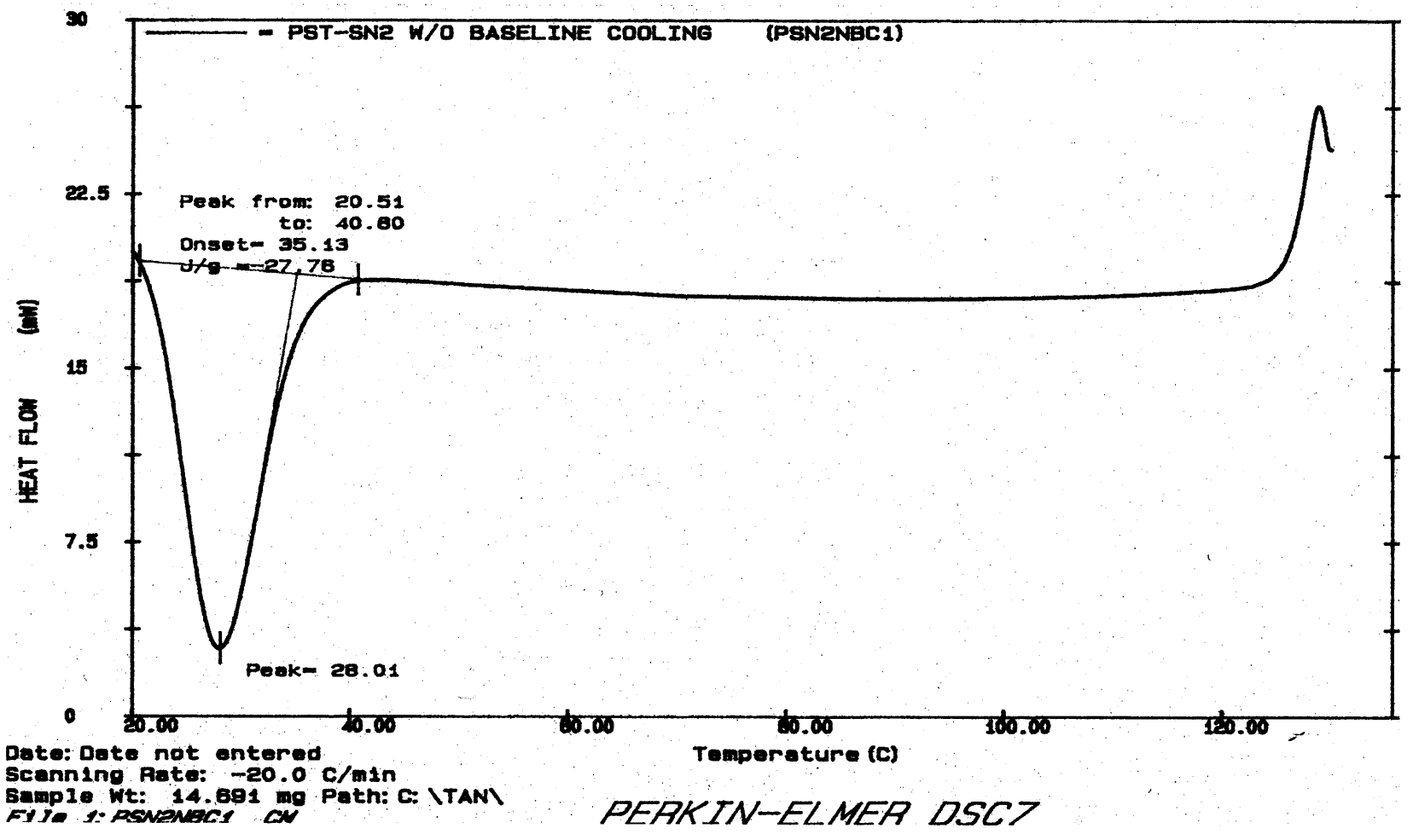

Figure A.35 DSC thermogram of neutralized PST/coated hydrotalcite composite, prepared by solution mixing, during the cooling scan.

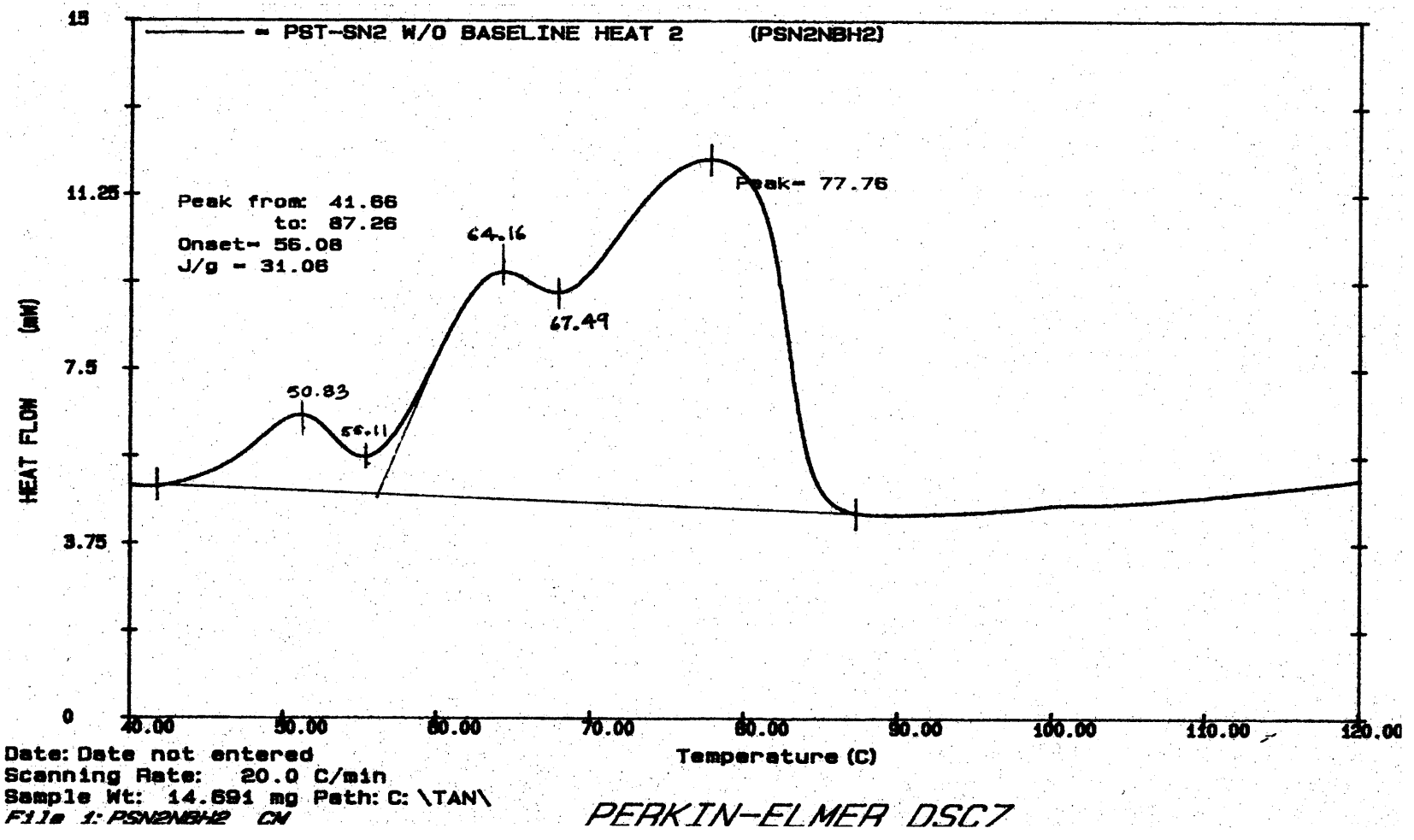

Figure A.36 DSC thermogram of neutralized PST/coated hydrotalcite composite, prepared by solution mixing, during the second heating scan.

APPENDIX B

MELT RHEOLOGY PLOTS

In this Appendix, the plots resulted from the melt rheology data for PST and its composites at shear rates of $2s^{-1}$ and $5s^{-1}$ are presented. The plot of the torque vs. time of PLLA is also included. No further experiments were performed since instability of this polymer occurred.

From Figure B.2 torque data for PST-pel are quite steady up to $10s^{-1}$, whereas at $20s^{-1}$ torque decreases presumably for the reasons mentioned below. From Figure B.2 torque data for PLLA-pel are downswing at all shear rates. Figures B.4 and B.5 show viscosity of PST-pel and PST-melt at 130^0C and $5s^{-1}$ shear rates. Viscosity values are fairly stable over long period of times and as discussed earlier PST-melt has a slighter lower viscosity than PST-pel. In Figures B.6 to B.11 obtained at different shear rates, only the average of values up to 100 sec was calculated and included along with % CV in Table 4.4.

The serious instabilities observed in Figures B.6 to B.11 at extended times, may be due to the high shear rates during the experiment. According to Tadmor and Gogos (1978), at shear rates exceeding 10^{-2} or 10^{-1} s^{-1} there is fracture of the polymer melt initiating at the melt-air interface of the plate perimeter. The elastic energy at this point becomes greater than the energy needed to fracture the polymer melt. As a result, the "saw tooth" pattern observed in the melt rheology plots may be related to the creation of such a secondary flow, commonly referred as "cigar" flow, represented by the "cones" rolling in the direction of the upper rotating plate in Figure B.1. From the 3-dimensional

prospective view that is presented in Figure B.1, one could observe that, as the plate is rotating, at the tangent point between the two cones, fluid may be coming out of the space between the plates reducing the torque. When the space in between the two cones becomes larger, the cones are separated, and then the material outside the perimeter may snap back (partially) in the flow region, increasing the torque. The process is cycling, giving rise to the "saw tooth" pattern.

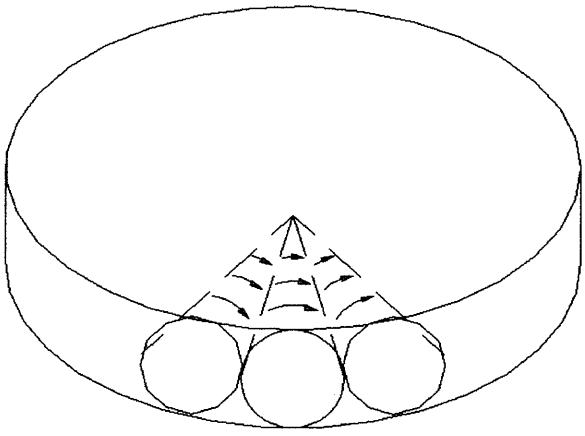

Figure B.1 3-Dimensional view of the secondary flow pattern at shear rate of $2s^{-1}$.

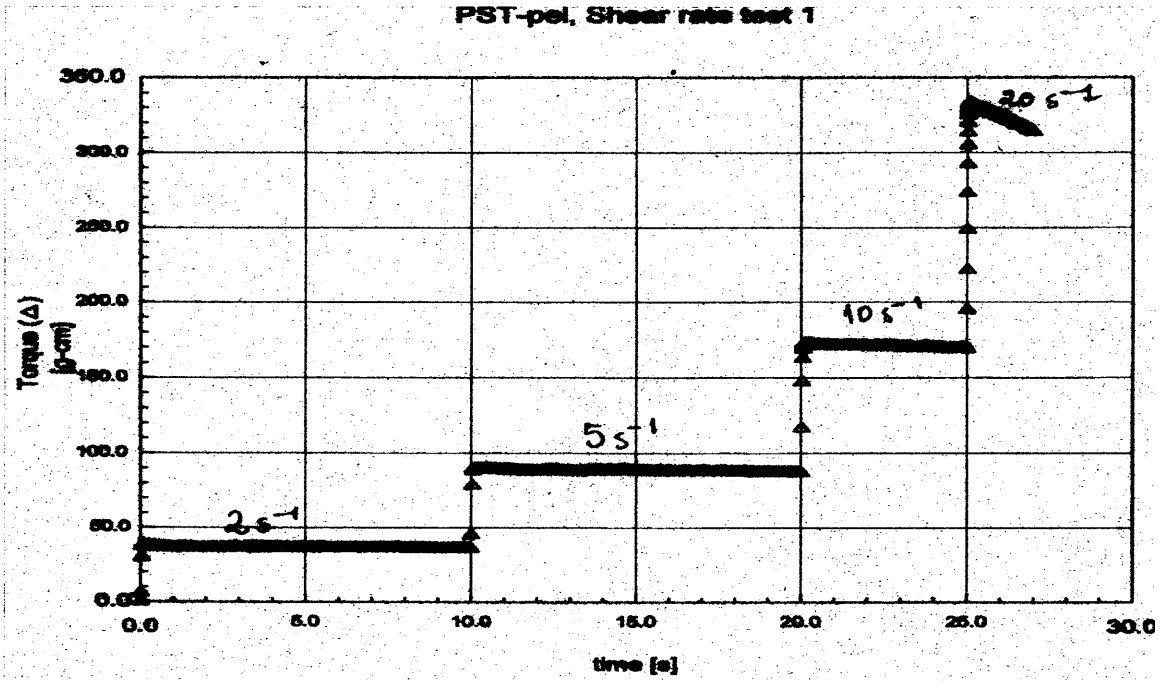

Figure B.2 Plot of torque vs. time of PST-pel at different shear rates at 130^{0}C.

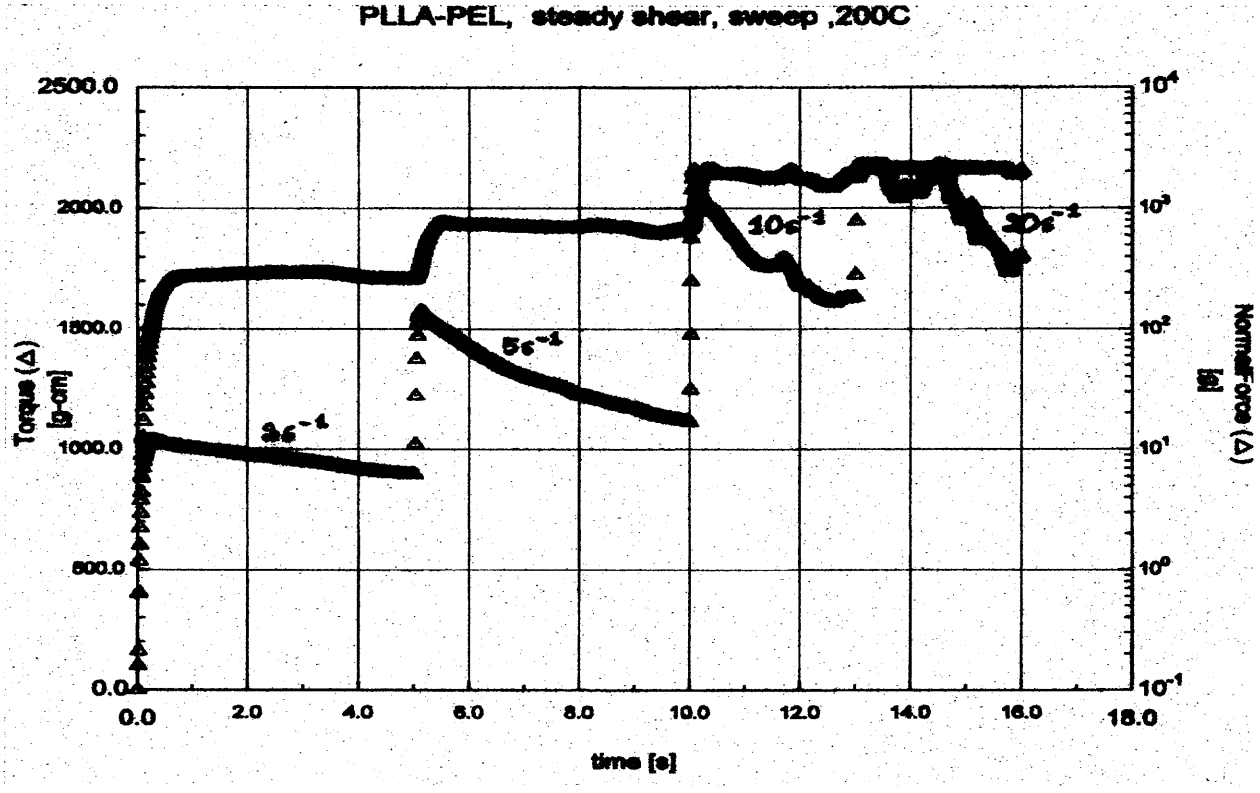

Figure B.3 Plot of torque or normal force vs. time for PLLA-pel at different shear rates at 200^{0}C. Lower curves, torque; higher curves, normal force.

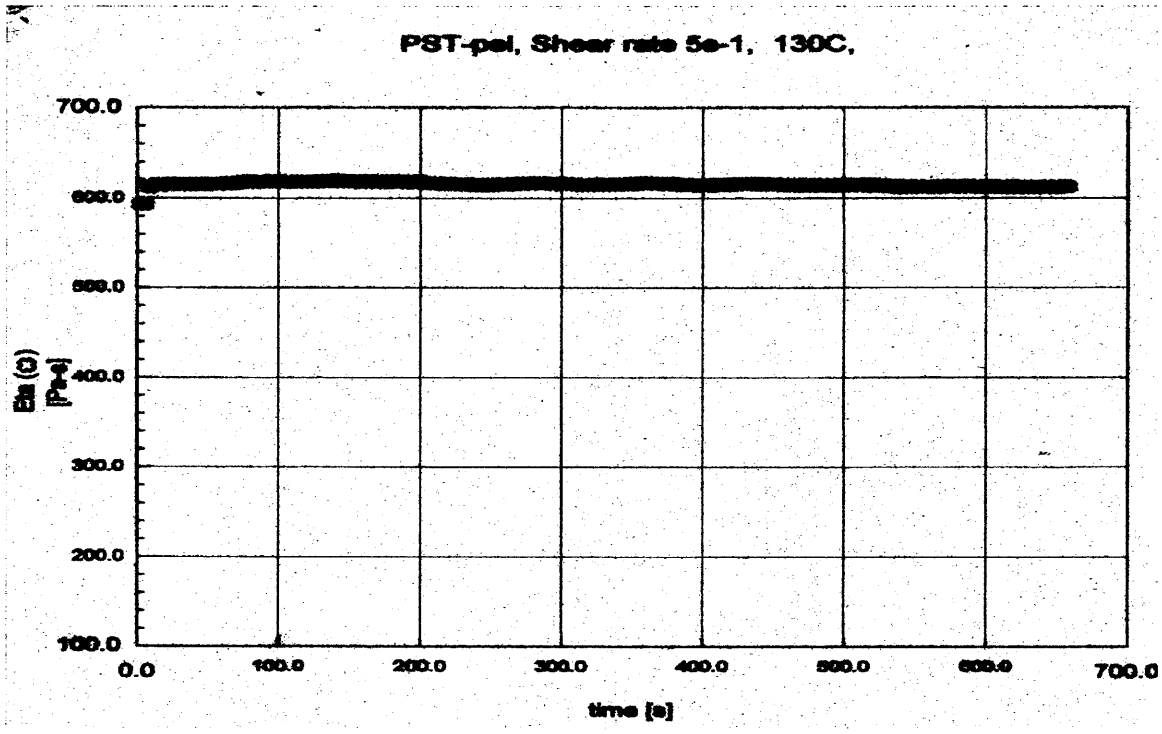

Figure B.4 Plot of viscosity Eta vs. time for PST-pel at $5s^{-1}$ shear rate.

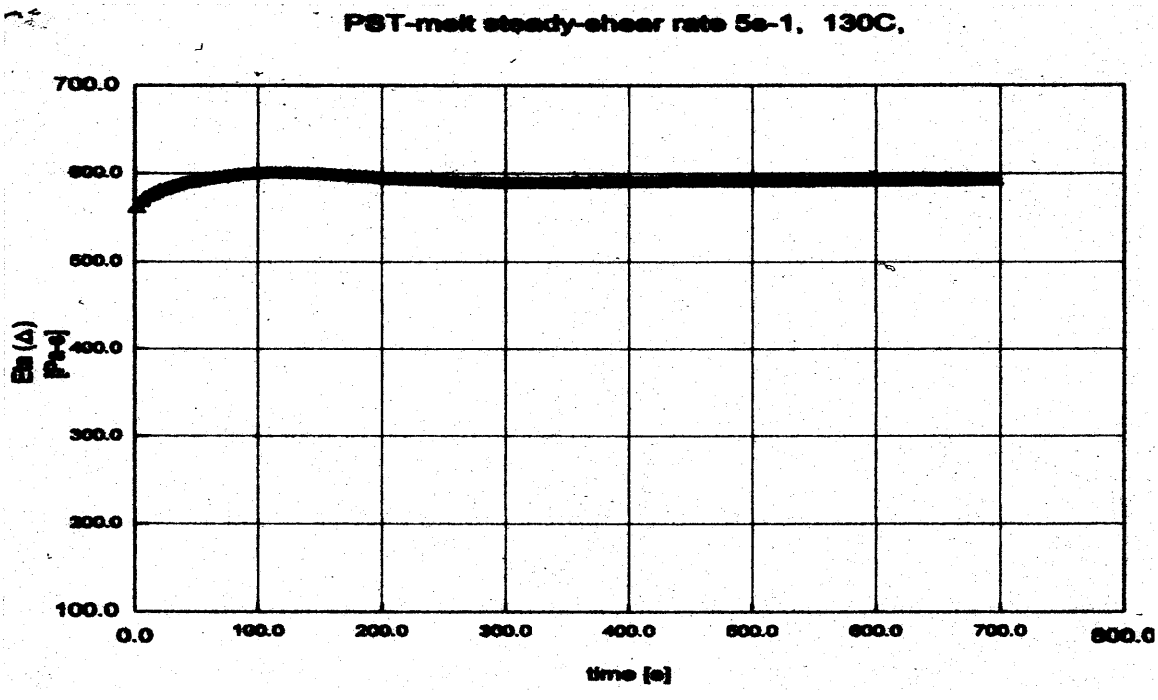

Figure B.5 Plot of viscosity Eta vs. time for PST-melt at $5s^{-1}$ shear rate.

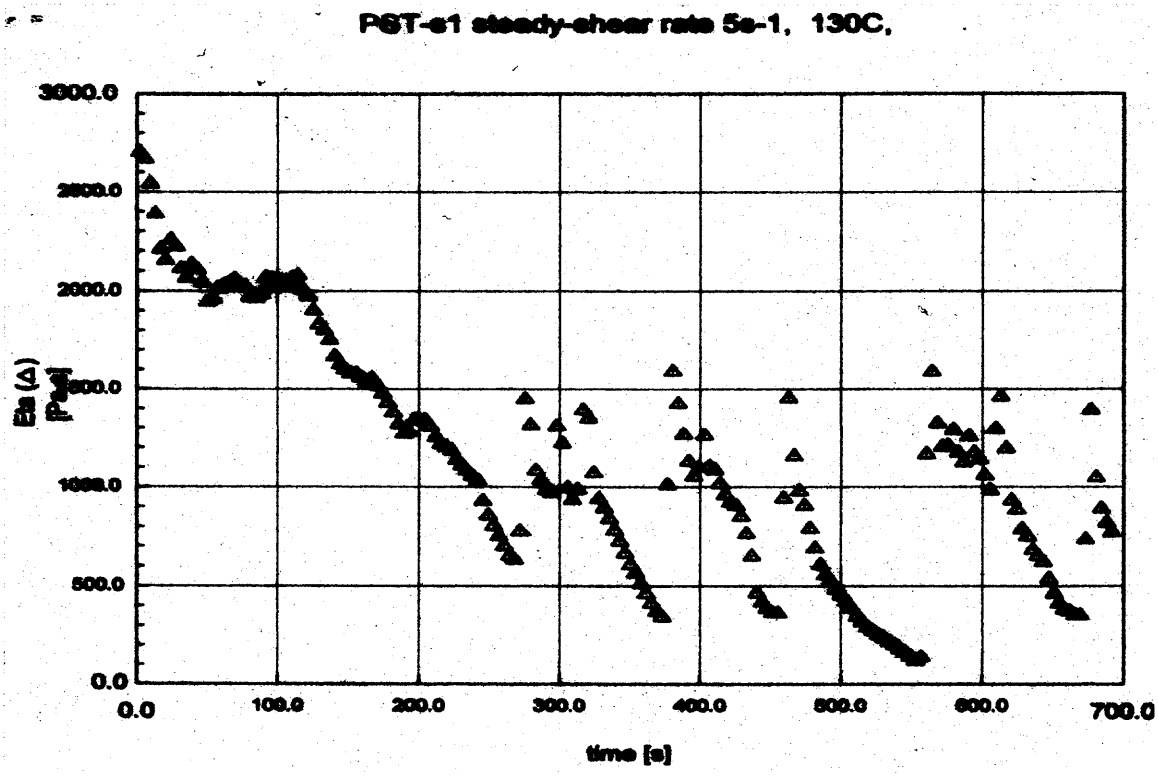

Figure B.6 Plot of viscosity Eta vs. time for PST/uncoated hydrotalcite composite, produced by solution mixing, at $5s^{-1}$ shear rate.

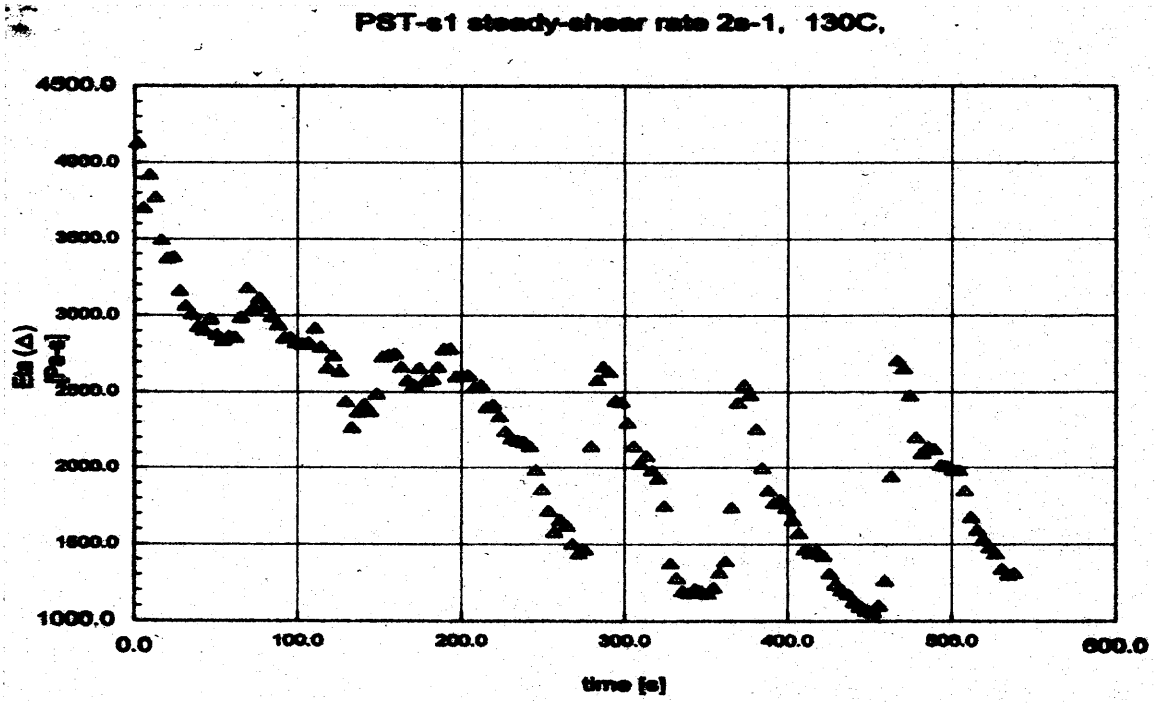

Figure B.7 Plot of viscosity Eta vs. time for PST/uncoated hydrotalcite composite, produced by solution mixing, at $2s^{-1}$ shear rate.

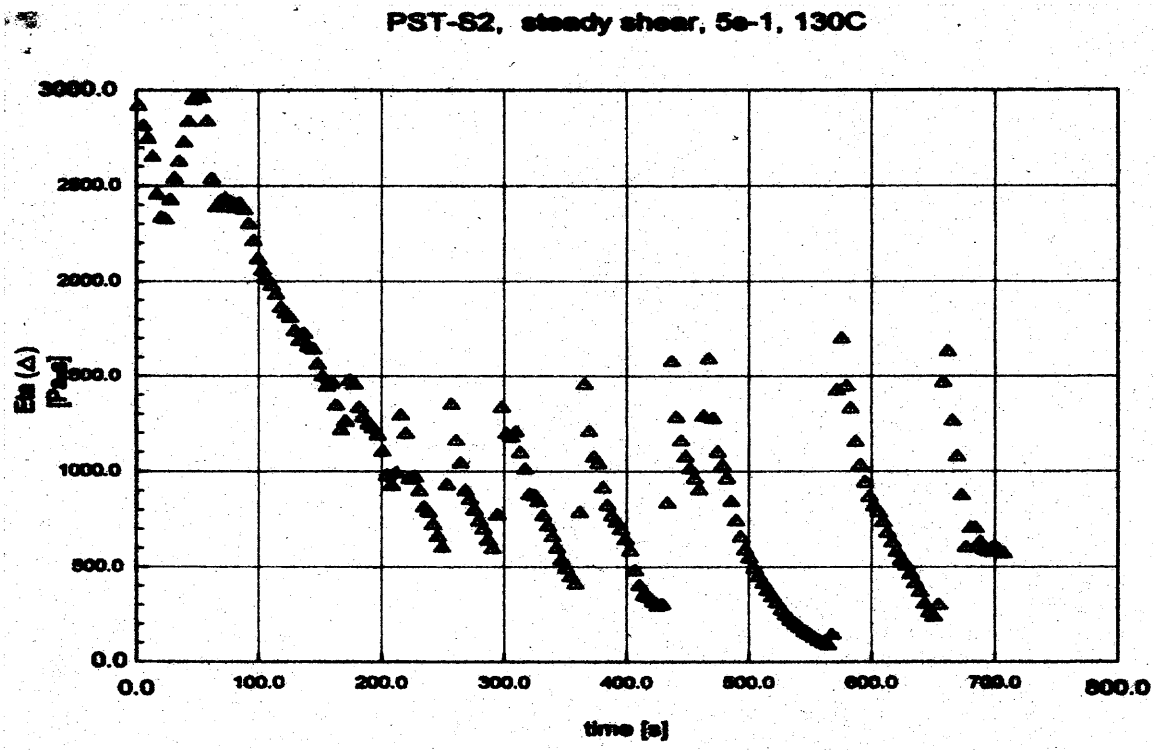

Figure B.8 Plot of viscosity Eta vs. time for PST/coated hydrotalcite composite, produced by solution mixing, at $5s^{-1}$ shear rate.

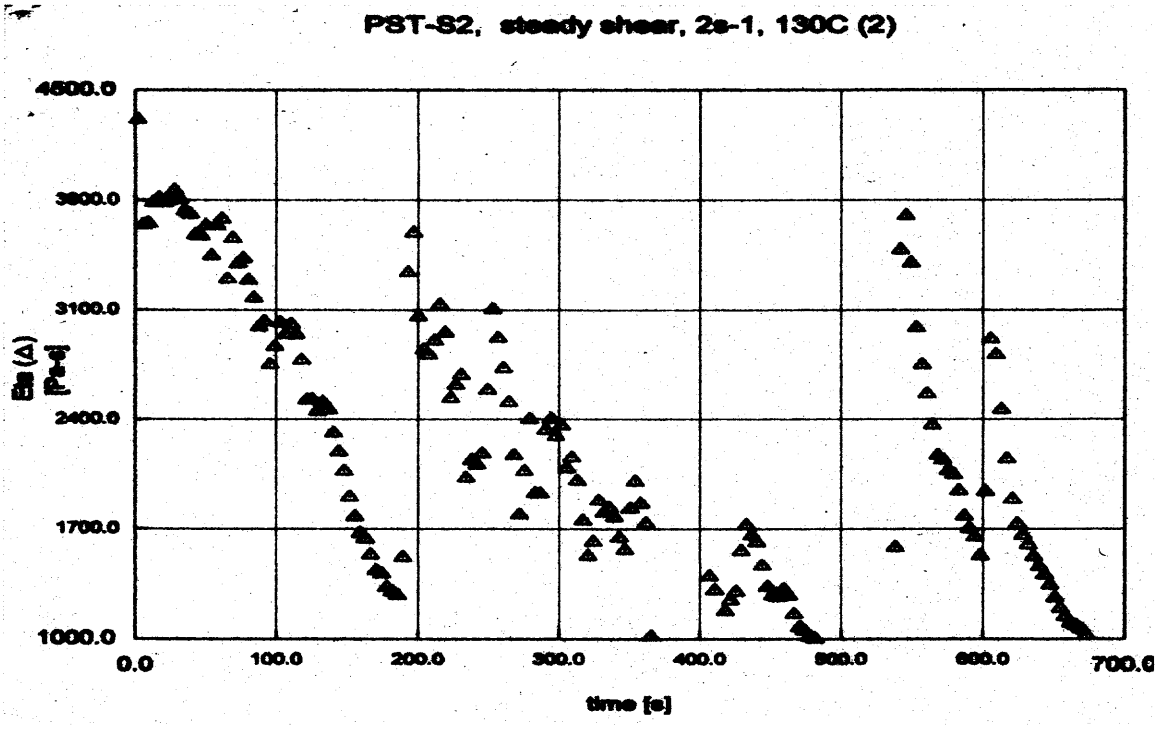

Figure B.9 Plot of viscosity Eta vs. time for PST/coated hydrotalcite composite, produced by solution mixing, at $2s^{-1}$ shear rate.

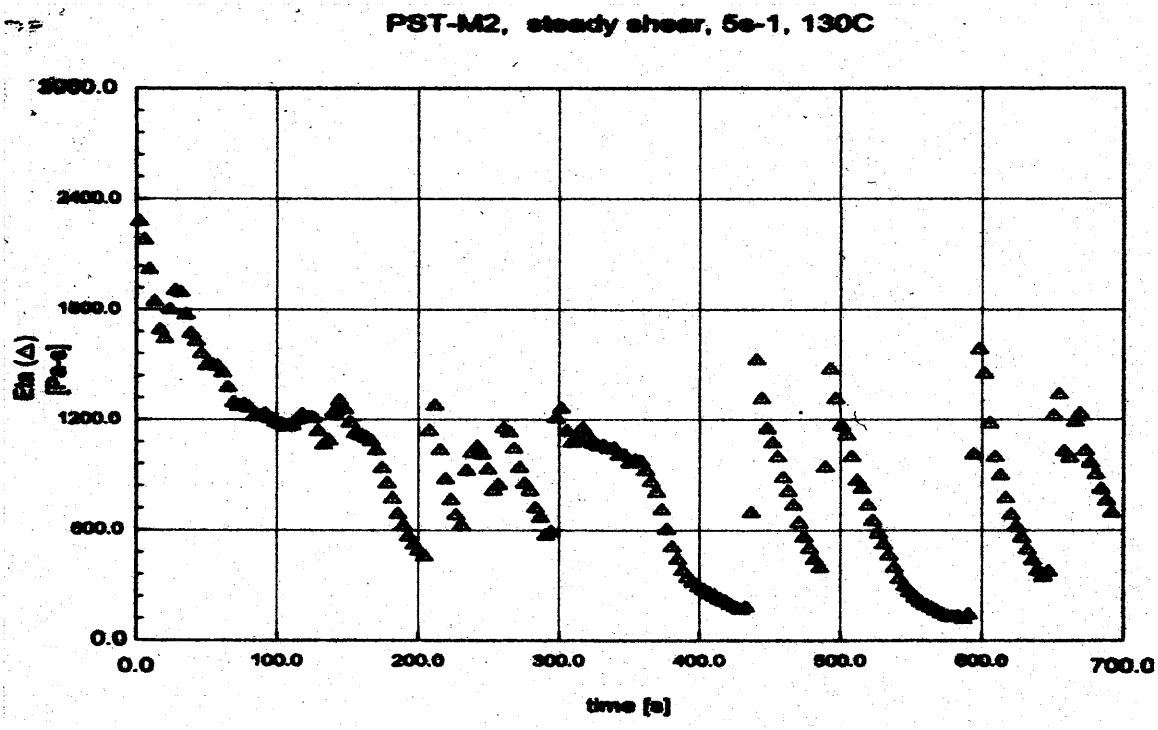

Figure B.10 Plot of viscosity Eta vs. time for PST/coated hydrotalcite composite, produced by melt processing, at $5s^{-1}$ shear rate.

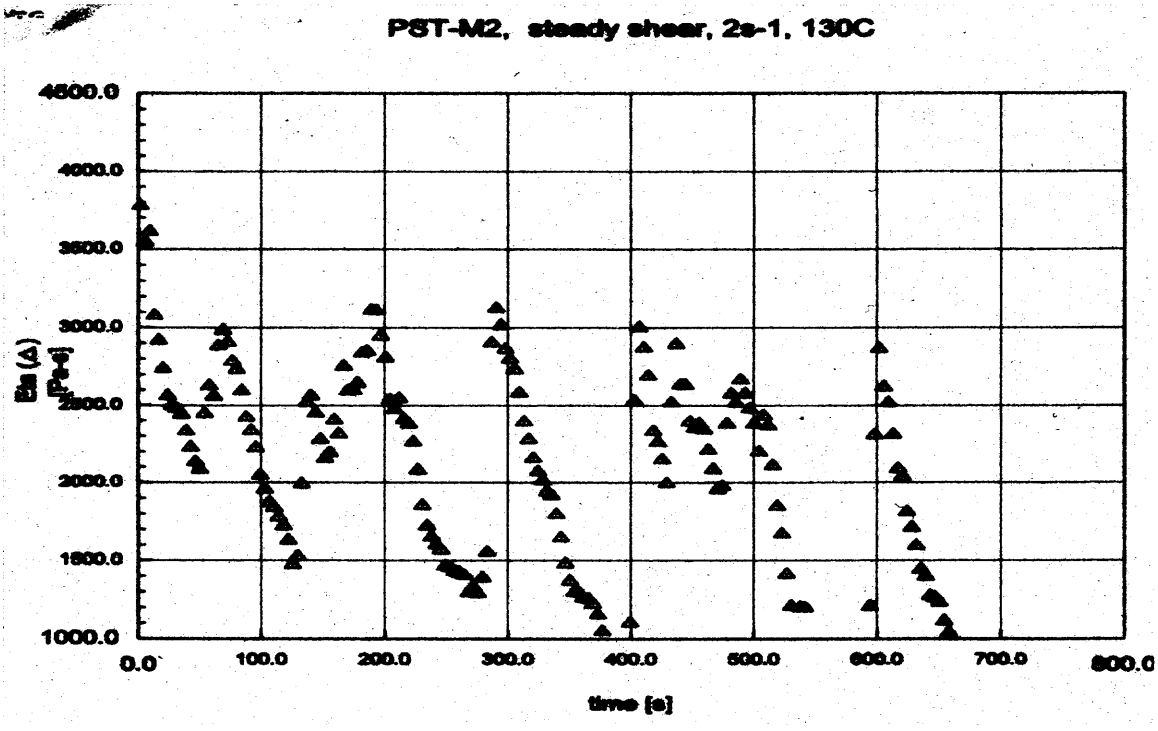

Figure B.11 Plot of viscosity Eta vs. time for PST/coated hydrotalcite composite, produced by melt processing, at $2s^{-1}$ shear rate.

REFERENCES

Calandreli L., Immirzi B., Malinconico M., Volpe M. G., Oliva A., and Ragione F. D., "Preparation and characterization of composites based on biodegradable polymers for *in vivo* application", Polymer, **41**, 8027 (2000).

Carlino S., "The intercalation of carboxylic acids into layered double hydroxides: a critical evaluation and review of the different methods", Solid State Ionics, **98**, 73 (1997).

Doobon Yuhwa., Co. LTD. (2002). CLC-120 Hydrotalcite. [Brochure]. Japan: Research Department.

Engin N. O. and Tas A. C., "Manufacture of macroporous calcium hydroxyapatite and tricalcium phosphate bioceramics", Retrieved July 2002 from the World Wide Web: http://mete.metu.edu.

Fujibayadhi S., Neo M., Kim H., Kokubo T., and Nakamura T., "A comparative study between *in vivo* bone ingrowth and *in vitro* apatite formation on Na_2O-CaO-SiO_2 glasses", Biomaterials, **24**, 1349 (2003).

Gomes M. E., Ribeiro A. S., Malafaya P. B., Reis R. L., and Cunha A. M., "A new approach based on injection moulding to produce biodegradable starch-based polymeric scaffolds: morphology, mechanical and degradation behaviour", Biomaterials, **22**, 883 (2001).

Gomes M. E., Godinho J. S., Tchalamov D., Cunha A. M., and Reis R. L., "Design, processing and biological behaviour of starch based scaffolds for bone and cartilage tissue engineering", Proc. of the 60th SPE Ann. Tech. Conf., 2648 (2002).

Hench L. L., Biomaterial science: An introduction to materials in medicine, Academic Press, (1996).

Kellomäki M., Niiranen H., Puumanen K., Ashammakhi N., Waris T., and Törmälä P., "Bioabsorbable scaffolds for guided bone regeneration and generation", Biomaterials, **21**, 2495 (2000).

Kim Y. H., The KIST website: "An overview on Biodegradable polymers in biomedical application", ICS-UNIDO EDP EGM, Retrieved July 2002 from the World Wide Web: http://biomaterials.kist.re.kr .

Kyowa Chemical Industry Co., LTD. (1972, May). DHT-4A Hydrotalcite-like compound. Japan, Research Center.

Laurencin C. T., Attawia M. A., Lu L. Q., Borden M. D., Lu H. H., Gorum W. J., and Lieberman, J. R. " Poly(lactide-co-glycolide)/hydroxyapatite delivery of BMP-2-producing cells: a regional gene therapy approach to bone regeneration", Biomaterials, **22**, 1271 (2001).

Leonor I. B., Ito A., Onuma K., Kanzaki N., and Reis R. L., "*In vitro* bioactivity of starch thermoplastic/hydroxyapatite composite biomaterials: an *in situ* study using atomic force microscopy", Biomaterials, **24**, 579 (2003).

Lewandrowski K. U., Bondre S. P., Wise D. L., and Trantolo D. J., "Healing of osteochondral osteotomies after fixation with a hydroxyapatite-buffered polylactide. A histomorphometric and radiographic study in rabbits", Bio-Medical Materials and Engineering, **12**, 259 (2002).

Lutton C., Read J., and Trau M., "Nanostructured Biomaterials: a Novel Approach to Artificial Bone Implants", Australian Journal of Chemistry, **54**, 621 (2001).

Ming S., Garreau H., Vert M., "Structure-property relationships in the case of the degradation of the massive aliphatic poly(a-hydroxy acids) in aqueous media, Part 1: Poly(D,L-lactic acid)", Journal of Materials Science: Materials in Medicine, **1**, 123 (1990).

Malafaya P. B., Elvira C., Gallardo A., Stappers F., Roman J. S., and Reis R. L., "Processing of starch-based microparticles and porous architectures for the controlled release of drugs", Proc. of the Polymer Processing Society Conf., PPS 2002, Guimarães, Portugal, June 2002.

Mitsunaga T., Okada K., Nagase and Y., "Properties of Biodegradable Resin/Clay Nanocomposites", Proc. of the Polymer Processing Society Conf., PPS 2002, Taipei, Japan, Nov. 2002.

Närhi T. O., Jansen J. A., Jaakkola T., Ruijter A., Rich J., Seppälä J., and Yli-Upro A., "Bone Response to degradable thermoplastic composite in rabbits", Biomaterials, **24**, 1697 (2003).

Paul M. A., Alexandre M., Degée P., Henrist C., Rulmont A., and Dubois P., " New nanocomposite materials based on plasticized poly(L-lactide) and organomodified montmorillonites: thermal and morphological study", Polymer, **44**, 443 (2003).

Pohl H. A., Anal. Chem., **26,** 1614 (1954).

Ray S. S., Okamoto M., Yamada K., and Ueda K., " New and novel polylactide-layered silicate nanocomposites: preparation, materials properties and melt rheology", Proc. of the Polymer Processing Society Conf., PPS 2002, Taipei, Taiwan, Nov. 2002.

Ray S. S., Yamada K., Okamoto M. and Ueda K., "New polylactide-layered silicate nanocomposites. 2. Concurrent improvements of material properties, biodegradability and melt rheology", Polymer, **44**, 857 (2003).

Reis R. L., Gomes M. E., Godinho J. S., Tchalamov D., Cunha A. M., "A range of processing methodologies for designing adequate tissue engineering scaffolds based on natural origin degradable polymers", Proc. of the 59th SPE Ann. Tech. Conf., 2555 (2002).

Reis R. L., "Polymers in tissue engineering: basic principles, main challenges and characterization requirements", Proc. of the 60th SPE Ann. Tech. Conf., 2680 (2002).

Rhee S. H., "Effect of molecular weight of poly(ε-caprolactone) on interpenetrating network structure, apatite-forming ability, and degradability of poly(ε-caprolactone)/silica nano-hybrid materials", Biomaterials, **24,** 1721 (2003).

Schiller C. and Epple M., "Carbonated calcium phosphates pH-stabilising fillers for biodegradable polyesters", Biomaterials, **24**, 2037 (2003).

Sousa R. A., Mano J. F., Reis R. L., Cunha A. M., and Bevis M. J., "Mechanical performance of starch based bioactive composite biomaterials molded with preferred orientation", Polymer Engineering and Science, **42**, 1032 (2002).

Tadmor Z., and Gogos C., Principles of Polymer Processing, Wiley-Interscience, Haifa, Israel, Hoboken, New Jersey (1978).

Törmälä P., Kellomaki M., and Bonfield W., "Bioactive and biodegradable composites of polymers and ceramics or glasses and method to manufacture such composites", International Patent WO 99/11296 (1999).

Vert M., Li M. S., Spenlehauer G., and Guerin P., "Bioresorbability and biocompatibility of aliphatic polyesters", Journal of Materials Science, **3**, 432 (1992).

Zhang X., Goosen M. F. A., Wyss U., and Pichora D., "Biodegradable polymers for orthopedic applications", J. M. S. Rev. Macromol. Chem. Phys., **C33(1)**, 81 (1993).